For Reference

NOT TO BE TAKEN FROM THIS ROOM

For Reference

NOT TO BE TAKEN FROM THIS ROOM

Ex libris
universitatis
albertaensis

QUAECUMQUE VERA

UNIVERSITY OF ALBERTA
LIBRARY

Regulations Regarding Theses and Dissertations

Typescript copies of theses and dissertations for Master's and Doctor's degrees deposited in the University of Alberta Library, as the official Copy of the Faculty of Graduate Studies, may be consulted in the Reference Reading Room only.

A second copy is on deposit in the Department under whose supervision the work was done. Some Departments are willing to loan their copy to libraries, through the inter-library loan service of the University of Alberta Library.

These theses and dissertations are to be used only with due regard to the rights of the author. Written permission of the author and of the Department must be obtained through the University of Alberta Library when extended passages are copied. When permission has been granted, acknowledgement must appear in the published work.

This thesis or dissertation has been used in accordance with the above regulations by the persons listed below. The borrowing library is obligated to secure the signature of each user.

Please sign below:

| Date | Signature | Institution |
|---|---|---|

THE UNIVERSITY OF ALBERTA

# TURBULENT ENTRY REGION
# OF
# VISCOELASTIC FLUIDS

BY

© PETER JOSEPH CATANIA

A DISSERTATION
SUBMITTED TO THE FACULTY OF GRADUATE STUDIES
IN PARTIAL FULFILMENT OF THE REQUIREMENTS
FOR THE DEGREE OF MASTER OF SCIENCE
IN CHEMICAL ENGINEERING

DEPARTMENT OF CHEMICAL AND PETROLEUM ENGINEERING

EDMONTON, ALBERTA
DECEMBER, 1968

UNIVERSITY OF ALBERTA

FACULTY OF GRADUATE STUDIES

The undersigned certify that they have read, and recommend to the Faculty of Graduate Studies for acceptance, a thesis entitled "Turbulent Entry Region of Viscoelastic Fluids" submitted by P.J. Catania in partial fulfilment of the requirements for the degree of Master of Science in Chemical Engineering.

# ACKNOWLEDGEMENTS

The author wishes to express his gratitude for financial support provided by the National Research Council of Canada, and to Dow Chemical Company who donated the polymer.

I am especially indebted to my supervisor, Professor Frederick A. Seyer, for providing the necessary guidance and knowledge necessary to complete this work. The excellent workmanship and organization of Mr. Walsh and his colleagues was indeed appreciated. A special appreciation is due to Miss J. Juanillo, my future wife, for providing many hours of assistance in the preparation of this final dissertation.

## LIST OF FIGURES

Page

1.1 Newtonian Laminar Velocity Profile Development 3

1.2 Newtonian Pressure Profile 5

1.3 Newtonian Turbulent Velocity Profile Development 11

3.1 Schematic of Experimental Apparatus 28

3.2 Upstream Reservoir 2" Brass Pipe 30

3.3 Upstream Reservoir ½" Brass Pipe 31

4.1 Friction Factor - Reynolds Number 37

4.2 $\Delta P/\rho V^2/g_c$ versus $x/RN_{Re}$ 38

4.3 Newtonian Contraction Losses 40

4.4 Friction Factor - Reynolds Number 0.20% Separan AP-30 44

4.5 Friction Factor - Reynolds Number 0.01% Separan AP-30 45

4.6 Pressure Losses ½" Pipe 47

4.7 Pressure Losses 2" Pipe 48

4.8 Pressure Profile 0.20% Separan AP-30 2" Pipe 50

4.9 Vena Contracta Effect 52

4.10 Pressure Profile 0.01% Separan AP-30 ½" Pipe 55

4.11 Contraction Loss and Entry Length Measurement 56

4.12 Contraction Losses for ½" Pipe 58

4.13 Contraction Losses for 2" Pipe 59

Page

4.14 Entry Lengths for 0.01% Separan AP-30 63

4.15 Entry Lengths for 0.20% Separan AP-30 64

4.16 Dimensionless Contraction Loss - Deborah Number 70

4.17 Dimensionless Contraction Loss - Reynolds Number 71

A-1 Equipment Test Section A-2

A-2 Manometer Indicating Fluids A-5

A-3 Viscosity and Specific Gravity Temperature Relations - Sugar Solution #1 A-6

A-4 Viscosity and Specific Gravity Temperature Relations - Sugar Solution #2 A-7

B-1 Low Flow Rate Calibration B-5

B-2 High Flow Rate Calibration B-6

C-1 Flow Curves C-2

C-2 Relaxation Time - Shear Stress C-3

D-1 Pressure versus Downstream Distance for Water in 2" Pipe D-11

D-2 Pressure versus Downstream Distance for Sugar Solution #1 in 2" Pipe D-12

D-3 Pressure versus Downstream Distance for Sugar Solution #2 in 2" Pipe D-13

D-4 Pressure versus Downstream Distance for Sugar Solutions #1 and #2 in 2" Pipe D-14

D-5 Pressure versus Downstream Distance for Water in ½" Pipe D-15

D-7 Pressure versus Downstream Distance for Sugar Solution #2 in ½" Pipe D-17

D-8 Pressure versus Downstream Distance for Sugar Solutions #1 and #2 in ½" Pipe D-18

Page

E-1 Pressure Profiles for 0.20% Separan AP-30 in 2" Pipe E-16

E-2 Pressure Profiles for 0.20% Separan AP-30 in 2" Pipe E-17

E-3 Pressure Profiles for 0.20% Separan AP-30 in 2" Pipe E-18

E-4 Pressure Profiles for 0.20% Separan AP-30 in ½" Pipe E-19

E-5 Pressure Profiles for 0.20% Separan AP-30 in ½" Pipe E-20

E-6 Pressure Profiles for 0.20% Separan AP-30 in ½" Pipe E-21

E-7 Pressure Profiles for 0.20% Separan AP-30 in ½" Pipe E-22

E-8 Pressure Profiles for 0.01% Separan AP-30 in 2" Pipe E-23

E-9 Pressure Profiles for 0.01% Separan AP-30 in 2" Pipe E-24

E-10 Pressure Profiles for 0.01% Separan AP-30 in 2" Pipe E-25

E-11 Pressure Profiles for 0.01% Separan AP-30 in ½" Pipe E-26

E-12 Pressure Profiles for 0.01% Seperan AP-30 in ½" Pipe E-27

E-13 Pressure Profiles for 0.01% Separan AP-30 in ½" Pipe E-28

E-14 Pressure Profiles for 0.01% Separan AP-30 in ½" Pipe E-29

E-15 Pressure Profiles for 0.01% Separan AP-30 in ½" Pipe E-30

E-16 Pressure Profiles for 0.01% Separan AP-30 in ½" Pipe E-31

Page

E-17 Pressure Profiles for 0.01% Separan AP-30 in ½" Pipe E-32

E-18 Pressure Profiles for 0.01% Separan AP-30 in ½" Pipe E-33

## LIST OF TABLES

Page

1.1 Newtonian Hagenbach Correction Factors 9

4.1 Variation of Hagenbach Correction Factors 41

4.2 Turbulent Entry Length 42

B-1 0-25 Imp. G.P.M. Calibration (High Sensitivity) B-2

B-2 0-65 Imp. G.P.M. Calibration (Low Sensitivity) B-3

B-2 0-170 Imp. G.P.M. Calibration B-4

D-2 Newtonian Pressure Drops (Water) D-5

D-3 Pressure Drops for Sugar Solution #1-2" Pipe D-7

D-4 Pressure Drops for Sugar Solution #1-½" Pipe D-8

D-5 Pressure Drops for Sugar Solution #2-2" Pipe D-9

D-6 Pressure Drops for Sugar Solution #2-½" Pipe D-10

E-2 Contraction Losses and Entry Lengths for 0.20% Separan AP-30 2" Pipe E-3

E-3 Contraction Losses and Entry Lengths for 0.20% Separan AP-30 ½" Pipe E-4

E-4 Contraction Losses and Entry Lengths for 0.01% Separan AP-30 2" Pipe E-5

E-5 Contraction Losses and Entry Lengths for 0.01% Separan AP-30 ½" Pipe E-6

E-6 Pressure Drops for 0.20% Separan AP-30 2" Pipe E-7

Page

E-7 Pressure Drops for 0.20% Separan AP-30 ½" Pipe E-9

E-8 Pressure Drops for 0.01% Separan AP-30 2" Pipe E-11

E-9 Pressure Drops for 0.01% Separan AP-30 ½" Pipe E-13

## ABSTRACT

Turbulent flow drag reduction in recent years has received considerable attention in the engineering literature. While many authors purport to have quantitatively defined the drag reduction, it is clear that under some conditions extremely large entry lengths occur and therefore, there may be serious errors in their measurements.

Entry lengths and contraction losses have been determined for both Newtonian and drag reducing non-Newtonian fluids. The drag reducing fluids considered were 0.01% and 0.20% by weight of Separan AP-30 in water. Data were obtained in 2 inch and 1/2 inch pipes over Reynolds numbers ranging from approximately $10^3$ to $4 \times 10^5$. Data obtained with the Newtonian fluids are in good agreement with the available data.

For the viscoelastic materials, the contraction losses owing to the sharp-edged 6 to 1 cross-sectional area reduction were found to be as much as 75% more than Newtonian fluids at similar conditions. The measured entry lengths, although suffering from an appreciable amount of scatter, have been found to be much larger than for the turbulent flow of Newtonian fluids and pass through a maximum. For the 0.20% solution, entry lengths in the order of 200 diameters were found at a Reynolds number of $2 \times 10^4$. Similar entry lengths were found for the 0.01%

solution at a Reynolds number of $3 \times 10^5$. These observations have important consequences when it is noted that the experimental pipelines for studying these materials, are generally designed by assuming turbulent Newtonian entry lengths of about 50 diameters.

Dimensional considerations indicate that the contraction losses depend on a dimensionless group which includes the relaxation time of the material, $\theta$. It was found however, that this single dimensionless group was insufficient to interpret the results qualitatively. Other dimensionless groups such as the generalized Reynolds number was also shown to be insufficient.

# TABLE OF CONTENTS

Page

LIST OF FIGURES i

LIST OF TABLES v

ABSTRACT vii

I INTRODUCTION

1.1 General 1

1.2 Entry Length and Contraction Losses 2

II BACKGROUND AND THEORY FOR DRAG REDUCING FLUIDS

2.1 General 15

2.2 Constitutive Equations 17

2.3 Drag Reduction and Velocity Profiles 20

2.4 Pressure Losses and Dimensional Analysis 22

III EXPERIMENTAL EQUIPMENT AND PROCEDURE

3.1 Experimental Equipment 27

3.1.1 General 27

3.1.2 Pump and Measuring System 27

3.1.3 Entrance Region and Pressure Taps 29

3.1.4 Pressure Measurements 32

3.1.5 Experimental Fluids 32

3.1.6 Rheological Properties 33

3.2 Procedure 34

3.2.1 Preparation of Polymer Solution 34

3.2.2 Data Collection 34

Page

IV DISCUSSION OF RESULTS

4.1 Newtonian Analysis 36

4.2 Analysis for Viscoelastic Fluids 42

4.2.1 Drag Reduction and Unusual Effects 42

4.2.2 Contraction Losses 53

(i) Measurement 53

(ii) Correlations 57

4.2.3 Entry Lengths 62

4.2.4 Dimensional Analysis 67

V CONCLUSIONS AND RECOMMENDATIONS

5.1 Conclusions 72

5.2 Recommendations 74

APPENDICES

A Equipment Specifications

B Flow Calibration

C Physical Properties

D Newtonian Pressure Profiles

E Viscoelastic Pressure Profiles

F Sample Calculations

G Nomenclature

H Bibliography

# CHAPTER I

# INTRODUCTION

## 1.1 GENERAL

One of the many problems confronting the engineer is to define entry length and contraction losses for various flow geometries either experimentally or theoretically. Recently, owing to the many practical implications, a large number of studies have considered the properties of drag-reducing additives in turbulent flow. In this turbulent regime by the use of pressure measurements and velocity profiles determined in a region-free of entry effects drag reduction can be defined experimentally.

In addition to drag reduction, analyses as discussed by Philipoff and Gaskins (60) and others (28,49) may lead to the determination of the normal stress difference. The entry region and associated contraction losses are closely coupled with the study of heat and mass transfer (34) in these systems: that is, heat transfer coefficients have been noted to be lowered in proportion to the amount of drag reduction.

It is therefore imperative to have a quantitative analysis concerning the length required for entry effects to become negligible. In the past this problem has been dealt with in a qualitative sense (48, 66) indicating entry

lengths similar to those in the Newtonian transition regime (63). No quantitative analyses are as yet available to determine experimentally the magnitude of the entry lengths relative to Newtonian values.

Therefore, the purpose of this study was to consider experimentally the turbulent entry lengths for drag-reducing systems in round tubes. Equally important is the magnitude of the contraction losses. However, before such an analysis commences an understanding of the analyses of laminar and turbulent flow for Newtonian fluids as well as the analysis for laminar non-Newtonian flow will be discussed in some detail. This background, based on available analyses, serves as a framework for interpreting the experimental results and is also an indication of the complexity of the problem.

## 1.2 ENTRANCE LENGTHS AND CONTRACTION LOSSES

The entry length may be defined as that distance required for a fluid flowing from an infinite upstream reservoir into a capillary or pipe to a point where the downstream flow is fully developed. Three non-independent pieces of information are generally sufficient to characterize the flow in the entry: entry lengths, contraction losses and velocity profiles. As indicated on Figure (1.1) for laminar flow, the fluid enters the pipe from a large reservoir and

FIGURE (1.1)
NEWTONIAN LAMINAR VELOCITY
PROFILE DEVELOPMENT

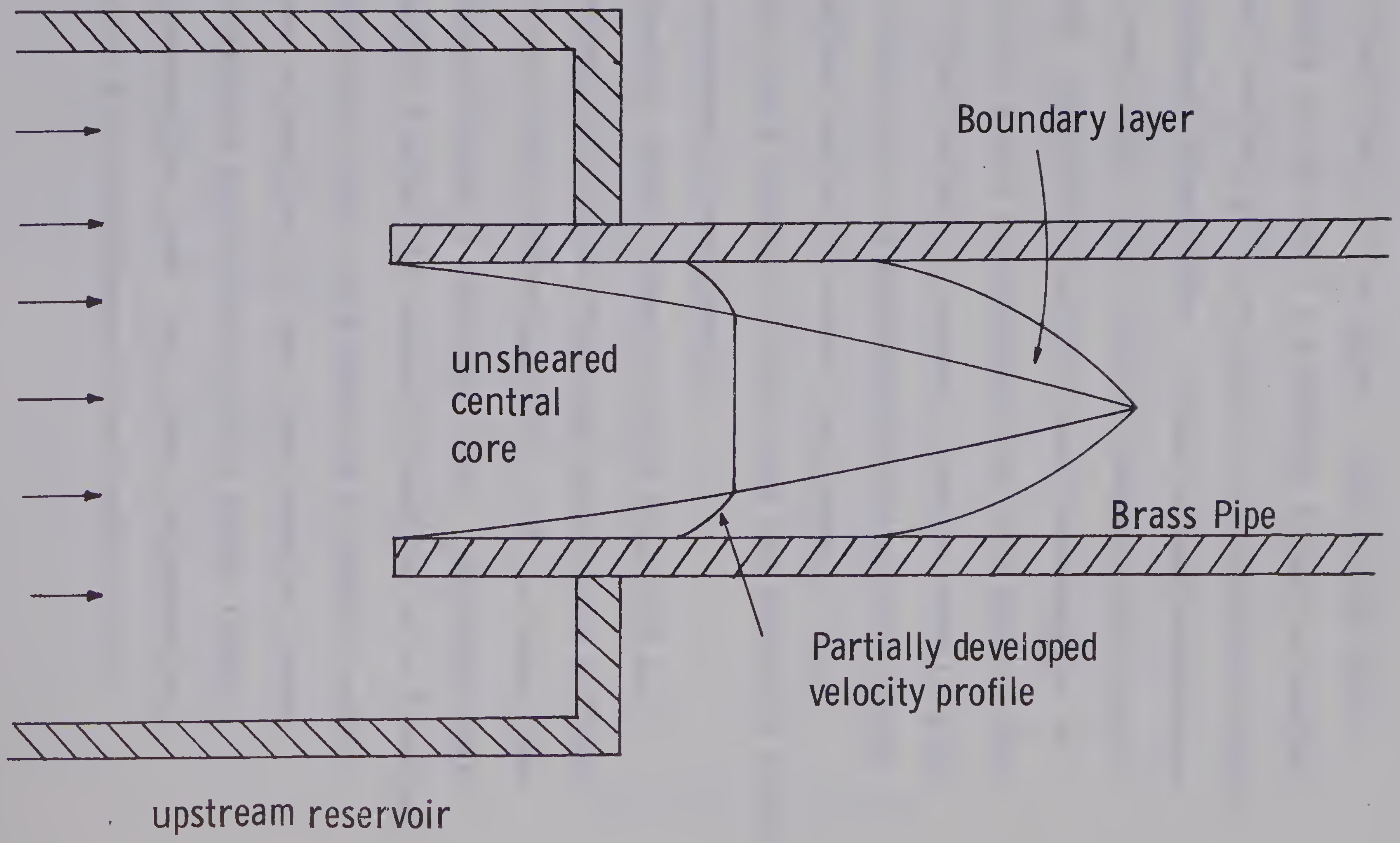
Boundary layer
unsheared
central
core
Brass Pipe
Partially developed
velocity profile
upstream reservoir

a uniform velocity distribution is generally assumed to prevail at the start of the pipe. Due to the frictional resistance at the wall a boundary layer is created at the wall and gradually encroaches on the uniform stream as the flow proceeds downstream. Since at any downstream position the total mass flux remains constant the flow in the undisturbed, unsheared, central core accelerates to compensate for the fluid retardation near the wall. This change of the steam velocity causes a greater static pressure reduction than for the corresponding well-developed pipe flow. Beyond the point where the boundary layer encompasses the cross section of the tube the velocity profile continues an asymptotic development.

As a result, entry length can be measured as a distance downstream where the velocity profile is a fixed percentage of being fully-developed (20, 33) or where the pressure gradient becomes a constant (30). In purely viscous non-Newtonian fluids the velocity profile is a function of the flow behavior index and yields as a result, entry lengths that are a function of the flow behavior index. Figure (1.2) indicates qualitatively the entry length ($L_e$) and the contraction loss ($\Delta P_c$) for a hypothetical run when pressure drop measurements are used as the criteria.

FIGURE(1.2)
NEWTONIAN PRESSURE PROFILE

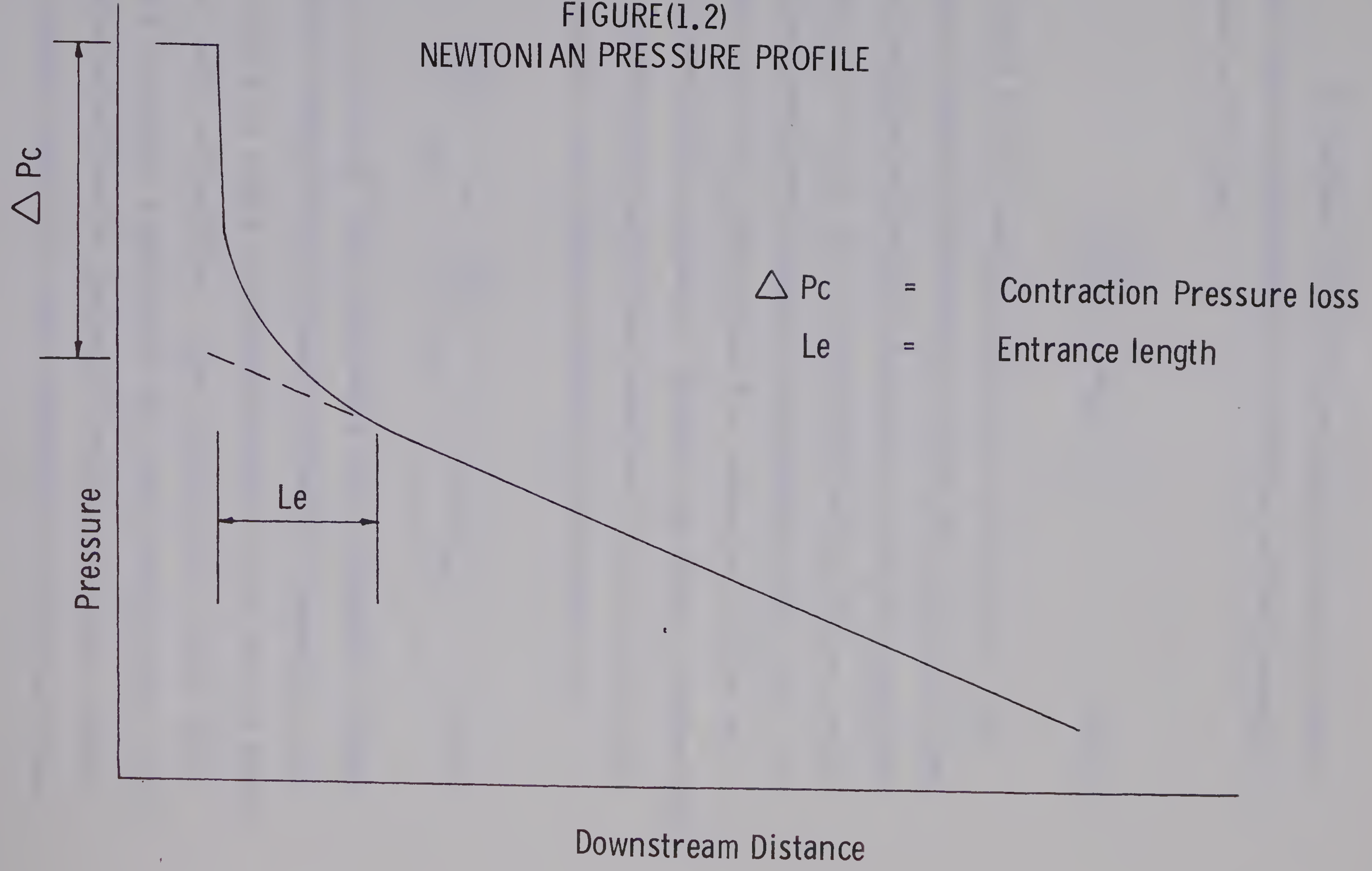

In laminar flow of Newtonian fluids the entry lenth may be expressed as a function of the Reynolds number as follows:

$$\frac{L_e}{D} = KN_{Re} \tag{1.2.1}$$

in which K is a constant equal to 0.0555 (20). For purely viscous non-Newtonian fluids the value of K has been reported as being a function of the flow behavior index (6, 13, 21, 76). For viscoelastic fluids, entry lengths have been observed to be shorter (28, 30), or longer (55,77) than those for Newtonian fluids at similar Reynolds numbers. Metzner and White (47) show that for viscoelastic solutions equation (1.2.1) can be rewritten for flow between parallel flat plates as:

$$\left(\frac{L_e}{b}\right)_{VE} = \left(\frac{L_e}{b}\right)_{PV} + \sigma(n,s)N_{ws} \tag{1.2.2}$$

where the second term represents the incremental change in entry length due to elastic effects. Depending upon the values of n and s the coefficient $\sigma(n,s)$ may be negative, zero, or positive. The variation of $\sigma(n,s)$ thus offers a partial explanation why entry lengths for viscoelastic solutions in laminar flow can be larger, greater and possibly equal to their counterpart Newtonian values.

Considering Newtonian laminar flow in a pipe free of end effects one can write Poiseuille's equation as:

$$\frac{\Delta P_{DEV}}{\rho V^2/g_c} = 32.0 \frac{L}{RN_{Re}} \qquad (1.2.3)$$

The above can be extended to purely viscous non-Newtonian fluids by replacing the Reynolds number by the generalized Reynolds number (46) as indicated by Drexler (28). The excess pressure arising from several effects can be incorporated into equation (1.2.3) as follows (28):

$$\frac{\Delta P_{TOT}}{\rho V^2/g_c} = 32.0 \frac{L}{RN_{Re}} + \phi \qquad (1.2.4)$$

Here $\Delta P_{TOT}$ is the total pressure drop over the length L and $\phi$ is referred to as the Hagenbach correction factor. With reference to equation (1.2.4) the contraction loss can be empirically expressed as:

$$\Delta P_c = \phi \frac{\rho V^2}{g_c} \qquad (1.2.5)$$

Astarita and Greco ( 6 ) recently have expressed a similar relationship between the dimensionless contraction loss and the Reynolds number as:

$$\frac{\Delta P_c}{\rho V^2/g_c} = \frac{K_1}{N_{Re}} + K_2 \qquad (1.2.6)$$

where $\frac{K_1}{N_{Re}}$ is the Couette correction factor and $K_2$ is equivalent to $\phi$, the Hagenbach correction factor. Their data and analysis indicate that for any Reynolds number less than a critical Reynolds number of about 146 the dimensionless contraction loss becomes inversely proportional to the Reynolds number. The proportionality constant was experimentally determined to be 795. Beyond the critical Reynolds number the dimensionless contraction loss was found to be a constant equal to 5.48. Both $K_1$ and $K_2$ were reported for a specific ratio of reservoir to tube diameter $\beta$, and one would assume that these variables could be highly sensitive to the geometry of the contraction section. Other authors have reported the Hagenbach factor as a constant as indicated by Table (1.1). It is interesting to note that these semi-empirical values grossly underestimate the value of contraction loss. The semi-empirical approaches assumed that at the pipe entrance or at some imaginary section upstream there exists a flat

## TABLE (1.1)

## Newtonian Hagenbach Correction Factors

| Author | Reference | $\theta$ |
|---|---|---|
| Astarita | 6 | 5.48 |
| Bogue | 13 | 2.16 |
| Campbell and Slattery | 18 | 2.18 |
| Christiansen and Lemmon | 20 | 2.274 |
| Collins and Schowalter | 21 | 2.33 |
| Tomita | 75 | 2.20 |

velocity profile. In reality, the experimental evidence of Uebler (87) and the analysis of Wang and Longwell (78) show that the velocity profile is not flat for a sharp-edged contraction. In addition, the presence of a vena contracta (6, 58) downstream of the contraction would prove to be impossible if the profile was indeed flat.

The spectrum of values of $\phi$ is due in part to the other assumptions and the particular analysis; for example, solving the equations of motion by neglecting no terms (78), by Pohlhausen's Momentum Integral Technique (13), by the introduction of a stream function (21) or a similarity transformation (1). Significantly, the usual assumptions that the hydrostatic pressure is a function of axial position only and that radial momentum transfer by convection is negligible, have been the cause of some controversies (23,24,78).

Extending the analysis of laminar flow contraction losses to non-Newtonian fluids, Astarita (7) determines that for both weakly and highly elastic solutions the dimensionless contraction loss was inversely proportional to the Reynolds number (as indicated by equation 1.2.6). The constant of proportionality was suggested to be a function of the flow behavior index only, and have values smaller and larger than Newtonian fluids. In turbulent flow there are few analyses available which provide a general prediction of entry lengths and the attendant

FIGURE(1.3)
NEWTONIAN TURBULENT VELOCITY
PROFILE DEVELOPMENT

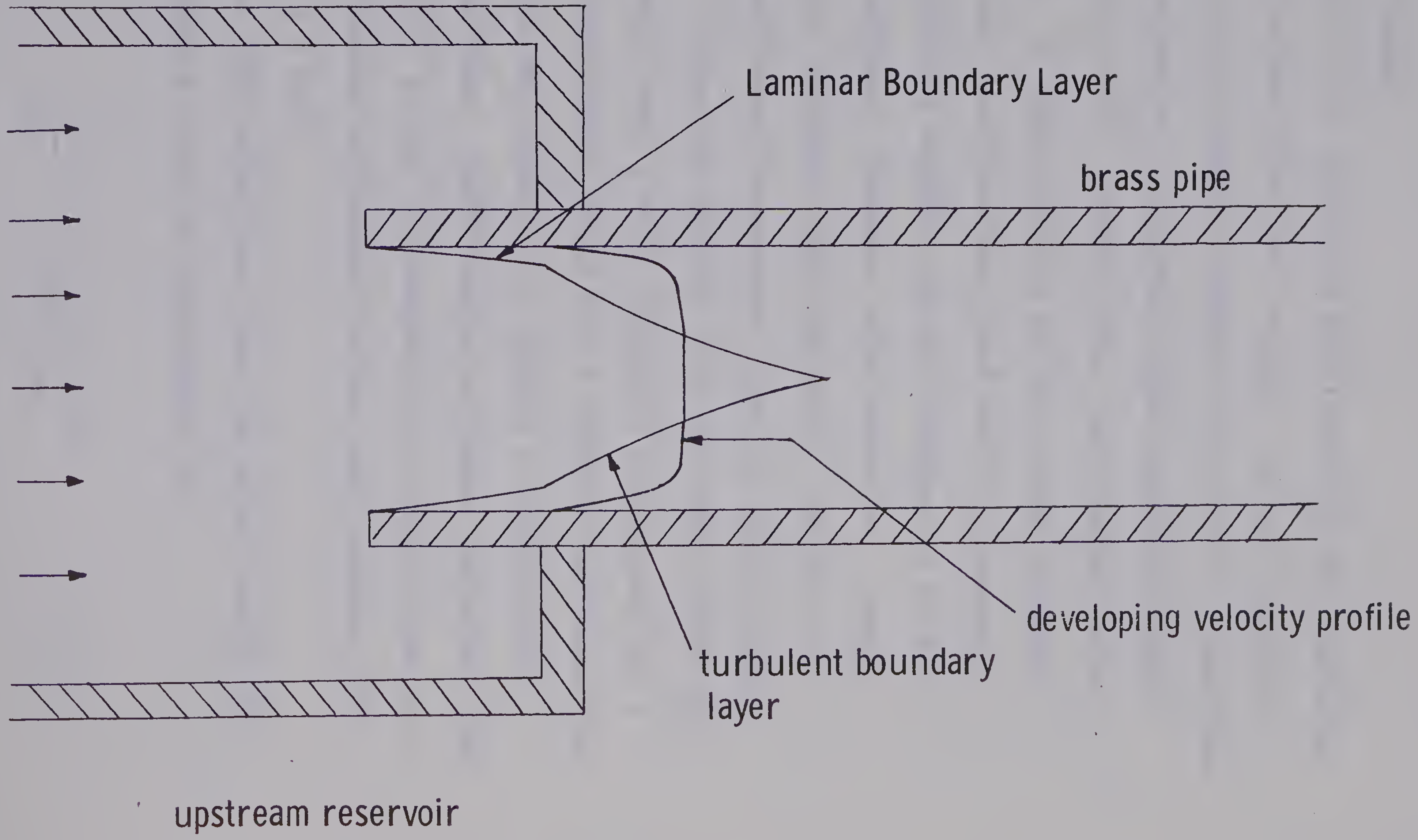
Laminar Boundary Layer
brass pipe
developing velocity profile
turbulent boundary layer
upstream reservoir

contraction losses.

Figure (1.3) indicates qualitatively the features of the entry in the turbulent regime. In this regime, the boundary layer remains laminar only up to a transition point which occurs at a boundary layer Reynolds number roughly equal to $10^5$. Beyond this, the boundary layer is turbulent. A large portion of the excess pressure loss occurs near the pipe entry and how this pressure loss is distributed between the two regimes is of yet not clearly defined. However, with accurate, closely spaced pressure readings near the entry, one can in principle predict the downstream location where transition occurs. Olson and Sparrow (59) use this device and show as a result that a vena contracta is present for a sharp-edged contraction while for a smoothed entrance the laminar portion was observed to extend a considerable distance downstream. Experimental evidence indicates that entry lengths of 25 and 15 diameters can result from non-induced and induced turbulence in the entry geometry for a $N_{Re} = 5.0 \times 10^5$.

Latzko (35) determined that the entry length for induced turbulence could be represented as:

$$\frac{L_e}{D} = 0.693\ N_{Re}^{1/4} \qquad (1.2.7)$$

However, the above formula yields shorter entry lengths that have been found experimentally. Barben and Jones (11)determined that for a $N_{Re} = 4.0 \times 10^5$ the velocity profile was not developed at 41 diameters downstream while Latzko's theoretical formula would have given an entry length of 17 diameters. Kirsten (38) measured entry lengths of 50 to 100 diameters depending upon the Reynolds numbers while Nikuradse (35) obtained fully-developed flow at 25 to 40 diameters for induced turbulent flow; the 40 diameter value was obtained at a $N_{RE} = 9.0 \times 10^5$.

A more recent analysis was made by Ross (62) who predicted pressure losses for Newtonian fluids by considering the integral momentum and continuity equations and utilizing available boundary layer equations. The results indicated that the pressure losses in the entry were a weak function of the Reynold number for Reynolds numbers in the order of $10^6$. Theoretically, this indicates that the dimensionless contraction losses are constant.

Generally, the available data for turbulent flow indicate that the entry lengths vary widely and in a complex way on the geometry of the entrance, the Reynolds number and even on the means of measurement. An additional although dependent factor, which has been largely ignored in the papers mentioned previously, is the turbulence level of the entering stream. The importance of turbulence in the free stream as well as in the entrance geometry is

concisely discussed in a recent paper by Dalla Lana and Christiansen (22).

At pipe Reynolds numbers near 2100, or equivalently "transition Reynolds numbers", entry lengths larger than those at high Reynolds numbers have been observed (63). These data are also presented in condensed form in Hinze (35). In the present context, these data may be especially important as some evidences exist to show that for the flow of viscoelastic fluids, transitional flow may prevail to Reynolds numbers in excess of 30,000 (66).

# CHAPTER II

# BACKGROUND AND THEORY FOR DRAG-REDUCING FLUIDS

## 2.1 GENERAL

Unlike Newtonian fluids which are capable of exhibiting only viscous responses, a viscoelastic solution is capable of exhibiting both viscous and elastic-like responses to a deformation. These responses depend in general upon the instantaneous deformation rate and the total deformation. It has been shown in recent literature (5, 50, 51) that the elastic nature may be considered to be governed by what has been termed a Deborah and a Weissenberg number (3, 35, 67). The Deborah number representing the ratio of the natural time of the fluid to the residence time of the material in the process defines whether the flow is one in which the elastic properties of the fluid are likely to predominate. For rapid deformations: that is, where the residence time is much smaller than the natural time of the fluid the elastic properties of the solution predominate. At the other extreme, the fluid relaxes relatively quickly as it moves through the flow field so as to adjust substantially to the immediate surroundings. In this limiting case, the fluid becomes indistinguishable from a purely viscous fluid. The Weissenberg number representing the

intuition as a parameter in addition to the Reynolds number defined as the ratio of inertial to viscous forces.

In the immediate vicinity of the sudden contraction, and within the developing boundary layer the rate of deformation experienced by a fluid element, changes rapidly with position downstream. Equivalently, from a Lagrangian point of view, the rapid changes in deformation rate may be viewed as rapid changes with respect to time. Thus, as has been shown in an earlier boundary layer analysis (44), large values of the Deborah number may be expected to occur at the leading edge of the tube and for some distance downstream of the leading edge. Furthermore, it has been shown that the large Deborah numbers may lead to a substantial thickening of the boundary layer (44,75,80) which in the case of flow in the entrance of a tube or channel (47,51) may be expected to result in a solid-like region immediately inside the entrance.

Similar effects owing to elasticity occur in the central core where continuity requires that acceleration must occur as governed by the growing boundary layer. The deformations in this region have been termed elongational flow (5,77) where it has been shown as in the previous paragraph that the limiting or high Deborah number behavior of the fluid is a solid-like response. For the viscoelastic fluids, for which a thickened boundary layer is expected

to occur, there will be a tendency to increase acceleration of the central core. At sufficiently high Deborah numbers within the core, the acceleration would be inhibited and the growth of the boundary layer must be modified in order to accommodate the resistance to high deformation rates.

The coupled and competing effects of a tendency toward a thickened boundary layer and a resistance to large accelerations within the core region imply that large changes may occur in the pressure profile of viscoelastic fluids as compared to those of Newtonian fluids. The presence of a solid-like region implies increased contraction losses must occur for viscoelastic fluids. Both effects are dependent on a Deborah number of the flow which in turn depends directly on the fluid relaxation time.

## 2.2 CONSTITUTIVE EQUATIONS

Before analyzing entry length, a constitutive equation must be chosen to represent the flow behavior. In the available literature Metzner and Reed (26,46) develop and employ a power law model for purely viscous solutions. This power law is expressed as:

$$T_w = K' \left( \frac{8V}{D} \right)^{n'} \qquad (2.2.1)$$

where n' is the flow behavior index and K' is the consistency index. Qualitatively, the larger the value of K' the more "viscous" is the solution while n' describes the degree of non-Newtonian behavior. Using

equation (2.2.1) and the Fanning friction factor definition the generalized Reynolds number arises naturally

$$N_{Re}' = \frac{D^{n'} V^{2-n'} \rho}{g_c K' 8^{n'-1}} \qquad (2.2.2)$$

For this study the fluid properties n' and K' have been chosen to adequately represent the viscous nature of the polymeric solutions. Many constitutive equations have been developed to portray the elastic properties of interest and two of these constitutive equations discussed in the literature are the Coleman and Noll and the Convected Maxwell models.

The Coleman and Noll constitutive equations as discussed in the literature (81,82) have stresses not dependent on the instantaneous deformations but on the entire history: that is, strains in the distant past have lesser effects than in the recent past. The mathematical elegance of this formulation however, is immediately lost when applying it to problems of interest. The truncated constitutive equation such as the second order approximation is only capable of predicting normal stress behavior at deformation rates that are so low as to be of little importance in engineering problems. Furthermore, a constant viscosity coefficient is maintained thus, limiting its usefulness to only slightly non-Newtonian fluids. In

comparison, the third order approximation introduces a variable viscosity but does not solve the problem insofar as normal stresses are concerned. Higher order approximations of fourth order and above only add to the complexity of the problem due to the presence of a larger number of material coefficients that must be determined experimentally. For the problem at hand the limited range of applicability of the Coleman and Noll constitutive equation suggests another equation must be chosen to portray the fluid properties.

Metzner, White and Denn (51) discuss in detail the Maxwell model and conclude that it is capable of predicting all experimental effects at least qualitatively, except for the assumption of a zero second normal stress difference. Recently, various authors (37,71,72) show that in reality this second normal stress difference is not zero and seems to be related to the first normal difference by a constant that is yet not clearly defined. Measurement of the first normal stress difference generally employs a jet thrust technique (48,83) for high shear rates and a cone and plate viscometer (86) at low shear rates. Middleman and Gavis (53) point out drawbacks to the former procedure. Other constitutive equations of equal complexity have been presented however, no single constitutive equation of a tractable complexity is available to universally depict the properties of polymer solutions.

As a first approximation it is assumed that the convected Maxwell model can portray the fluid properties such that

$$P_{ij} + \theta \frac{\delta P_{ij}}{\delta t} = 2\mu d_{ij} \qquad (2.2.3)$$

where

$$P_{ij} = P\delta_{ij} + T_{ij}$$

Here, P is an arbitrary hydrostatic pressure and $\frac{\delta}{\delta t}$ is the contravariant convective derivative (51). Thus, as a first approximation the significant elastic properties can be assumed to be governed by the relaxation time $\theta$.

## 2.3 DRAG REDUCTION AND VELOCITY PROFILES

Velocity profiles for polymeric solutions in turbulent flow can be used as a criteria in the determination of entry lengths and in determining the intermittency of the flow field. Recently, in developed flow: that is, in a flow field assumed to be free of all entry and exit effects experimental data indicate that the velocity profile can be expressed as (16,17,69):

$$u^+ = a \log y^+ + B\left(\frac{\theta u^{*2}}{\nu}\right) - C(\xi, f) \qquad (2.3.1)$$

The important features of the velocity profile equation are discussed in detail by Ernst (29), and other authors (52,69). The importance of this equation is that coupled with the definitions of the Fanning friction factor and average velocity a unique friction factor-Reynolds number correlation can be developed (32,41,42,69). This relationship quantitatively portrays the ability of the polymeric solutions to reduce frictional losses (19,31,66,70). The analysis of this phenomena has been documented experimentally by several authors (3,45,67) where a significant reduction of the turbulent drag as compared to the flow of a Newtonian fluid under similar conditions, is noted. Qualitatively, the drag reduction is displayed as a friction factor-Reynolds number plot having values of the friction factor as much as an order of magnitude lower than corresponding Newtonian values and in addition exhibit a strong diameter dependence.

Recent measurements indicate that drag reduction may be considered to be a function of elastic to viscous forces (45). Some investigators suggest that a stabilization of the flow to Reynolds numbers in excess of 2100 results directly from the fluids elastic properties. Not all polymers are drag-reducing (65). Some polymers, such as the 100 ppm considered in this study which has a flow

behavior index of unity (58), yield significant drag reduction. Also, data based on concentrations as low as 10 ppm (58) indicate that significant drag reduction is present even for minute quantities of polymer.

## 2.4 PRESSURE LOSSES AND DIMENSIONAL ANALYSIS

The measured presssure drop from an infinite upstream reservoir to a point downstream is composed of frictional losses in the upstream reservoir, in the entry, a loss due to the developing profile and frictional losses in the fully-developed section. In laminar flow, these effects as well as elastic contributions can be summarized as (56):

$$\frac{\Delta P_{TOT}}{\rho} = \Delta(KE) + F_{upstream} + F_{dev} + F_{entry} + \left[F_E + \Delta E\right] \quad (2.4.1)$$

In the above, $F_E + \Delta E$ are contributions owing to the elastic properties of the fluid. The term E is the internal elastic stored energy per unit mass and $F_E$ is the dissipative loss due to any unusual flow patterns caused by elasticity.

In viscoelastic fluids the unique ability to store and release quantities of energy is one phenomenon yet to be explained in detail and Astarita (4) suggests that an a priori understanding of the thermodynamics of

these systems is necessary. However, it is not clear that these elastic effects are additive. There exists the possibility of describing the total pressure loss as a function of the non-elastic terms where the function might depend upon the fluid relaxation time $\theta$. The non-elastic terms in equation (2.4.1) represent the kinetic energy difference for a fluid that flows from an infinite reservoir to some point downstream in fully-developed flow. F upstream represents the frictional losses in the upstream reservoir that are for most cases negligible when compared to $F_{dev}$ and $F_{entry}$: that is, the frictional losses in developed flow and in the entry region.

Feig (30) and Drexler (28) try to theoretically express the elastic stored energy, E, as:

$$E = P:S = \sum_{i}\sum_{j} P_{ij}S_{ji} \qquad (2.4.2)$$

where $P_{ij}$ is defined in the normal manner and $S_{ij}$ is a strain tensor that results from a deformation in a perfectly elastic solid subjected to simple shear (39). In the immediate vicinity of the contraction this assumption may be valid due to the solid-like behavior, however, further downstream the flow field is free from any solid-like behavior and in this region equation (2.4.2) is no longer applicable.

In turbulent flow, while in principle the same considerations apply as for laminar flow, the detailed analyses of entrance phenomena present difficulties that have not been overcome even for laminar flow. For viscoelastic fluids the problem is of course complicated by the complex nature of the fluid, thus, dimensional analysis will be applied as an aid to interpreting the experimental results.

Assuming that the contraction loss is a function of the usual variables in addition to the flow behavior and consistency indices, and the relaxation time we have

$$\Delta P_c = A(D,V,\rho,K',n',\theta,g_c) \qquad (2.4.3)$$

and similarly,

$$L_e = A_1(D,V,\rho,K',n',\theta,g_c) \qquad (2.4.4)$$

Applying the $P_i$ theorem we obtain:

$$\frac{\Delta P_c}{\rho V^2/g_c} = A\left[\frac{g_c K'}{D^{n'} V^{2-n'}\rho}, \frac{V\theta}{D}, n'\right] \qquad (2.4.5)$$

and

$$\frac{L_e}{D} = A_1\left[\frac{g_c K'}{D^{n},V^{2-n}\rho}, \frac{V\theta}{D}, n'\right] \qquad (2.4.6)$$

In general, these dimensionless groups can be rearranged in any manner provided their total number remains unchanged. As presented the three dimensionless groups are

the Reynolds number, a type of Deborah number and the flow behavior index.

Since Newtonian fluids possess small relaxation times the only important parameter is the Reynolds number. It has been shown that the dimensionless contraction loss can be either inversely porportional to or independent of the Reynolds number (6). The dimensionless entry length presented in Chapter I indicates a direct relationship with the Reynolds number.

For viscoelastic solutions the importance of any one of the three dimensionless groups is not known. Through the use of various polymeric solutions possessing a range of elastic properties one can determine experimentally, relationships between the dimensionless contraction loss or entry length and the dimensionless groups. The relaxation time used in the definition of the Deborah number is that which is determined in SLSF.[1] Using equation (2.2.3) the relaxation time in this case is defined as:

$$\theta = \frac{(P_{11} - P_{22})_w}{2T_w(\frac{8V}{D})} \qquad (2.4.7)$$

Qualitatively, the relaxation time determines how rapidly the stresses will decay to zero after the specimen is suddenly stretched and held at a constant deformation. It then becomes apparent

---

[1] SLSF refers to steady laminar shear flow

that the flow field has a spectrum of values. Near the entry as previously discussed the rapid changes in deformation may be viewed, from a Lagrangian viewpoint, as rapid changes with respect to time. In this limit, the calculation of relaxation time using equation (2.2.3) becomes complex since it now becomes a function of time. However, these relaxation times are related to those defined by equation (2.4.7) which can be evaluated experimentally. The Deborah number will thus be defined using the relaxation times obtained in SLSF.

# CHAPTER III

## 3.1 EXPERIMENTAL EQUIPMENT AND PROCEDURE

### 3.1.1 GENERAL

The experimental program consisted of measuring pressure losses and entry lengths for dilute aqueous solutions of a polymer additive Separan AP-30, as it flowed through a sudden 6 to 1 diameter contraction. Pressure taps were located before and after the contraction. Figure (3.1) is a schematic representation of the experimental equipment.

### 3.1.2 PUMP AND MEASURING SYSTEM

The pump used in this study was a Moyno 2L10H having a variable speed drive capable of delivering a 190 Imp.Gal./Min. output flow. To prevent the discharge pressure from fluctuating, a surge system consisting of two 10 foot schedule 80 P.V.C. pipes were connected to the discharge line. This limited the output pressure fluctuations to a ±5% deviation.

Flow rates were measured using a 2" Foxboro Magnetic Transmitter in a vertical position and a Model 696 Magnetic to Current Converter. These were recorded using a Beckman Type S-II Dynograph. For recording purposes, the rated 10 to 50 milliamp output signal was

FIGURE(3.1)
SCHEMATIC OF EXPERIMENTAL APPARTUS

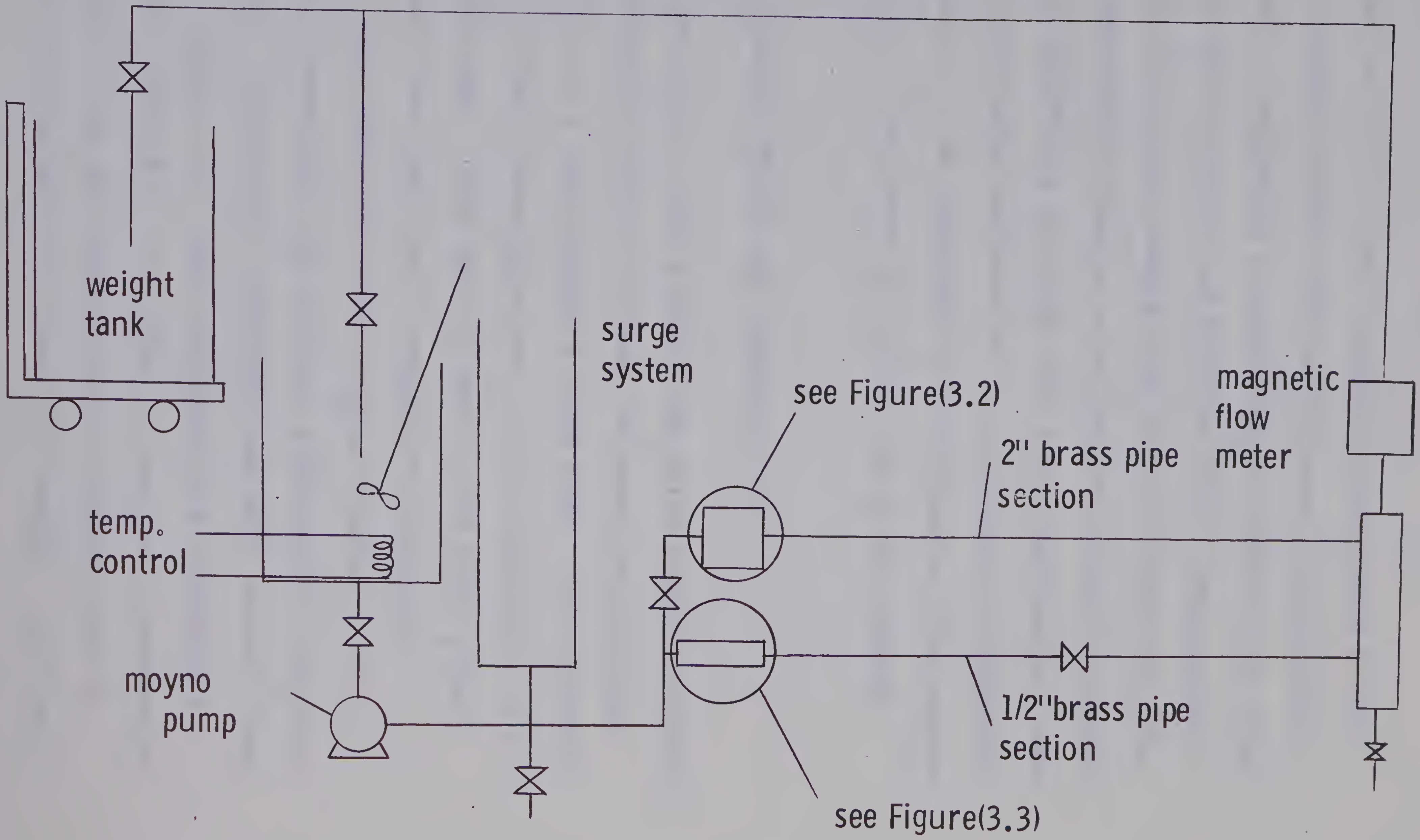
weight tank
temp. control
moyno pump
surge system
see Figure(3.2)
2" brass pipe section
magnetic flow meter
1/2"brass pipe section
see Figure(3.3)

converted to a 1 to 5 volt signal by connecting a 100 ohm, 2% resistor across the output leads. Calibration consisted of employing a weigh tank for small flow rates up to 65 Imp.Gal./Min. and friction factor measurements for high flow rates ranging from 30 to 190 Imp.Gal./Min. These measurements coupled with the well-known Von Karman equation determined the high flow rate calibration. Data for the flow meter calibration are presented in Appendix B, Tables 1-3. As indicated in the Appendix, the maximum deviation in flow rates is within 1½% of the maximum output.

### 3.1.3 ENTRANCE REGION AND PRESSURE TAPS

For the 2" test section the entry region consisted of a contraction from a 12 inch, 18 inch long upstream reservoir to a 2 inch standard brass pipe. The reservoir for the 1/2 inch brass pipe was a 3 foot section of a 3 inch brass pipe. Both the 1/2 and 2 inch brass pipes protruded 1 inch into their respective reservoirs. Figures (3.2) and (3.3) are schematic diagrams of the upstream reservoirs and indicate positions of the pressure taps. In addition, pressure taps were located along the test sections and their positions are tabulated in Appendix A, Table A-1. In order to minimize disturbances formed near or on the pressure taps, the tap holes on the test sections were 1/32 inch in diameter, with each

FIGURE(3.2)
UPSTREAM RESERVIOR - 2" BRASS PIPE

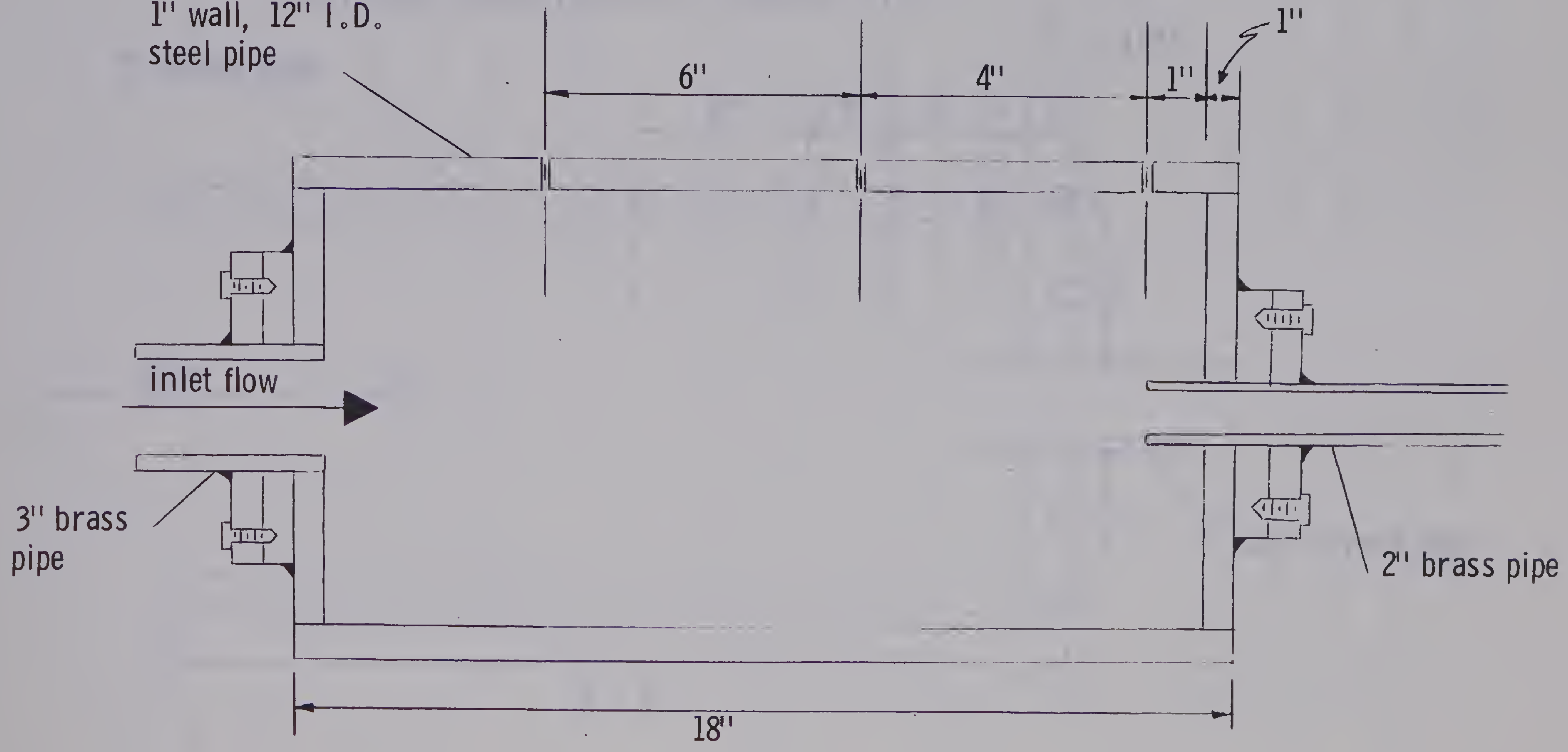
1" wall, 12" I.D.
steel pipe
6"
4"
1"
1"
inlet flow
3" brass
pipe
2" brass pipe
18"

FIGURE(3.3)

UPSTREAM RESERVIOR - 1/2" BRASS PIPE

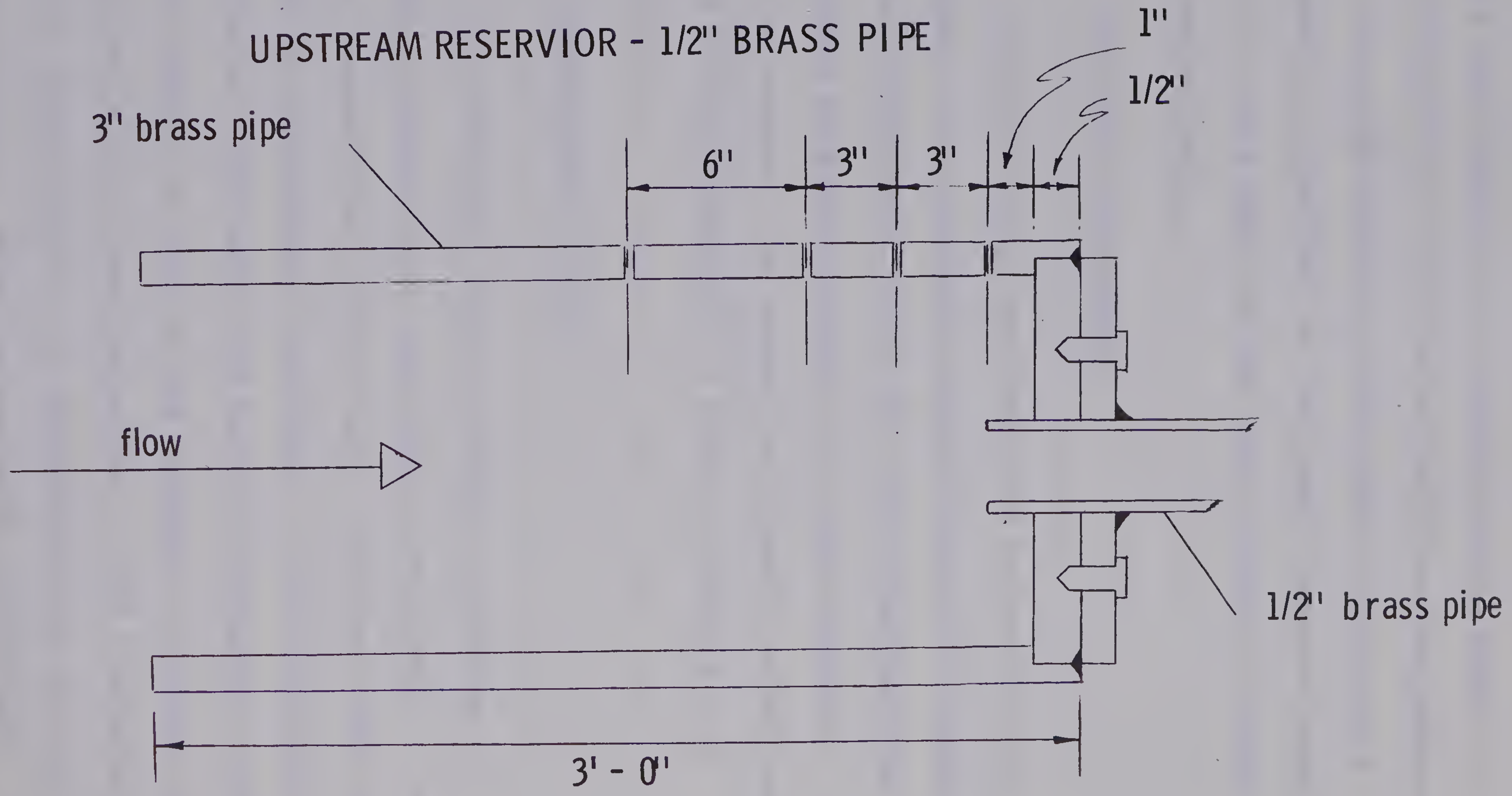
1"
1/2"
3" brass pipe
6"
3"
3"
flow
1/2" brass pipe
3' - 0"

pressure tap connected to a purge line in order to remove trapped air from the tap and from the pressure lines. The pipe diameter calibration in Table A-2 of Appendix A, resulted in the inner diameters being 0.1721 ft. and 0.0521 ft. for the 2" and 1/2" brass pipes respectively.

### 3.1.4 PRESSURE MEASUREMENTS

Pressure drops were measured by two 60 inch manometers. One manometer measured from 0-60 inches of 0-dichlorobenzene, while the other measured from 0-60 inches of water resulted in a more flexible measuring system. The temperature-density relationship for the 0-dichlorobenzene is given in Table A-3 of Appendix A.

### 3.1.5 EXPERIMENTAL FLUIDS

Two Newtonian and two polymer solutions of different concentration were used in this study. Water and two concentrated aqueous sugar solutions were used to test the experimental technique. The viscoelastic solutions of 0.20% and 0.01% having viscosities corresponding roughly to that of the Newtonian solutions were used as the elastic test solutions. This viscoelastic additive, Separan AP-30, is manufactured by the Dow Chemical Company. When the partially hydrolized

polyacrylamide (molecular weight of $3 \times 10^6$) is dissolved in water the resulting solution usually has a time stability: that is, resistant to significant degradation after an initial amount of degradation. This degradation is believed to stem from a partial or complete breakdown of the inter or intra molecular forces or a combination of these. However, the 0.01% solution indicated a complete degradation for shear rates exceeding $10^5$ $\sec^{-1}$. This degradation or decrease in drag reduction was found to be irreversible and similar in magnitude to effects noted by Savins (65) with soap solutions that were drag reducing.

### 3.1.6 RHEOLOGICAL PROPERTIES

Assumed elastic and viscous properties of the experimental fluids were estimated from data available in the literature (57,66) and have been reproduced in Appendix C.

## 3.2 PROCEDURE

### 3.2.1 PREPARATION OF POLYMER SOLUTION

Owing to degradation of the solutions it is important that each solution being tested is treated in a similar manner and the following procedure for dissolving the solute was adhered to. The solute was added to the tank filled to a height of 3 feet of tap water, and stirred with an agitator for a period of several hours. Coupled with this, the pump was running at a moderate speed and continued to do so for six hours. Afterwards, the solution was left unsheared for the remainder of the day and night.

The above procedure did degrade the solutions to a small extent however, significant, partially irreversible, drag reduction loss for the 0.01% solution occurred at high shear rates in the 1/2" pipe. This phenomena occurred even after only minutes of taking data. Others (66) have noted that the same solution remained stable to further shearing for several days.

### 3.2.2 DATA COLLECTION

In order to minimize degradation pressure readings were taken in the order of the 2 and 1/2 inch pipes respectively and after every few runs retakes were done to check if significant degradation had occurred. In

the case of the 0.2% solution the reruns checked within experimental error except for the 0.01% solution where irreversible, non-controllable degradation occurred over a short, continuous experimental period at high shear rates. To investigate this phenomena, experimental runs were made from the low to high shear rates and the reverse employing a fresh solution at each start. The results yielded two different friction factor-Reynolds number curves over the same range of Reynolds numbers. These effects are discussed in more detail in Chapter IV.

# CHAPTER IV

# DISCUSSION OF RESULTS

## 4.1 NEWTONIAN ANALYSIS

To test the validity of the experimental technique Newtonian fluids were used in both laminar and turbulent flow. As illustrated in Figure (4.1) the friction factor-Reynolds number correlations for fully-developed laminar and turbulent flow in a smooth pipe correspond, within experimental error, to the theoretical values. The maximum absolute deviation for the experimental runs were within 5%. The results for laminar flow given in detail in Table (A-2) of Appendix A, were used for the determination of the pipe diameters. In the entrance region, only four pressure profiles for laminar flow were obtained due to the inability to measure the very small pressure drops. These as well as the turbulent pressure profiles were used to confirm the empirical laminar and turbulent contraction losses and entry length correlations.

The laminar flow equation (1.2.4) as shown on Figure (4.2) yields a straight line with a slope of 32.0 and an intercept equal to 1.22. This intercept compares favorably with the values of 1.16 and 1.23 obtained by Bogue (13) and La Nieve (56) respectively, for flow in capillary tubes.

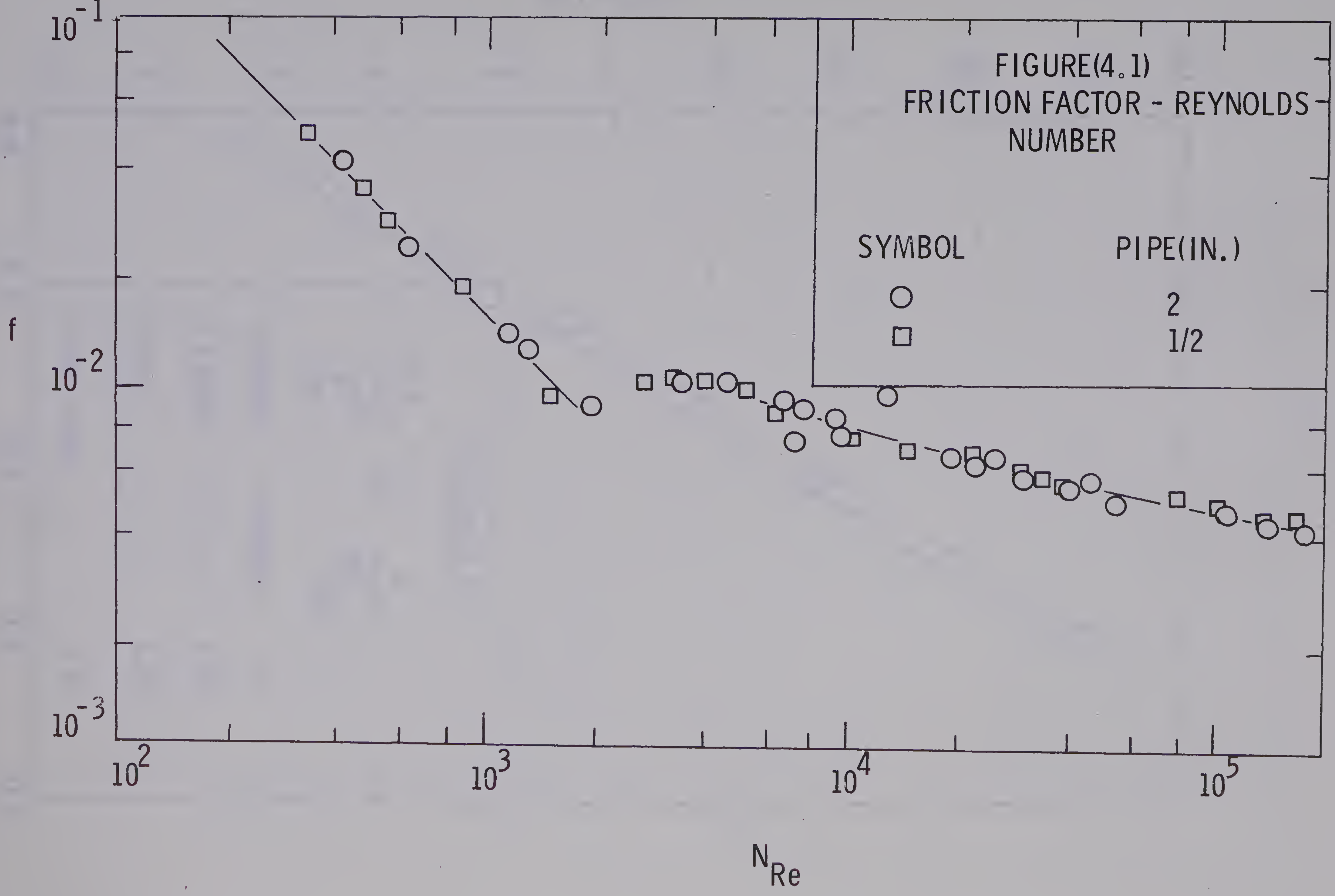
FIGURE(4.1)
FRICTION FACTOR - REYNOLDS
NUMBER

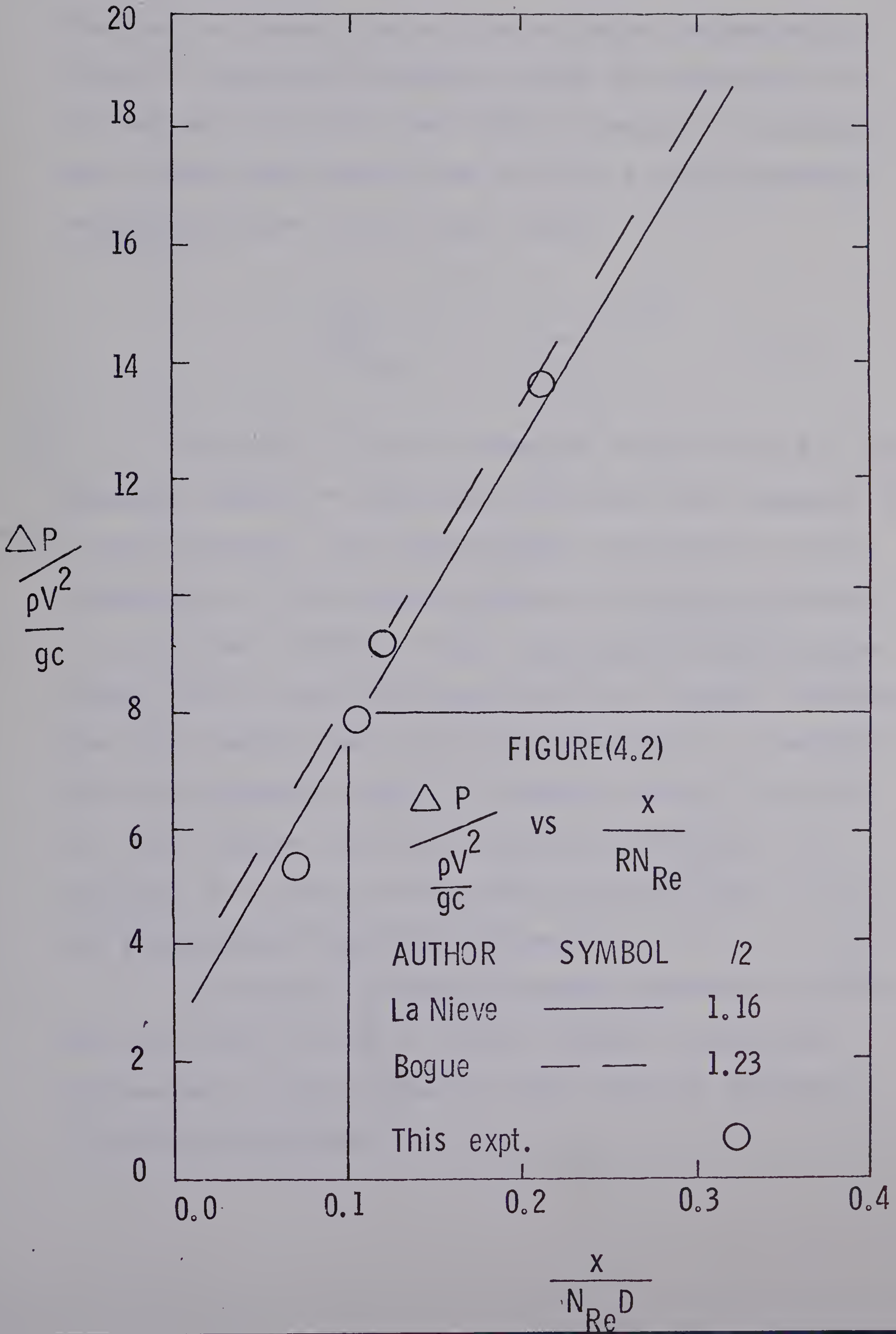

FIGURE(4.2)

$\frac{\Delta P}{\rho V^2 / gc}$ vs $\frac{x}{RN_{Re}}$

As noted and developed in the previous chapters the relationship between the dimensionless contraction loss can in general, be written as below for Newtonian fluids. Dimensional analysis yields no indications as to whether or not the flow field is laminar or turbulent. As a result, the form of the function A will presumably be different for the two flow fields.

$$\frac{\Delta P_c}{\rho V^2/g_c} = A\left(\frac{1}{N_{Re}}\right) \qquad (4.1.1)$$

Astarita (6) and La Nieve(56) suggest that for high Reynolds numbers in tubes with or without the presence of a vena contracta, the dimensionless contraction loss is independent of the Reynolds number and remains constant. In particular, Astarita found that the critical Reynolds number was 146 with the proportionality constant depending upon the diameter ratio of the contraction, $\beta$. Assuming that this argument holds for turbulent flow, a plot of log $(\Delta P_c)$ versus log (V) as indicated on Figure (4.3) resulted in a linear relationship having a slope of 2.0 but possessing a variable intercept.

In Figure (4.3) there is little discrepancy between data from the 1/2" and 2" tubes, however, substantial differences in the contraction loss occur as different fluids are considered.

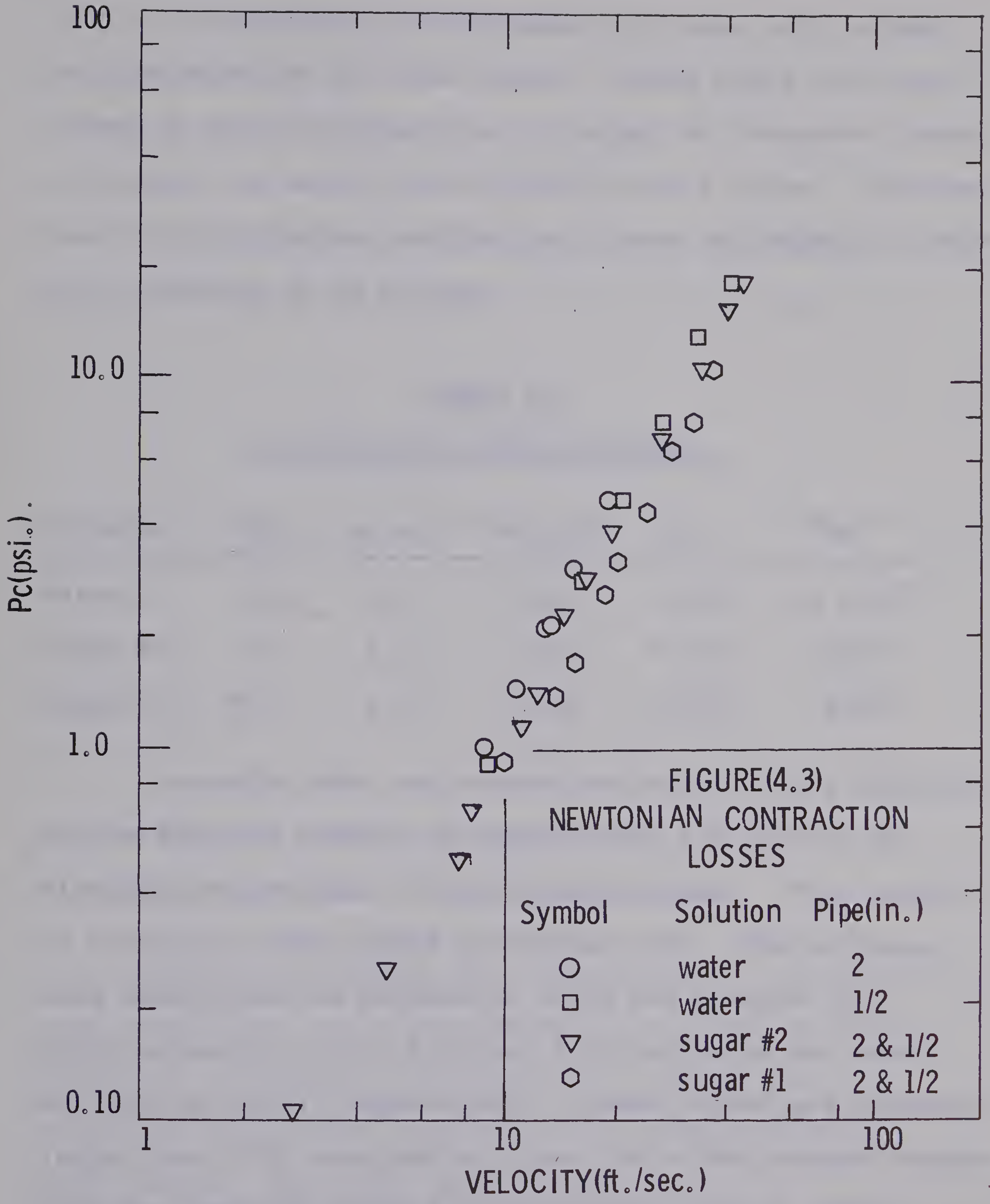

FIGURE(4.3) NEWTONIAN CONTRACTION LOSSES

If the density differences are taken into account the discrepancies are even larger. These facts are illustrated on Table (4.1) where the intercept or Hagenbach factor $\phi$ is given for each of the fluids in the 2" pipe. Included also in the table are contraction losses and Reynolds number for a velocity of 10 ft./sec.

TABLE 4.1

VARIATION OF HAGENBACH FACTOR

| Solution | $\mu$(cp) | Sp.Gr. | $\Delta P_c$(psi) | $\phi/2$ | $N_{Re}$ |
|---|---|---|---|---|---|
| Water | 1.0 | 1.0 | 1.25 | 1.068 | $1.6 \times 10^5$ |
| Sugar #2 | 7.0 | 1.15 | 1.00 | 0.920 | 26200 |
| Sugar #1 | 46.5 | 1.27 | 0.80 | 0.830 | 4360 |

Assuming that the correction factor $\phi$ is a function of the Reynolds number, it appears from the data to be directly proportional to the Reynolds number. This result is similar to that formed by Drexler (28). The entrance loss coefficient as defined by Olson and Sparrow (59) yield values of 1.136, 0.84 and 0.66 for water and sugar solution #2 and #1 respectively. These values are slightly larger than 0.55 obtained by Olson for a sharp-edged contraction for Reynolds numbers ranging from 16000 to 70000.

The measured entry length in turbulent flow for any experimental run was less than 17 diameters. Latzko's theoretical analysis reproduced below was developed for

induced turbulence.

$$\frac{L_e}{D} = 0.693\ N_{Re}^{\ 1/4} \qquad (4.1.2)$$

The results of this study are in reasonable agreement with this formula as indicated by Table (4.2).

TABLE 4.2

TURBULENT ENTRY LENGTH

| Reynolds Number | Theoretical ($L_e$) | Experiment ($L_e$) |
|---|---|---|
| 5230 | 8.5 | 7.30 |
| 37500 | 9.6 | 13.40 |
| $4.7 \times 10^5$ | 10.20 | 5.76 |
| $2.1 \times 10^5$ | 14.80 | 4.00 |

## 4.2 ANALYSIS FOR VISCOELASTIC FLUIDS

### 4.2.1 DRAG REDUCTION AND UNUSUAL EFFECTS

Before proceeding to a discussion of entry lengths and contraction loss measurements for the drag reducing material, a discussion concerning the method used in interpreting the data as well as the unusual behavior under certain flow conditions is discussed.

In determining the friction factor as well as the shear stress at the wall for each experimental run, it was assumed that the pressure loss measured over the

last two pressure taps represents the developed pressure loss. Based on this, the friction factor-Reynolds number data for each of the solutions are presented on Figures (4.4) and (4.5). The relationships as well as indicating considerable drag reduction present unusual effects that in the past have not been noticed or have not been clearly defined. One of the interesting properties depicted on Figure (4.4) is that the data from the larger pipe separate from the Newtonian curve at a lower Reynolds number. Savins (65) and Seyer (66) have noted this phenomena but no explanation is available at this time. Also, it is clear that beyond a certain Reynolds number the friction factors for the concentrated solution in the 2" pipe as shown on Figure (4.4) have a large amount of scatter relative to the other data. A more detailed analysis concerning this phenomena will be presented later in this section.

As the Reynolds number increases, it is noticed that the data tend to become parallel to the curve for Newtonian fluids. This may indicate that the flow is approaching fully-developed turbulent flow (68) in the sense of an intermittancy factor approaching unity. The intermittancy represents the percentage of time that the flow is turbulent for some given position downstream of the entrance. The only deviation from this approach to a parallel relationship is best exhibited by Figure (4.5)

FIGURE(4.4)

FRICTION FACTOR - REYNOLDS NUMBER 0.20% SOLUTION

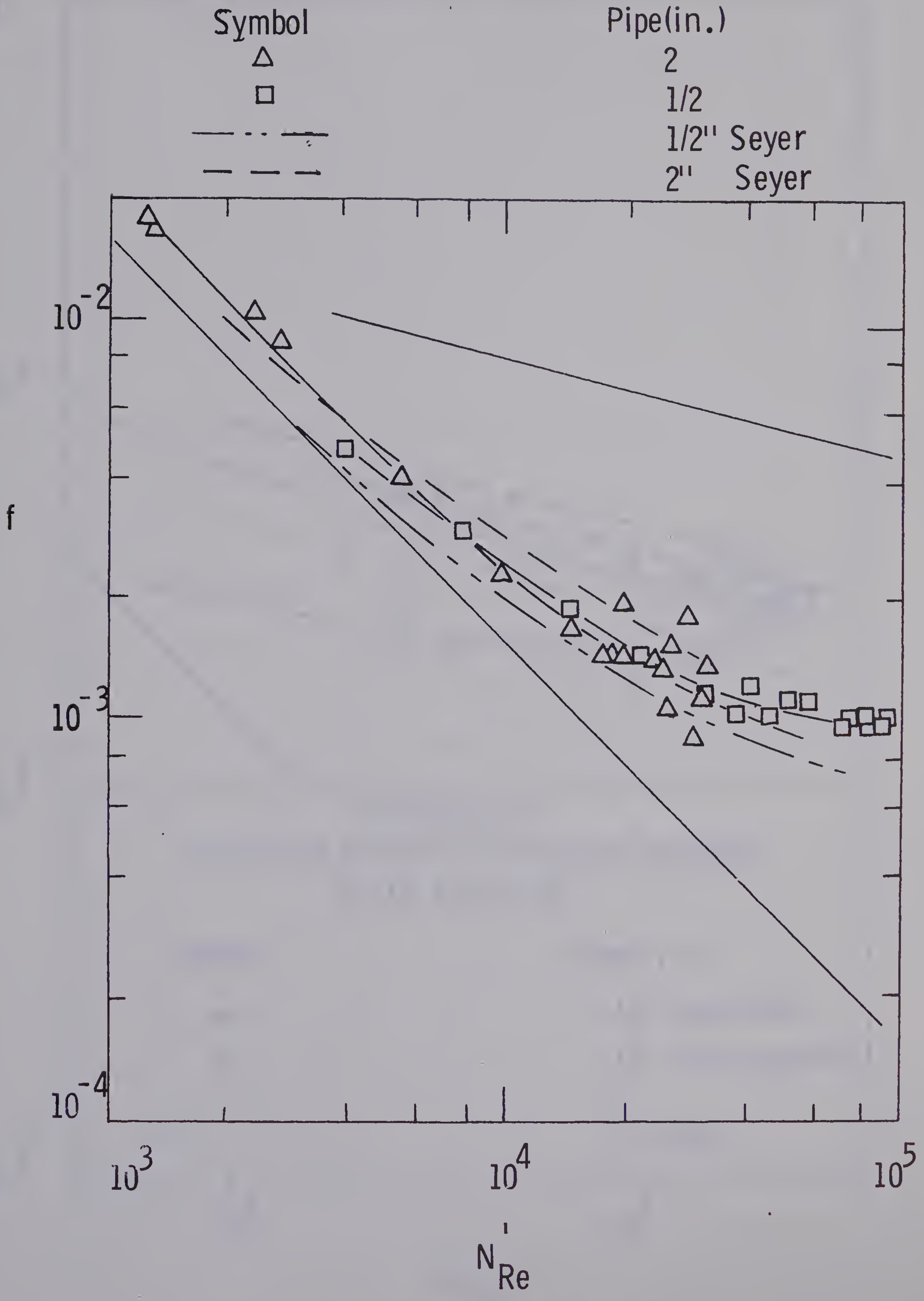

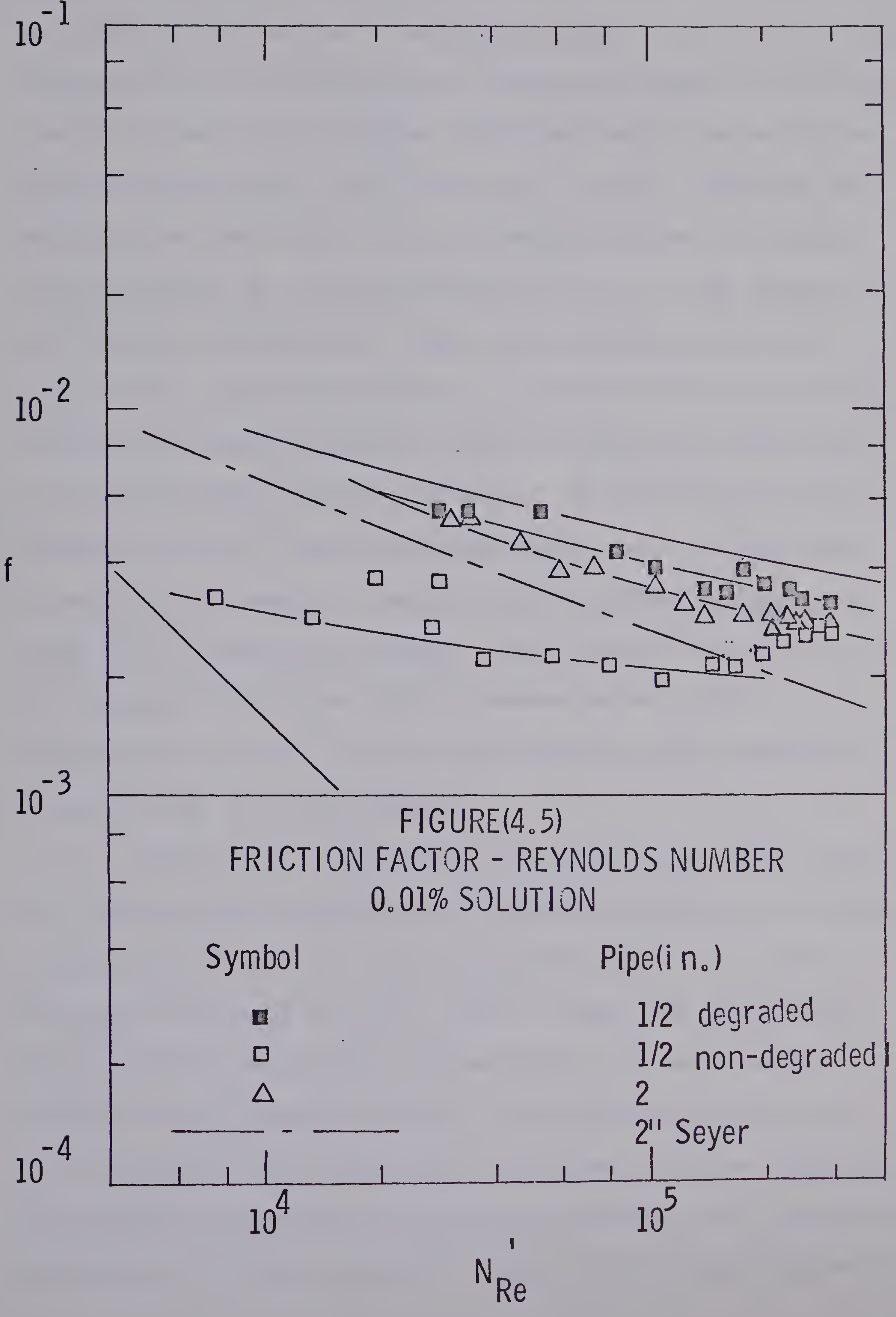

FIGURE(4.5)
FRICTION FACTOR - REYNOLDS NUMBER
0.01% SOLUTION

where the 0.01% solution undergoes a significant amount of degradation beyond a Reynolds number of $2 \times 10^5$. This degradation is reflected by a sharp decrease in the drag reduction and the decrease continues until the solution behaves essentially as a Newtonian fluid. Although the degradation was found to be irreversible over a period corresponding to the experimental runs, it was found to be slightly recoverable after the solution had been stored for a prolonged period. Savins (65) noticed this effect with soap solutions but no mention has been made concerning drag reducing systems. To comprehend this unusual effect, fresh solutions were made and data was taken in the order of low to high Reynolds numbers and high to low Reynolds numbers. The results gave rise to two distinct friction factor curves whose effects are discussed relative to the entry lengths and contraction losses later in this chapter.

To further illustrate the effects of drag reduction and significant degradation reference is made to Figures (4.6) and (4.7). As indicated by the data the 0.20% solution for both the 1/2" and 2" pipes was the better drag-reducing solution. In addition, it is clearly seen that for the two fresh 0.01% solutions used in the 1/2" pipe the drag reduction of 55% and 13% for the non-degradated and degradated solutions result in a significant distinction in the pressure losses. The highly degraded

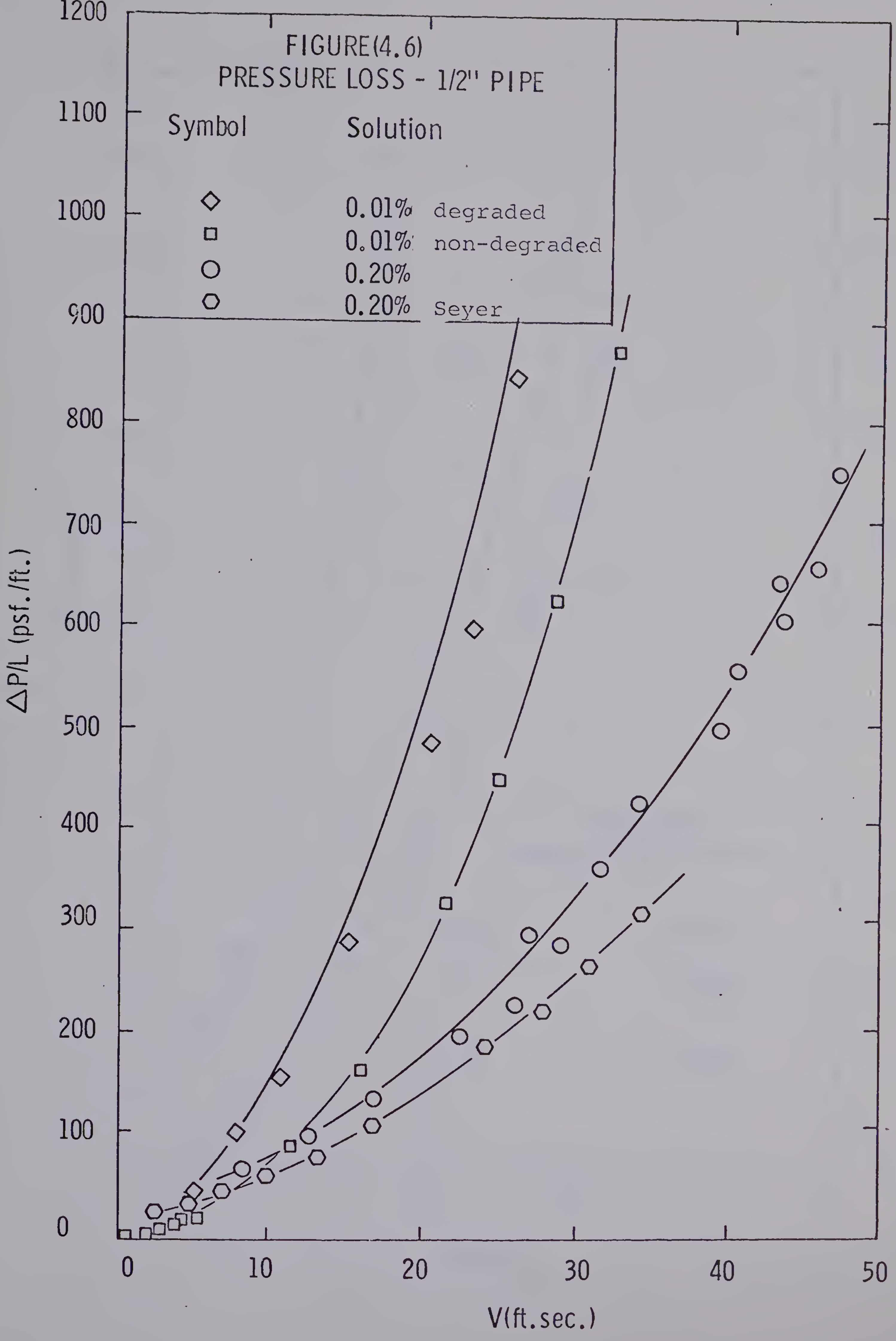
FIGURE(4.6)
PRESSURE LOSS - 1/2" PIPE

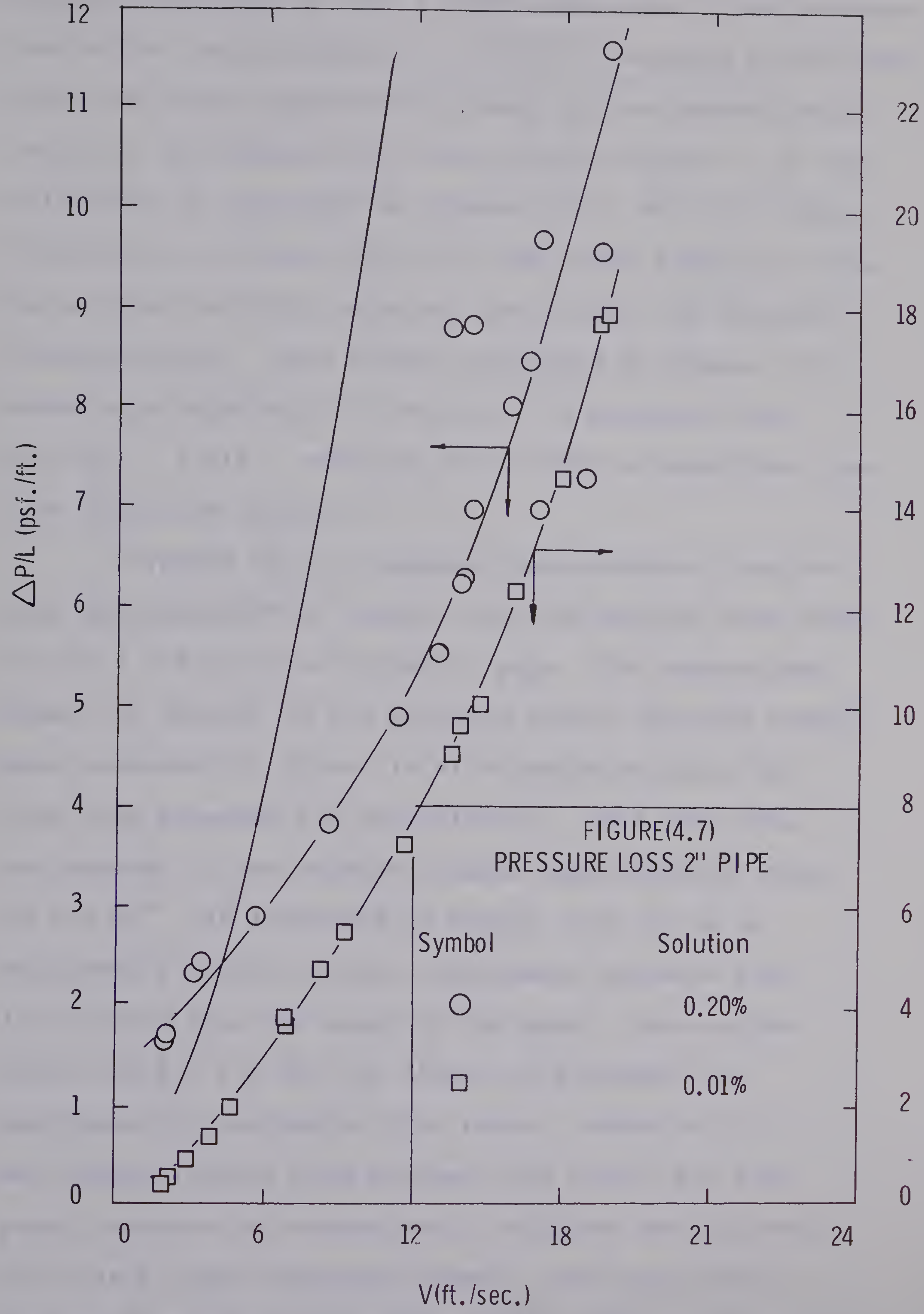

FIGURE(4.7)
PRESSURE LOSS 2" PIPE

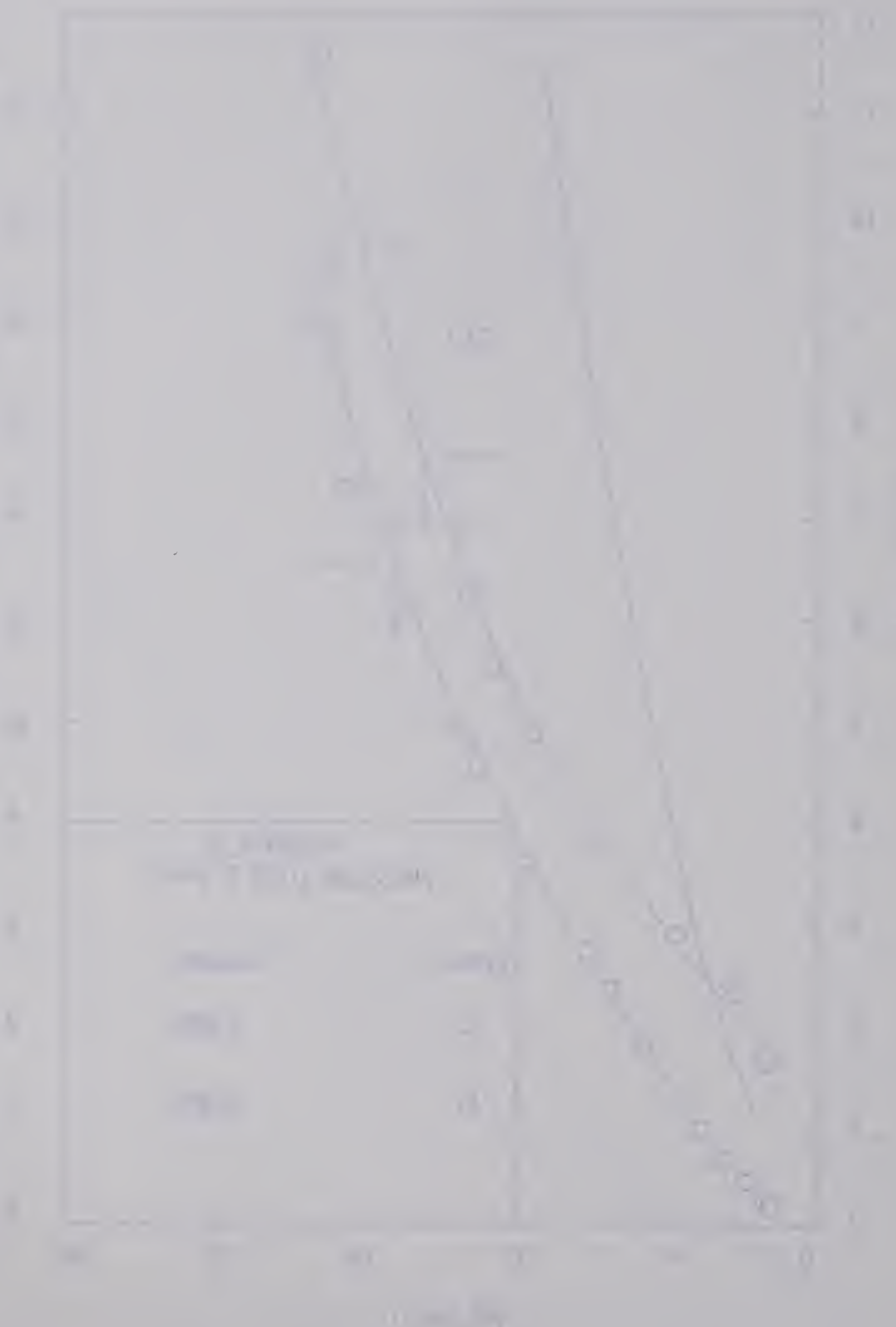

solution resulted in only a slight decrease in the pressure loss while the non-degraded solution resulted in the pressure loss being approximately equal to the percent drag reduction as measured from the friction factors. At low velocities as indicated on Figures (4.6) and (4.7) drag reduction is reversed: that is, the 0.01% solution is the better drag reducing solution, due in part to viscosity considerations. This is best displayed by Figure (4.6) where at a velocity of 5 ft./sec. the pressure loss for the 0.01% solution is an order of magnitude less than the 0.20% solution.

Typical data of pressure measurements along the pipe are presented in Figure (4.8) for several flow rates of the 0.20% solution in the 2" pipe. The unaccounted amount of scatter in the friction factor Reynolds number data presented in Figure (4.4) occurred whenever the flow rate exceeded 120 Imp.Gal./Min. This flow rate corresponds to the Reynolds number approximately equal to $2 \times 10^4$. As indicated on Figure (4.8) it is at this same flow rate where a noticeable pressure rise is obtained near the entry of the pipe. The maximum occurs at $\frac{L}{D} \simeq 8.0$ for all flows and increases in magnitude for increasing flow rates. Astarita (6) and others (28,59) have noticed this effect for both purely viscous and viscoelastic solutions and referred to it as a "vena contracta effect". For the case of laminar flow of viscoelastic solutions Metzner, White

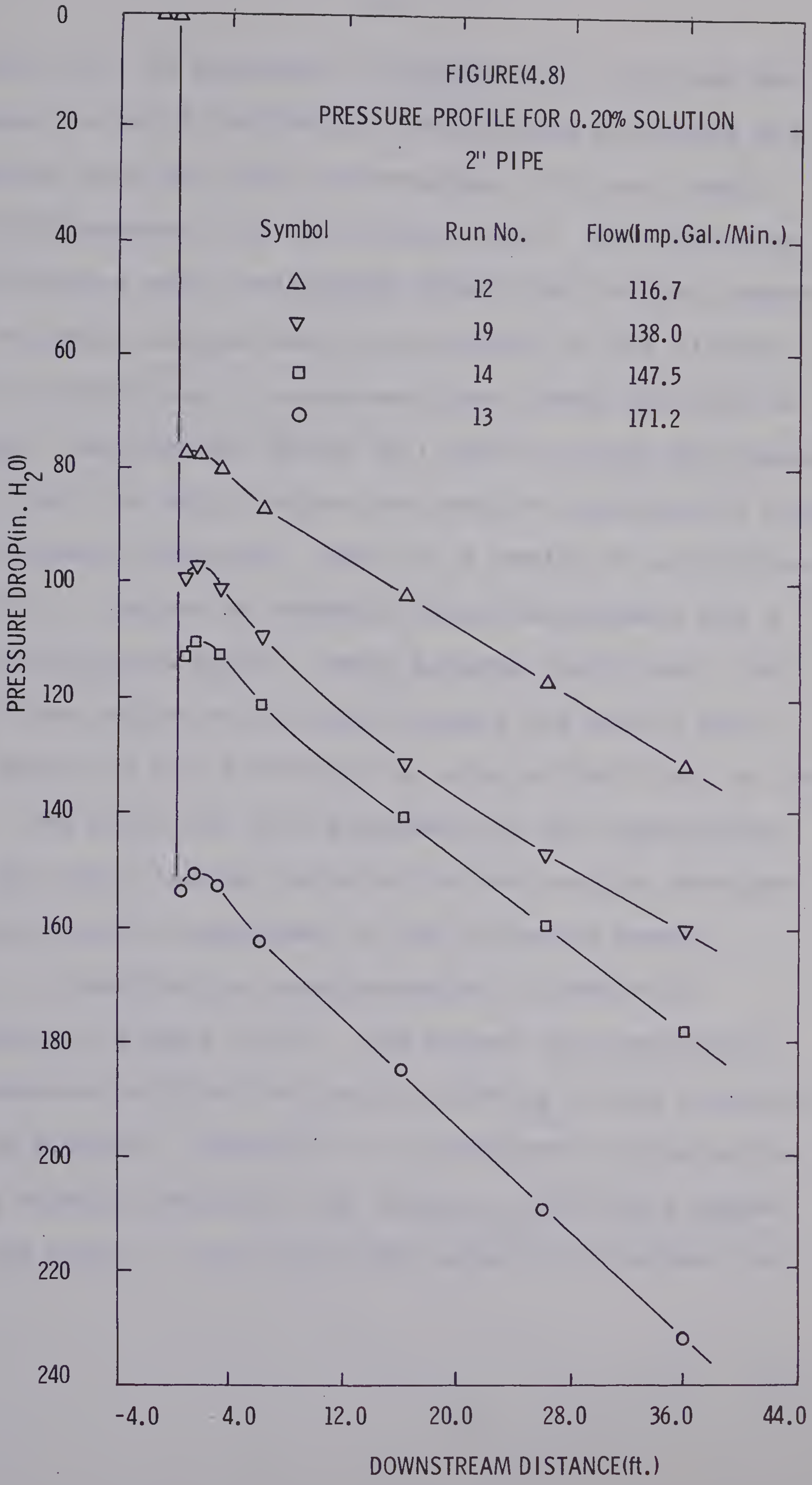

FIGURE(4.8)

PRESSURE PROFILE FOR 0.20% SOLUTION

2" PIPE

and Denn (51) as discussed in Chapter II, show that the stresses in rapid deformation, short-time processes are dependent upon the total deformation. In this limit, the fluid behaves like an elastic solid. For Newtonian fluids having small relaxation times, the Deborah number will be small and the solid-like region in the vicinity of the contraction of cross-sectional areas will not be present. Metzner and White (47) show at least for laminar flow, that the entry region can thus be conceived of having three distinct regions: that is, a region of solid-like behavior, a region of boundary layer development and a fully-developed region. Under extreme conditions, the solid-like region could extend across the entire duct thus requiring fluid fracture or slip of the fluid at the wall. The effect of this phenomena on the contraction loss and entry lengths relative to the results obtained in this study is explained in the following manner.

A qualitative interpretation is made with reference to Figure (4.9). The dotted line represents the pressure profile that would exist if a vena contracta was not present. However, the viscoelastic solution due to its elastic behavior, may create a solid-like region near the entry. This solid-like behavior in effect is

FIGURE(4.9)
VENA CONTRACTA EFFECT

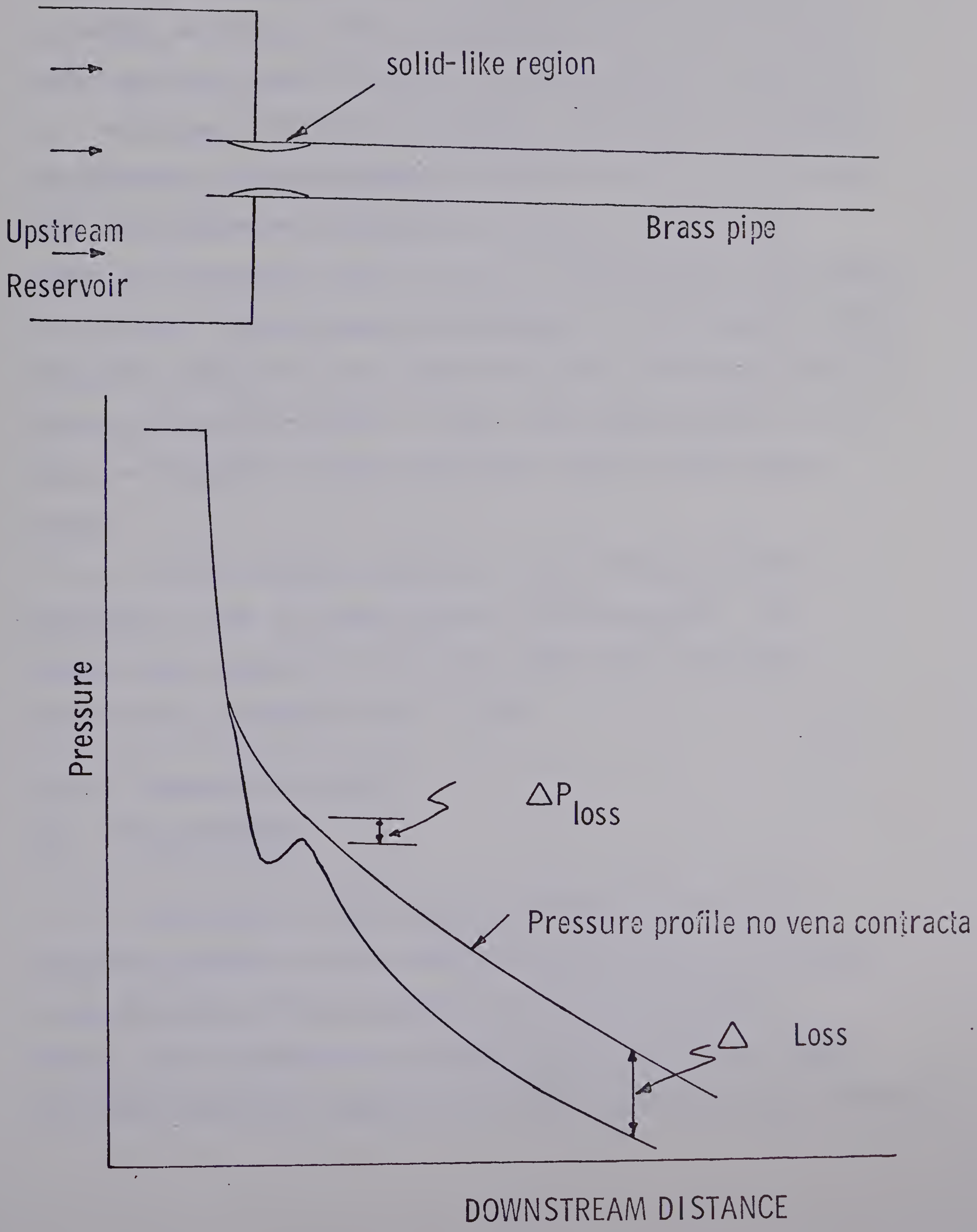
solid-like region
Upstream
Reservoir
Brass pipe
Pressure
ΔP loss
Pressure profile no vena contracta
Δ Loss
DOWNSTREAM DISTANCE

equivalent to a reduction of the total cross-sectional area which according to Bernoulli's equation causes the fluids velocity to increase. This in turn causes the pressure to reduce as shown. Once the fluid is beyond the reduced cross-sectional area it begins to deccelerate thus partially regaining its initial pressure. In this area however, the process is not completely reversible and an extra pressure loss occurs as indicated by $\Delta P_{LOSS}$. Beyond this region the generally lower level of acceleration experienced by the fluid allows normal development of the boundary layer since the response of the fluid would be essentially that of a purely viscous material. Thus, the overall effect is to cause an increase in the contraction loss by the amount $\Delta_{LOSS}$.

In this study, the only "vena contracta effect" noted was in the 2" pipe with the 0.20% solution. No effects were measured in the 1/2" pipe with the first pressure tap located at L/D = 5.60.

### 4.2.2 CONTRACTION LOSSES

#### (i) MEASUREMENT

The question arises as to whether or not the recorded pressure at the reservoir just above the entrance is in fact the actual pressure at the pipe entrance. Uebler (77) and Astarita (6) indicate that although there is a small pressure change due to the height and recirculation

the effect is negligible relative to the overall pressure contraction loss. Also, due to the unusual pressure curves obtained it is necessary to indicate how the entry lengths and contraction losses were determined. In addition to the solid-like behavior, pressure curves as shown on Figure (4.10) indicate that fully-developed flow was not achieved anywhere in the test section.

Figure (4.11) indicates qualitatively how the entry length and contraction losses were measured for both cases. Although curve 1 indicates the presence of a vena contracta at some point downstream the pressure loss becomes equal to that of a fully-developed flow field. Extrapolating this constant pressure loss per linear foot back to zero distance downstream, a contraction loss can be measured as ($\Delta P_c$). At the point downstream where the extrapolated line separates from the pressure profile, the distance measured is referred to as the entry length ($L_e$). For curve 2, fully-developed flow was not achieved within the test section. In this case, the contraction loss was determined by drawing a straight line connecting the two lowest pressure points and extrapolating to zero distance downstream where $(\Delta P)_2$ is measured. To determine the entry length, the assumed developed pressure loss over the later portion of the pipe's pressure profile was extrapolated to beyond a point where it separated from the pressure profile.

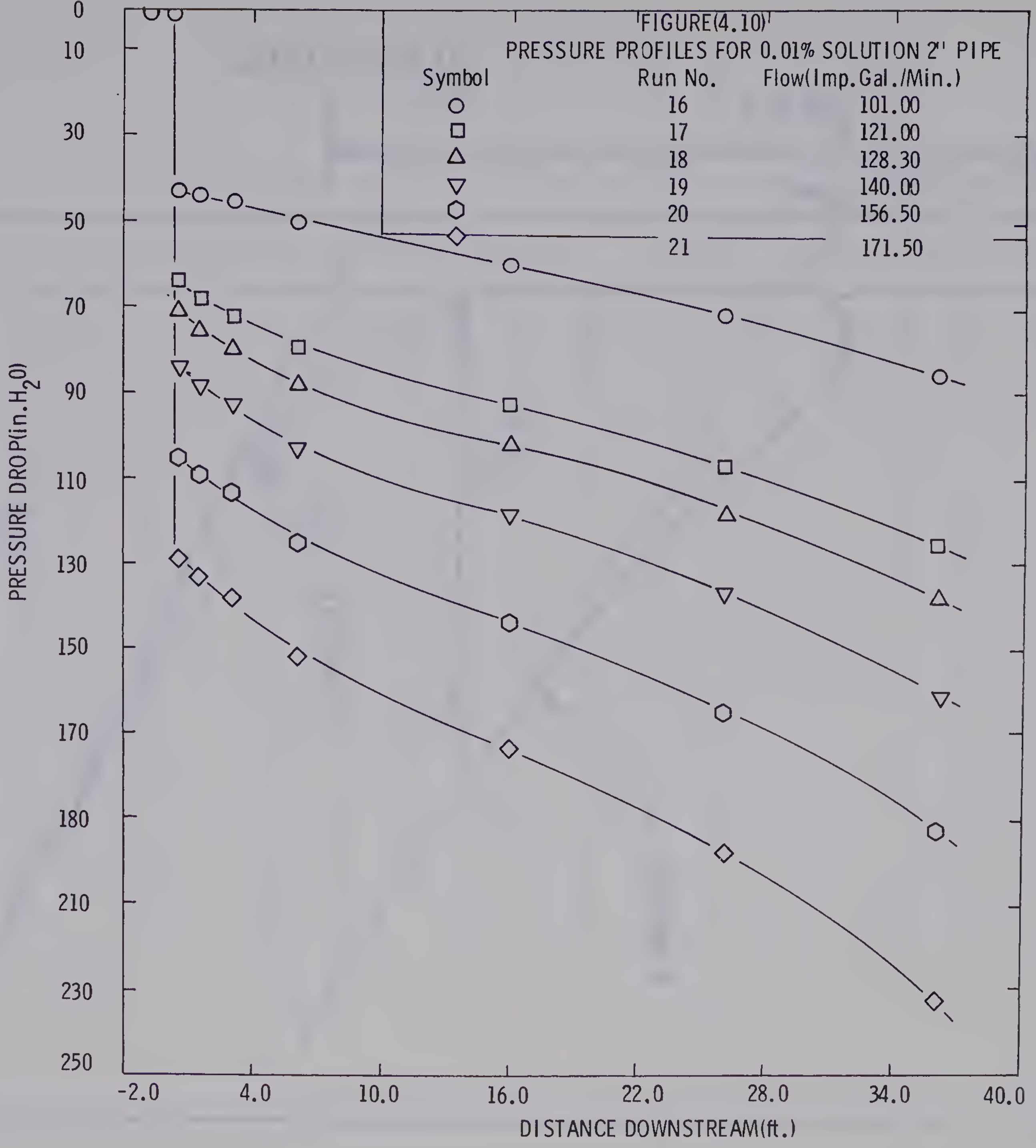

FIGURE(4.10)

PRESSURE PROFILES FOR 0.01% SOLUTION 2" PIPE

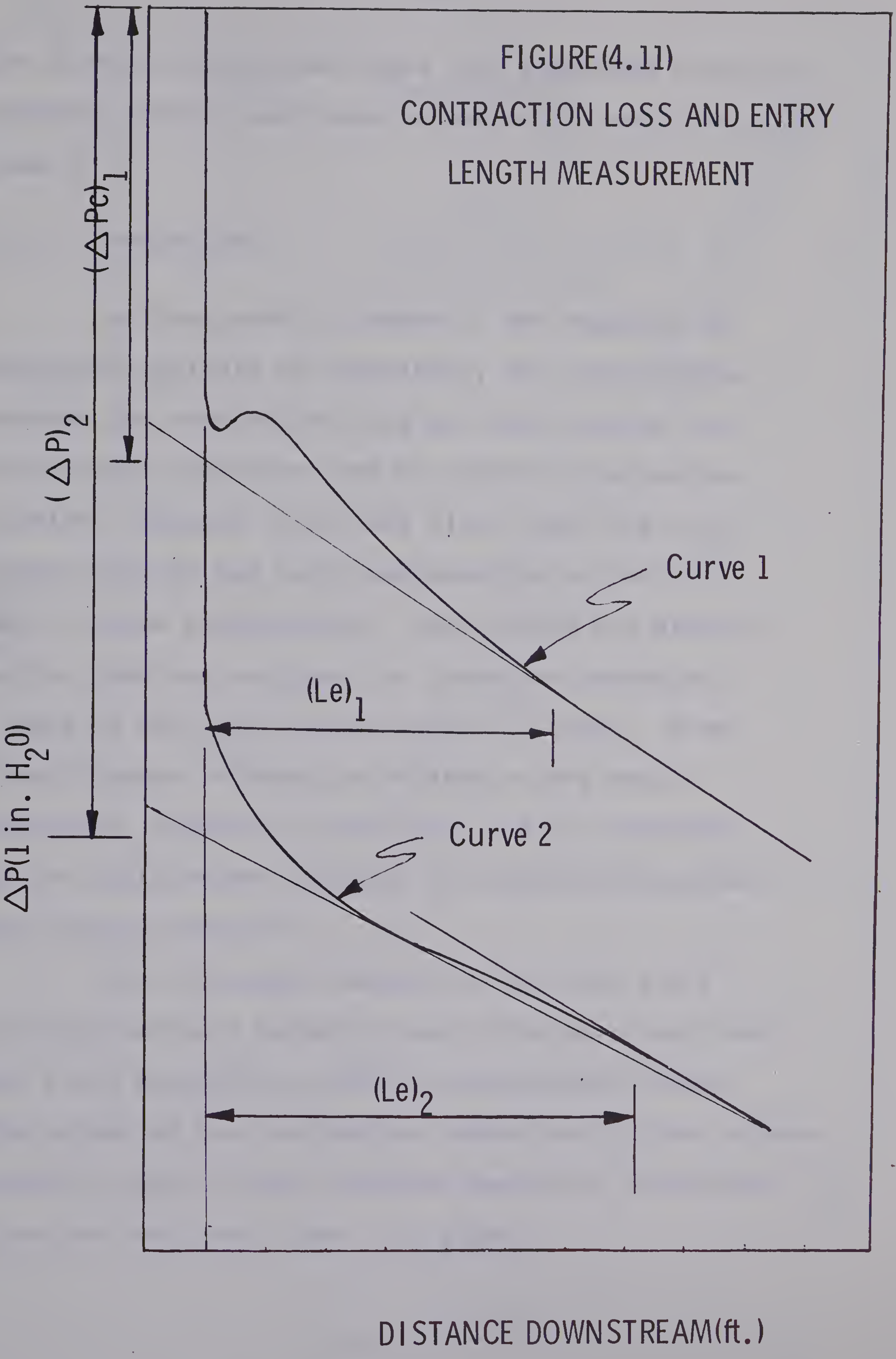

FIGURE(4.11)
CONTRACTION LOSS AND ENTRY LENGTH MEASUREMENT

The distance downstream where this separated from the pressure profile was taken as the entry length $(L_e)_2$ for case 2.

## (ii) CORRELATIONS

As developed in Chapter I and employed in Newtonian analysis of turbulence, the relationship between the contraction loss and the velocity for viscoelastic solutions can be plotted in a similar fashion. Figures (4.12) and (4.13) plot log $(\Delta P_c)$ versus log $(\dot{V})$ for each concentration in the 1/2" and 2" pipes respectively. The results are similar to the previous analyses for turbulent Newtonian fluids in that each relationship is linear. From these figures information related to the vena-contracta, degree of elasticity, and the magnitude of the contractions relative to turbulent Newtonian data can be analyzed.

One noticeable feature is that the 0.01% solution having a normal stress difference less than the 0.20% solution has smaller contraction losses. The values of the contraction losses are in fact approximately equal to the turbulent Newtonian contraction loss for both the 2" and 1/2" pipes.

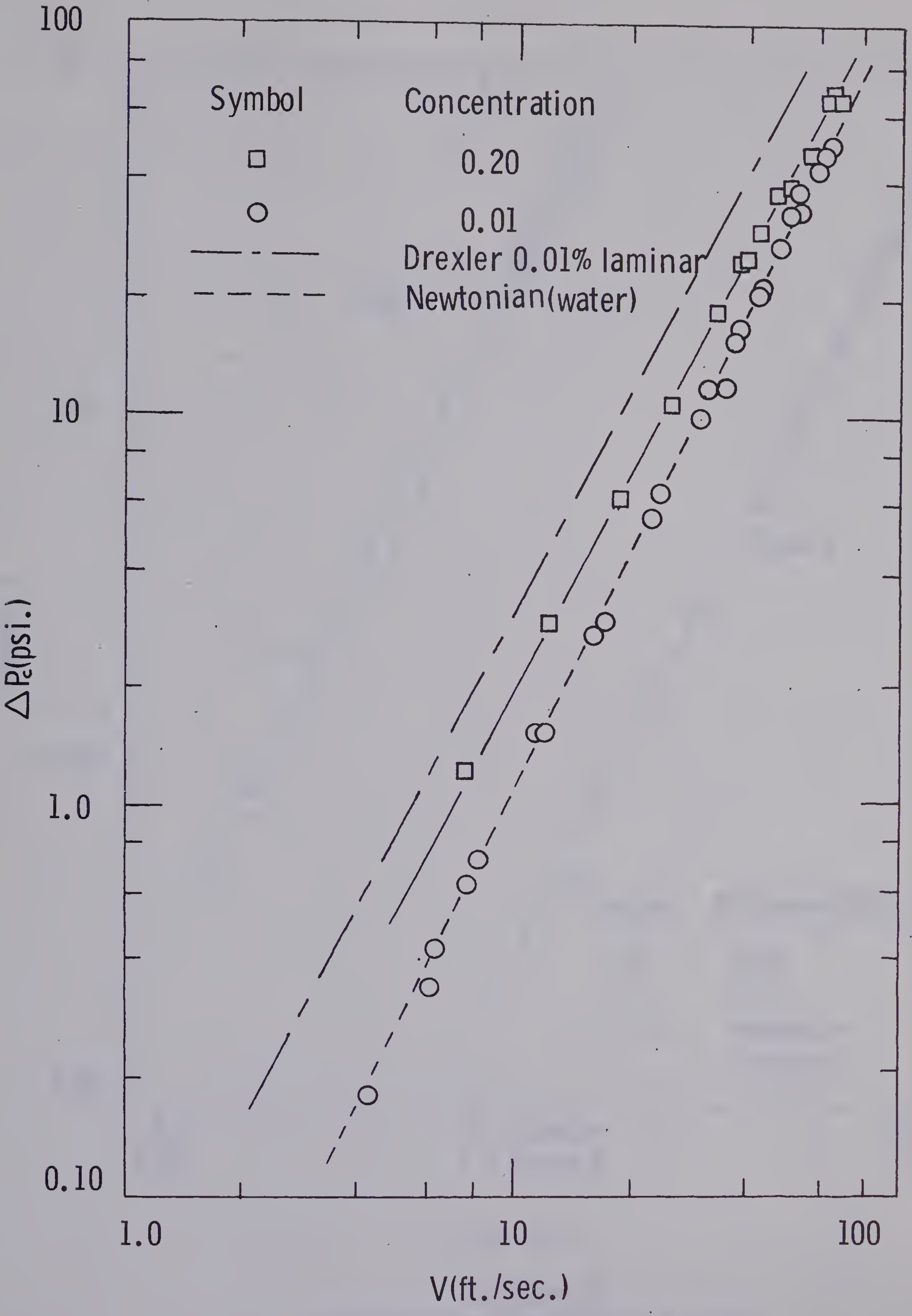

FIGURE(4.12)
CONTRACTION LOSSES FOR 1/2" PIPE

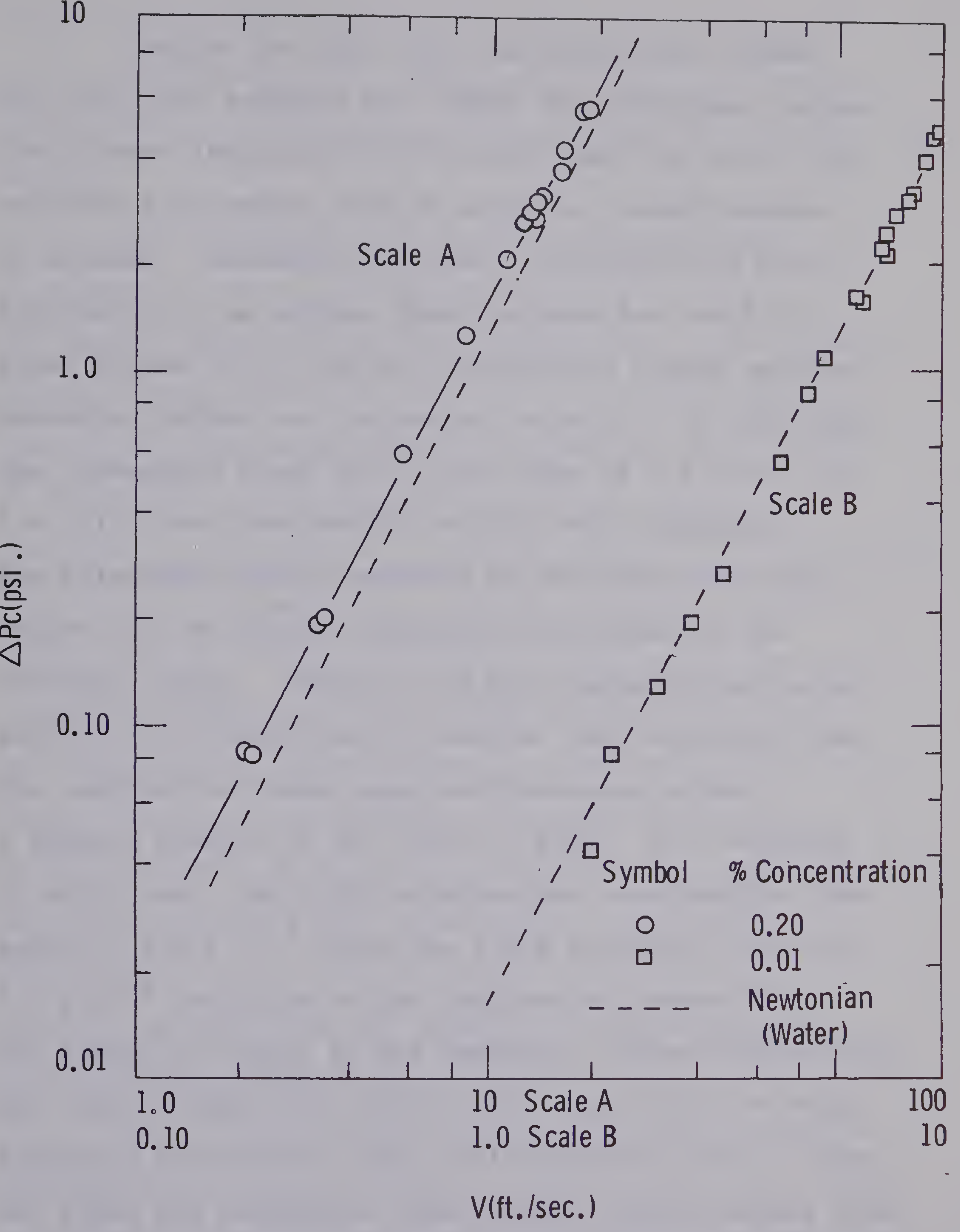

FIGURE(4.13)
CONTRACTION LOSSES FOR 2" PIPE

Despite the fact that the contraction losses for the 0.20% solution are larger than Newtonian values, the Figures indicate that they are less than the 0.01% solution for laminar flow in capillary tubes obtained by Drexler. Although not clearly indicated for the 2" pipe data, it is obvious from the data for the 1/2" pipe, Figure (4.12) that the contraction losses approach Newtonian values for increasing velocity. In this case, the relaxation times are in the order of 6.0 x $10^{-3}$ to 1.6 x $10^{-4}$ sec. decreasing as flow rate increases. The relaxation times, measured in the fully-developed region, may be indeed different from values in the entrance region. However, the data suggests that under similar flow conditions the smaller the relaxation time the contraction losses approach Newtonian values. A typical example is for the 1/2" pipe. At a velocity of 60 ft./sec. the 0.20% solution has a relaxation time equal to 1.6 x $10^{-4}$ while the 0.01% solutions value is 3.0 x $10^{-5}$ resulting in the contraction losses being 30% larger and equal to the Newtonian values respectively. One cannot extend this result for a particular solution. Examining the data for the 0.01% solution in the 2" pipe, one finds the relaxation times having values ranging from 1.0 x $10^{-3}$ to 3.0 x $10^{-5}$ sec. yet have contraction losses similar to Newtonian values. It would thus appear that in general, the additive effects of smaller relaxation

times and Bernoulli effect which increases as the flow rates increase cause the contraction losses for viscoelastic fluids to approach or become equal to Newtonian values.

For some flows, unusual vena contracta and significant degradation effects occurred. It was previously indicated that the presence of a vena contracta would increase the contraction loss. Although only at a flow rate beyond approximately 120 Imp.Gal./Min. or 13.5 ft./sec. was there any recorded effects, Figure (4.13) indicates that there is no sudden change in the contraction loss-velocity correlation. If the vena contracta effects commenced at this flow rate then a noticeable shift in the contraction loss correlation should prevail. As this was not the case, it was assumed that it existed closer to the entry and progressively moved downstream as the flow rate increased. Extra pressure taps closer to the entry are required to confirm this conclusion. The significant degradation for the 0.01% solution in the 1/2" pipe resulted in no measured difference to the contraction loss as indicated by Figure (4.12).

Since the solutions studied had weak to strong viscoelastic characteristics it seems probable that other viscoelastic solutions such as C.M.C. will have contraction losses lying within the results of this study under similar flow and geometrical conditions. Considering the 0.20%

solution at a velocity of 10 ft./sec. the data indicates that there exists a 23% and 74% increase in the contraction losses for the 2" and 1/2" pipes respectively. The elastic effects thus create a diameter dependence not previously noted for flow of Newtonian fluids. This diameter dependence is caused by the effect of elasticity being more pronounced for smaller diameter pipes. Also, this has been measured (66) in terms of drag reduction by noting that the friction factors decrease for decreasing diameters.

### 4.2.3 ENTRY LENGTHS

At the beginning of this chapter in Section 4.2.2 it was suggested that fully-developed flow was not achieved for certain flow rates for the 0.01% solution in the 2" pipe. Despite this, the contraction losses and entry lengths as discussed in more detail in section (4.2.2) can be estimated. The measured entry lengths are shown on Figure (4.14) and (4.15) and range from 20 to 180 diameters as the Reynolds number is increased. For this particular solution, drag reduction commenced at a Reynolds number approximately equal to $10^4$ and continued up to a maximum Reynolds number of $2.9 \times 10^5$.

As previously mentioned, entry lengths in the same order of magnitude as those obtained by Rotta (63) for Newtonian fluids, can in general be predicted for viscoelastic solutions. Seyer (67) experimentally predicts

FIGURE(4.14)

ENTRY LENGTHS FOR 0.01% SOLUTION

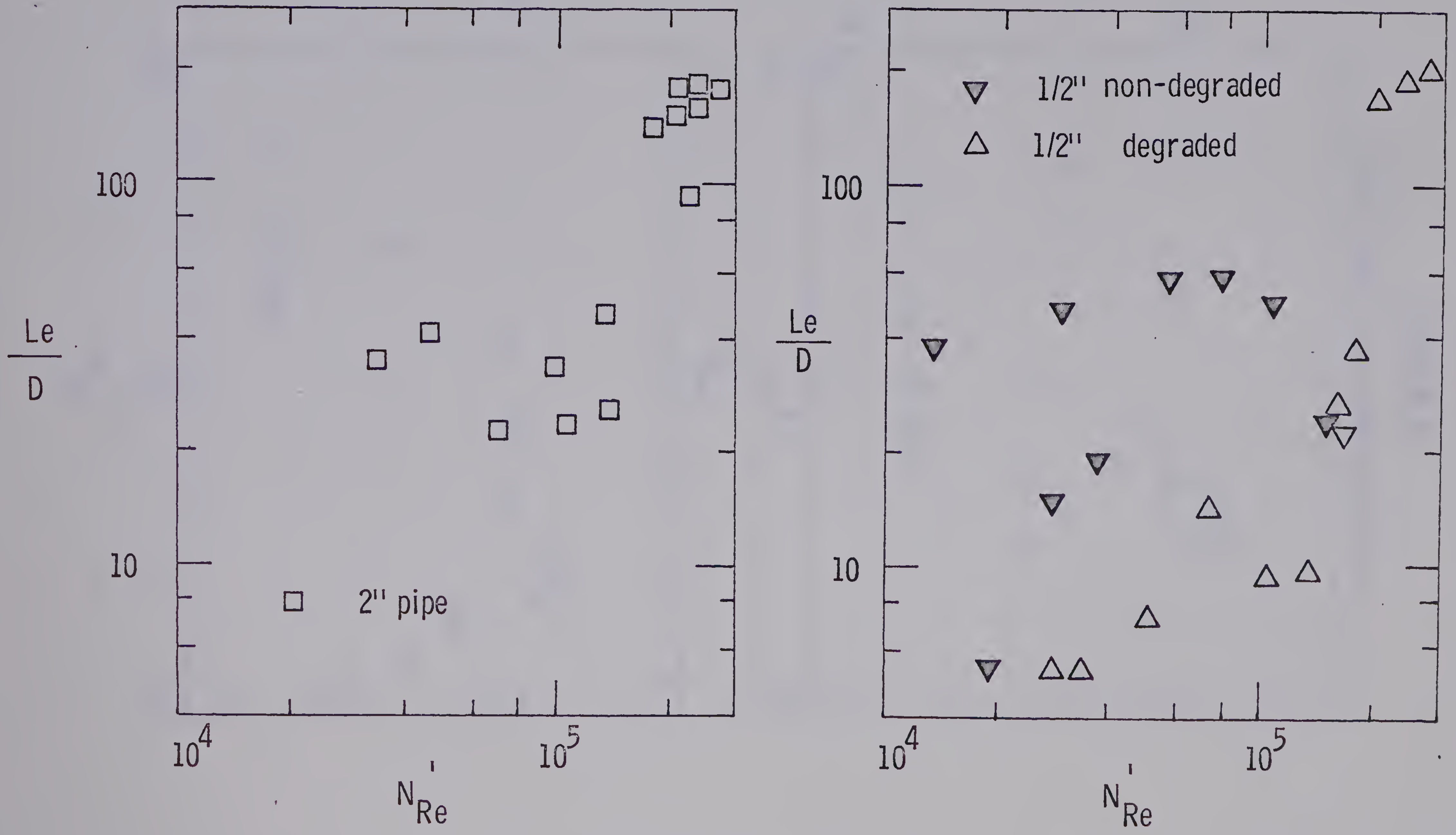

FIGURE(4.15)

ENTRY LENGTH FOR 0.20% SOLUTION

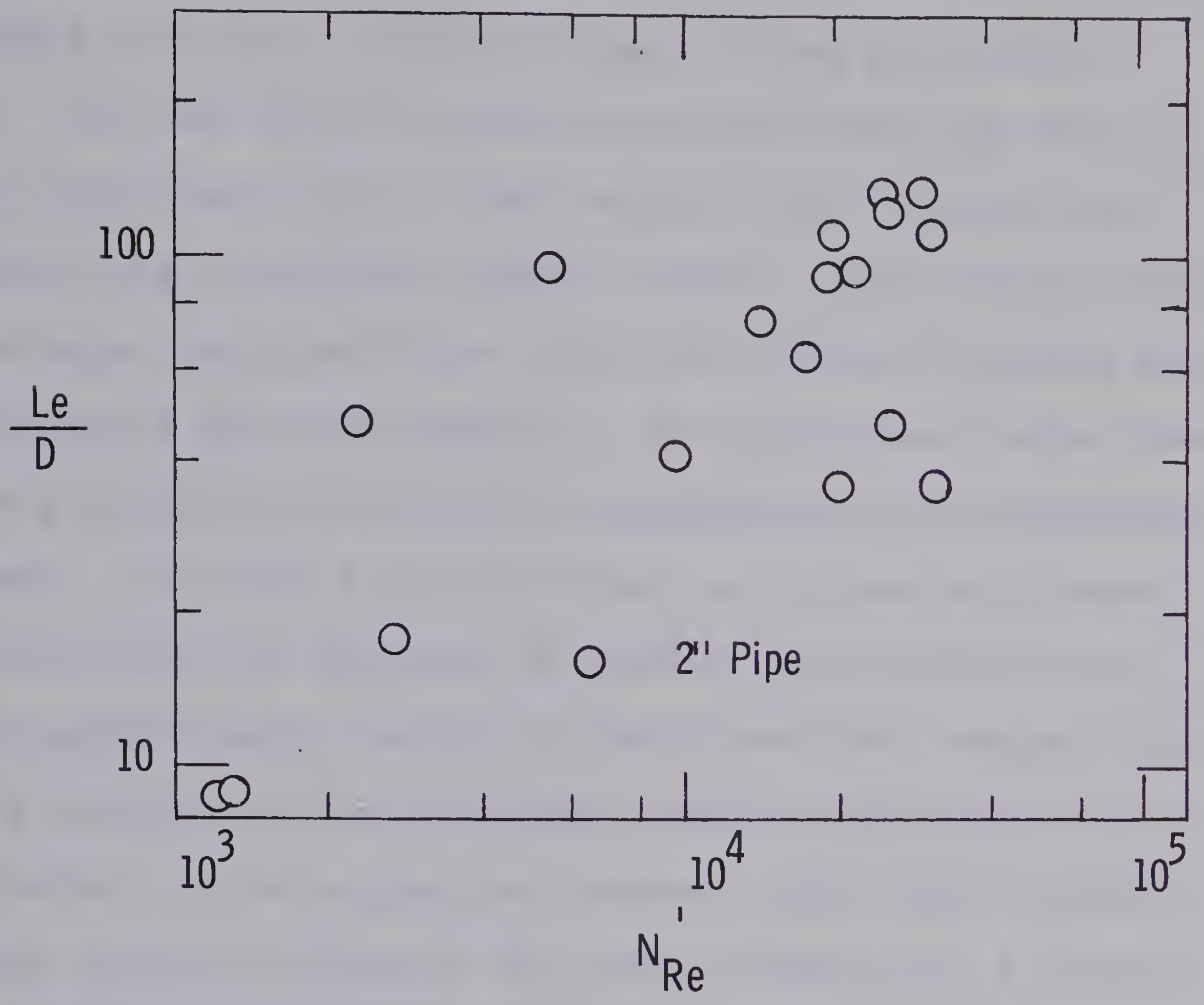

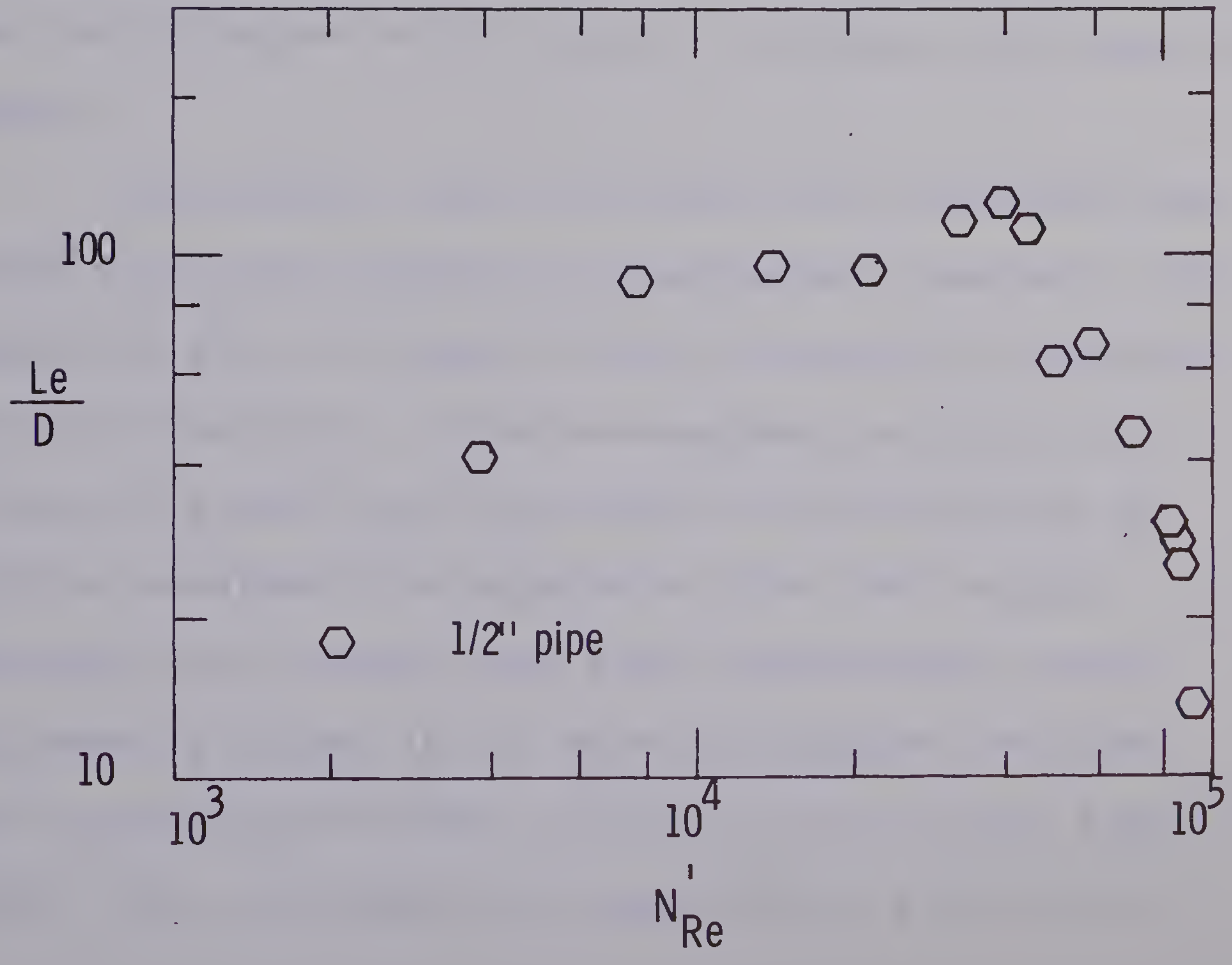

long entry lengths to extend up to Reynolds numbers in excess of 30000. In this range, it was also noticed by the use of velocity profiles that the flow is not fully-developed. Also, Rotta's data suggest that beyond the transition region, that is, approaching fully-developed turbulent flow the entry lengths decrease with increasing Reynolds numbers. In the laminar region the entry lengths are directly proportional to the Reynolds number. For the 0.01% solution, an increasing linear relationship as depicted by Figure (4.14) results in the maximum entry length of 200 diameters. Beyond this no relationship can be foreseen due to the limited amount of data. It is suggestive however, that these maximum entry lengths represent the entry lengths for a transition region beyond which they will decrease with Reynolds numbers.

In addition, the two fresh 0.01% solutions used in the 1/2" pipe resulted in considerable scatter. This scatter as shown by Figure (4.14) is noted for the non-degradated solution. This non-degraded solution had a friction factor curve that due to the stability of solution resulted in a separation from the laminar Newtonian curve rather than from the turbulent curve. Indicated by Figure (4.14) this non-degraded solution has a considerable amount of scatter for the low Reynolds number range and appears to pass through a maximum of

entry length of 60 diameters occurring at a Reynolds number of $8 \times 10^4$. Beyond this, the entry length decreases indicating an approach to fully-developed turbulent flow. For the degradated solution, the entry lengths continue to increase with Reynolds number until a maximum entry length of 200 is obtained at the maximum Reynolds number of $2.6 \times 10^5$. This suggests as for the 2" pipe data that the flow is in a transition state.

The highly elastic solution: that is, the 0.20% was the only solution at least for flow in the 1/2" pipe, that resulted in a well-defined relationship between the entry length and the Reynolds number. Figure (4.15) indicates a definite maximum entry length of 140 diameters occurring at a Reynolds number of $2.5 \times 10^4$. Beyond this Reynolds number, the entry lengths decrease as the flow field approaches fully-developed turbulent flow.

The presence of a vena contracta was discussed in detail in the preceding section and at that time no firm conclusion could be drawn relative to the effects on entry lenths. It becomes apparent as shown by Figure (4.15) that the presence of the vena contracta results in considerable scatter in the entry lenths. This scatter results in the entry lenths ranging from 35 to 130 diameters for the indicated Reynolds number range. Despite this, the entry lengths are seen to increase rapidly with Reynolds number and the maximum attained value corresponds to those in the 1/2" pipe.

In summarizing all of the above results, the following conclusions are reached. First, the entry lengths are always greater than the corresponding Newtonian values and extend up to a maximum of 200 diameters at a maximum Reynolds number of $10^5$. Second, the results indicate that the entry lengths pass through a maximum value presumably to occur within the transition region then, approach turbulent Newtonian values. Third, the presence of a vena contracta caused by the elastic nature of the fluid and the difficulties in reproducing data for the weak viscoelastic solution in the transition region resulted in a significant amount of scatter in the estimated entry lengths.

### 4.2.4 DIMENSIONAL ANALYSIS

The concept of dimensional analysis employed by Astarita (6) for Newtonian fluids and extended to viscoelastic fluids ( 7 ) in laminar flow is used for this analysis. Considering the dimensional analysis as presented in Chapter II and reproduced here, one has:

$$\frac{\Delta P_c}{\rho V^2/g_c} = A\left(\frac{1}{N_{Re}'}, \frac{V\theta}{D}, n'\right) \quad (4.2.1)$$

Neglecting the effects of n': that is, assuming it to be a constant value for each concentration, the above equation can be rewritten as:

Astarita's analysis considers only the generalized Reynolds number to determine the Hagenbach or Couette correction factors. Equation (4.2.1) indicates that an additional parameter, namely a Deborah number, may be important. For several values of the Reynolds number, data showing the relationship between contraction loss and the Deborah number are presented in Figure 4.16. For values of the Deborah number less than about 0.1 the dimensionless contraction loss is in close agreement with values that have been observed for Newtonian fluids. As the Deborah number approaches unity however, the contraction loss is seen to increase significantly relative to the low Deborah number or Newtonian value. At a Deborah number of 0.60 the dimensionless contraction loss for the 0.2% solution in the 1/2 inch pipe is 1.30 while the measured Newtonian value is 0.83 in the same pipe at roughly the same Reynolds number. Equivalently, these data at the noted conditions, indicate a 56% increase in the contraction loss owing to elastic effects.

In Figure 4.17 the dimensionless contraction loss has been plotted as a function of the generalized Reynolds number. Considering the Newtonian data, plotted as the solid triangles, a distinct effect of pipe diameter is noted. In view of the large contraction

ratio for the system, which was the same for both pipes, the difference in dimensionless contraction loss is somewhat surprising. Evidently some effect owing to differences in the entrance geometry of the two test sections has not been acounted for. In comparing data for the viscoelastic fluids with data for Newtonian fluids the geometry can be accounted for by comparing data obtained in the same test section.

Data for the dilute solutions (0.01%) are in general agreement with the Newtonian data. The rather large scatter in these data however, serve to mask any effect of geometry which may be present.

Comparing the 0.2% solution data, in the 1/2 inch pipe, with the data for the Newtonian fluid, it is observed that the contraction losses are significantly higher. This effect is of course equivalent to that noted in Figure 4.16 at Deborah numbers approaching unity. As a function of Reynolds number contraction losses for the 0.2% solution show a significant decrease as the Reynolds number increases. This effect is consistent with the observation that the Deborah number decreases modestly with increasing Reynolds number. For example over the range of Reynolds numbers observed in the 1/2 inch tube the Deborah number decreases from roughly 0.8 to a value of 0.4 at a Reynolds number of $10^5$.

Comparing the data for the 0.2% solution from the 1/2 inch and 2 inch pipes, it is clear that the data from the 2 inch pipe lie generally below those from the 1/2 inch pipe. Equivalently, the larger values of the Deborah number prevalent in the 1/2 inch tube at a given Reynolds number, serve to markedly increase the contraction loss.

This increase in contraction loss serves to more than offset the difference in contraction loss owing to geometry that was observed for the Newtonian fluid. Quantitatively, at a Reynolds number of $2.2 \times 10^4$ the Deborah numbers in the 1/2 and 2 inch pipes are 0.63 and 0.40 respectively.

In summary, the effect of elasticity is seen to be a substantial increase in the dimensionless contraction loss. The available data, being complicated by an unaccounted for geometric effect, are insufficient to quantitatively define the effect of elasticity.

FIGURE(4.16)
DIMENSIONLESS CONTRACTION LOSS VS DEBORAH NUMBER

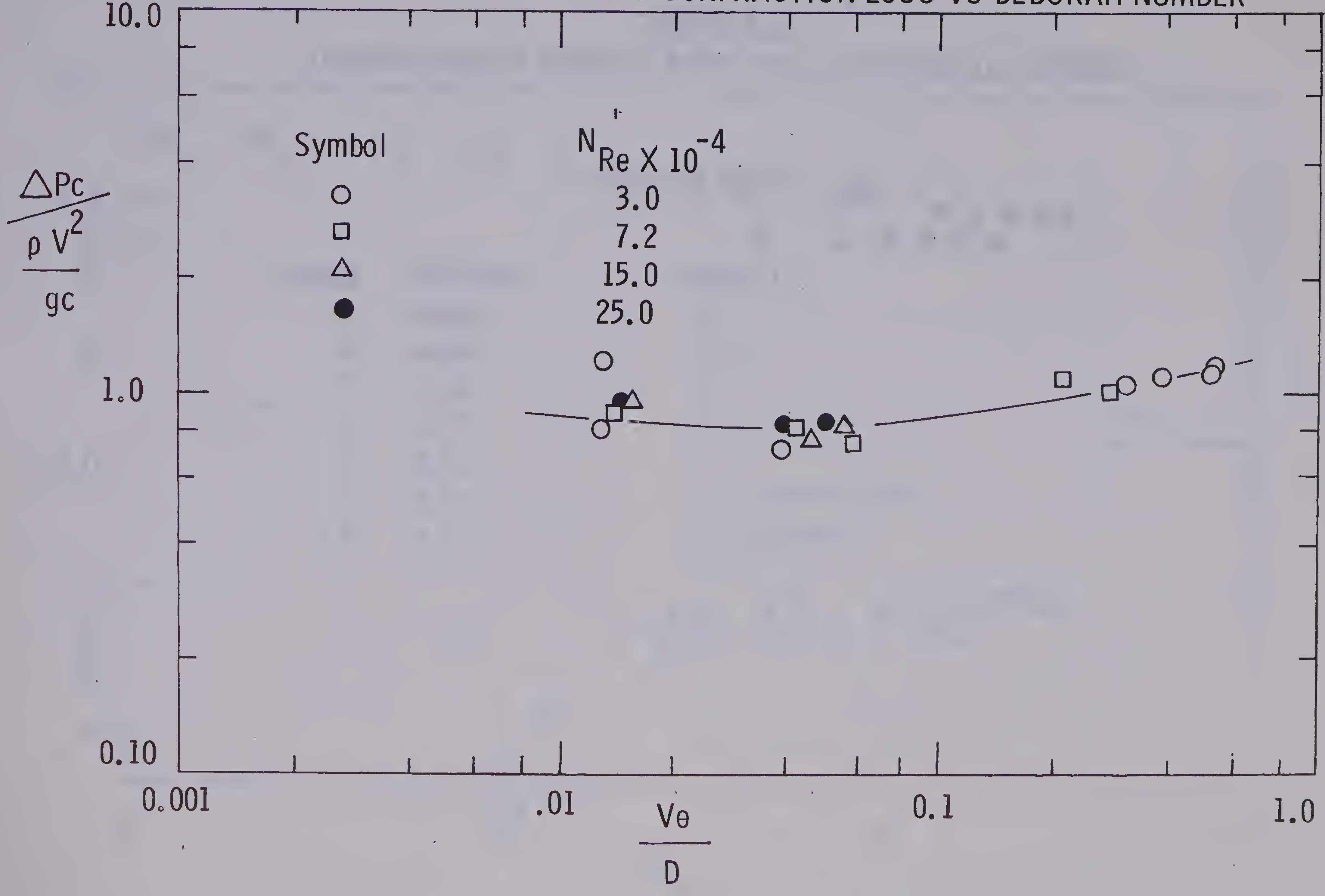

FIGURE(4.17)

DIMENSIONLESS CONTRACTION LOSS VS REYNOLDS NUMBER

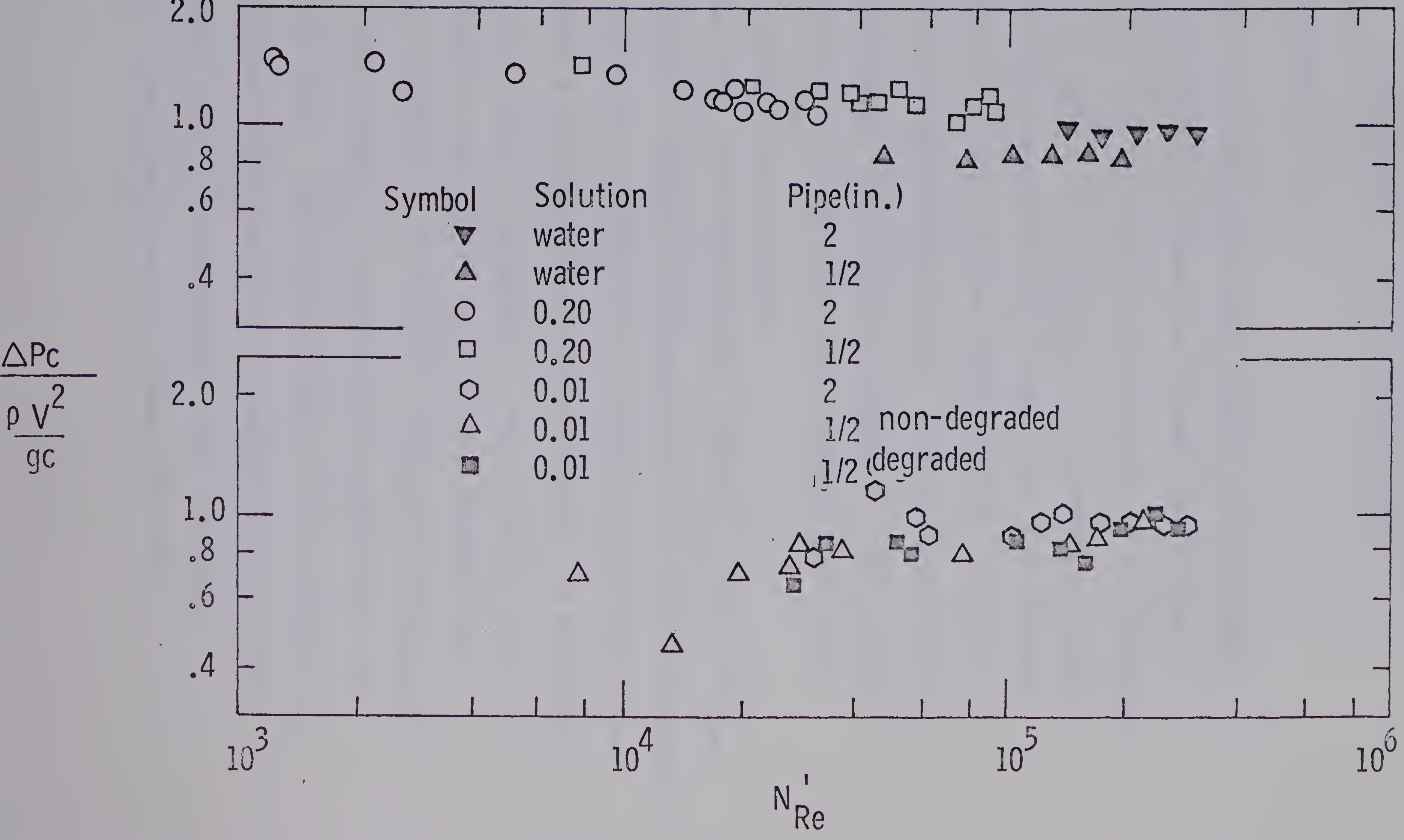

# CHAPTER V

# CONCLUSIONS AND RECOMMENDATIONS

## 5.1 CONCLUSIONS

For the flow conditions studied the turbulent Newtonian contraction losses were lower than those in laminar flow and decreased in proportion to the increasing fluid density. This density relationship apparent in the turbulent results do not appear for the laminar flows. Entry lengths for the turbulent flow results correspond to Latzko's theoretical formula with deviations occurring at high Reynolds numbers. Under these flow conditions the turbulent entry lengths were less than those predicted by Latzko.

For the 0.20% viscoelastic solution in the 2" pipe a vena contracta effect was detected for flow rates exceeding 120 Imp. Gal./Min. Although not detected below this value by the pressure profiles its existence cannot be ruled out. The vena contraction is assumed to stem in part from the elastic nature of the fluid under rapid deformations. Under these conditions, the fluid resists the deformation and as a result sets up a solid-like response near the entry of the tube. The overall effect is an increase in the contraction losses relative to turbulent Newtonian data. As the flow rate increases, the discrepancy between the viscoelastic and the Newtonian data

diminish. This is due to the increased Bernoulli effect which in the case for the 0.01% results in contraction losses equal to the Newtonian values.

The entry lengths, although suffering from significant scatter show a definite increase from those expected for Newtonian fluids. Entry lengths in the order of 200 diameters were found for the 0.20% and 0.01% solutions at Reynolds numbers approximately equal to $2 \times 10^4$ and $3 \times 10^5$ respectively. The maximum attained value presumably occurs within the transition region. Beyond the maximum, the entry lengths at least for the 0.20% solution, approach turbulent Newtonian values.

The use of dimensional analysis indicate that the dimensionless contraction losses depends upon a dimensionless group which includes the relaxation time of the material, $\theta$. It has been found however, that this single dimensionless group as insufficient to quantitatively interpret the results. In addition to the above group, the Reynolds number, although depicting the results for laminar flow, was not capable of describing the turbulent results. It is apparent that other dimensionless groups such as the elastio-inertial number must be considered in more detail before a definitive analysis of the entry phenomena can be obtained.

## 5.2 RECOMMENDATIONS

The following recommendations are:

1. A modification should be made to the pressure taps on the pipes near the entry to enable one to confirm that the measured pressure in the reservoir above the entry can be considered equal to that in the pipe. Also, with more taps located near the entry, a more detailed analysis can be obtained concerning the "vena contracta effect" or the solid-like behavior that was experimentally present for the 0.20% solution in the 2" pipe. These taps would have to be less than an $\frac{L}{D} = 8.0$. As an added feature, the pressure measurements would indicate the position where the boundary layer changes from a laminar to a turbulent condition as detected by an inflection point on the pressure curves.

2. Experimental studies should be conducted with other moderately or highly elastic solutions so as to yield a more comprehensive analysis.

3. Longer test sections especially for the larger diameter pipes is required in order to determine one way or another if the assumption that the pressure drop over the last section does indeed represent the developed pressure loss.

4. Velocity profiles would aid in the determination of the boundary layer growth and the evaluation of the shear stress at the wall in the entry region. These would allow one to theoretically determine the magnitude of the normal stresses and the previously mentioned boundary layer. In addition a more exact picture would be available concerning the solid-like behavior in the entry region for high flow rates in small or large pipes.
5. Coupled with the above, the relationship between the normal stress differences with radial position would enable one to employ other semi-empirical approaches.

# Appendix A

## Equipment Specifications

## A-1

## EQUIPMENT DIMENSIONS

With reference to Figure (A-1), Table (A-1) specifies the downstream and upstream pressure tap locations for both the 2" and 1/2" smooth brass pipes. The total length for the 2" and 1/2" test sections of 42.5' and 16.5' respectively resulted in the last pressure tap being 37 and 45 diameters upstream from the end.

| | 2" BRASS | | 1/2" BRASS | |
|---|---|---|---|---|
| TAP REFERENCE | TAP LOCATION* (FEET) | L/D | TAP LOCATION* (FEET) | L/D |
| 1A | -1.000 | 5.81 | -1.000 | 19.20 |
| 2A | -0.500 | 2.91 | -0.500 | 9.60 |
| 3A | 0.000 | 0.00 | -0.250 | 4.80 |
| 4A | - | - | 0.000 | 0.00 |
| 1 | 0.500 | 2.91 | 0.292 | 5.61 |
| 2 | 1.535 | 8.93 | 0.451 | 8.66 |
| 3 | 3.084 | 17.93 | 0.920 | 17.70 |
| 4 | 6.084 | 35.40 | 1.829 | 35.20 |
| 5 | 16.084 | 93.50 | 4.860 | 93.50 |
| 6 | 26.084 | 151.80 | 7.927 | 152.50 |
| 7 | 36.084 | 210.00 | 10.919 | 210.00 |
| 8 | - | - | 14.095 | 271.00 |

---

* Reference: Entrance to brass pipe test section.

## FIGURE A-1

## EXPERIMENTAL TEST SECTIONS

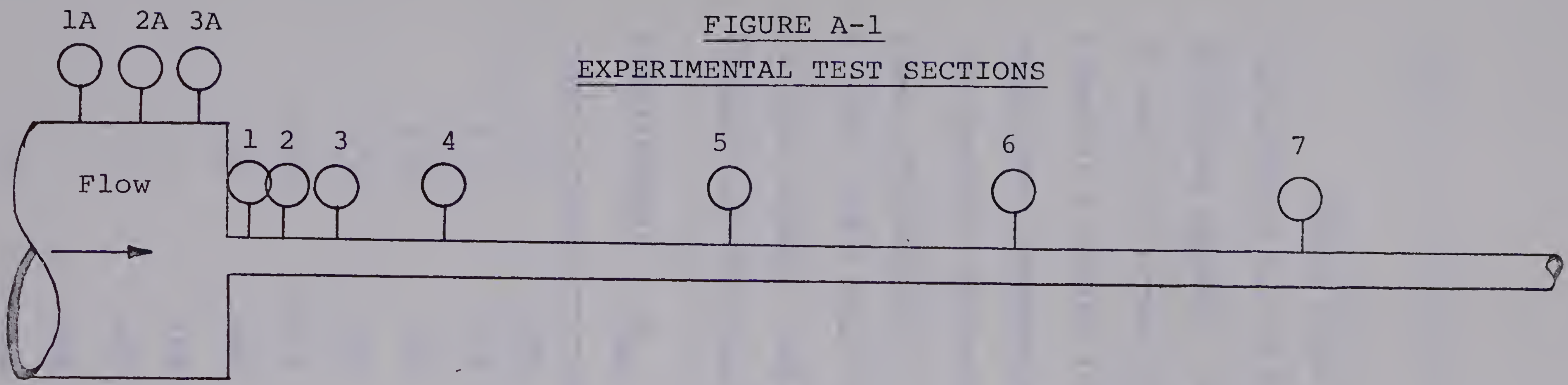
1A
2A
3A
1
2
3
4
5
6
7
Flow

2" Brass Test Section

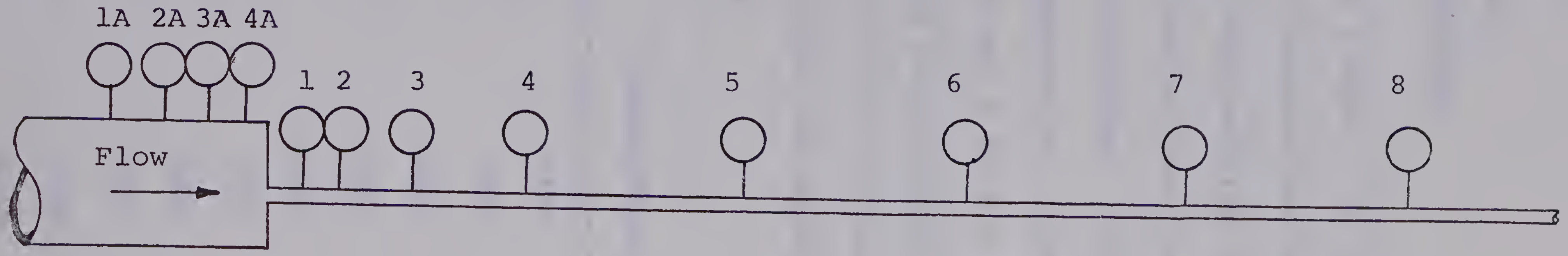
1A
2A
3A
4A
1
2
3
4
5
6
7
8
Flow

1/2" Brass Test Section

## TABLE 2

## TEST SECTION

Using sugar solution number 1 in laminar flow the calibration of the pipe diameters was done in the following manner. Using the manufacturer's data for the 2" and 1/2" brass pipes and knowing the flow rate an experimental friction factor is determined. This experimental value when compared to the theoretical value resulted in the absolute deviation of 5.0 and 2.9% for the 1/2" and 2" pipes respectively. Thus, the manufacturer's values of 0.1721' and 0.0521' for the I.D. of the pipes were used in this study. Table (A-2) lists the experimental and theoretical friction factors.

| PIPE (INCHES) | $N_{Re}$ | $f_{exp.}$ | $f_{theoretical}$ | DEVIATION |
|---|---|---|---|---|
| 1/2 | 326 | .0491 | .0494 | +.0003 |
| 1/2 | 470 | .0341 | .0348 | +.0007 |
| 1/2 | 538 | .0297 | .0282 | -.0015 |
| 1/2 | 860 | .0184 | .0180 | +.0005 |
| 1/2 | 1500 | .0107 | .0095 | -.0012 |
| 1/2 | 1900 | .0084 | .0088 | +.0004 |
| 2 | 416 | .0385 | .0396 | +.0011 |
| 2 | 607 | .0264 | .0257 | -.0007 |
| 2 | 882 | .0182 | .0184 | +.0002 |
| 2 | 1164 | .0138 | .0142 | +.0004 |
| 2 | 1302 | .0123 | .0128 | +.0005 |
| 2 | 1995 | .0080 | .0081 | +.0001 |

## TABLE A-3: MANOMETER FLUID DATA

Densities for the manometer fluids were obtained from Seyer (66). The fluids used were mercury and 0-dichlorobenzene. The temperature density relationships for water and 0-dichlorobenzene are given on Figure (A-2). The density of mercury was assumed to be a constant value of 13.550 $lbm/ft^3$.

## TABLE A-4: SUGAR SOLUTION DATA

For each of the two sugar solutions, a temperature viscosity and a temperature specific gravity relationship was determined by use of a Brookfield Viscometer and a Westfall balance respectively. Since most of the experimental runs were between a room temperature of 65.0°F to 85.0°F the relationships were determined within the same range as shown on Figures (A-3) and (A-4) for the sugar solution 1 and 2 respectively.

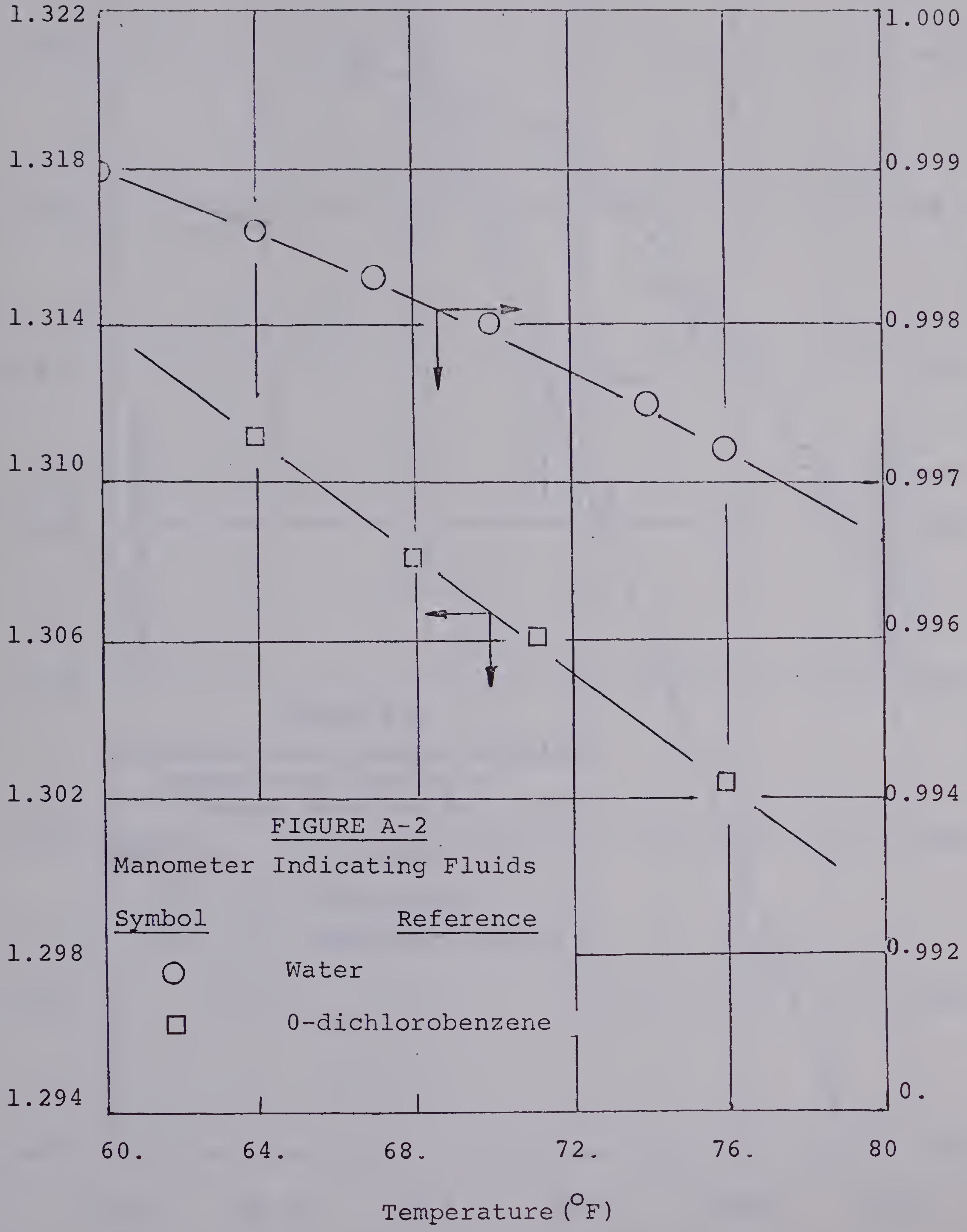

FIGURE A-2

Manometer Indicating Fluids

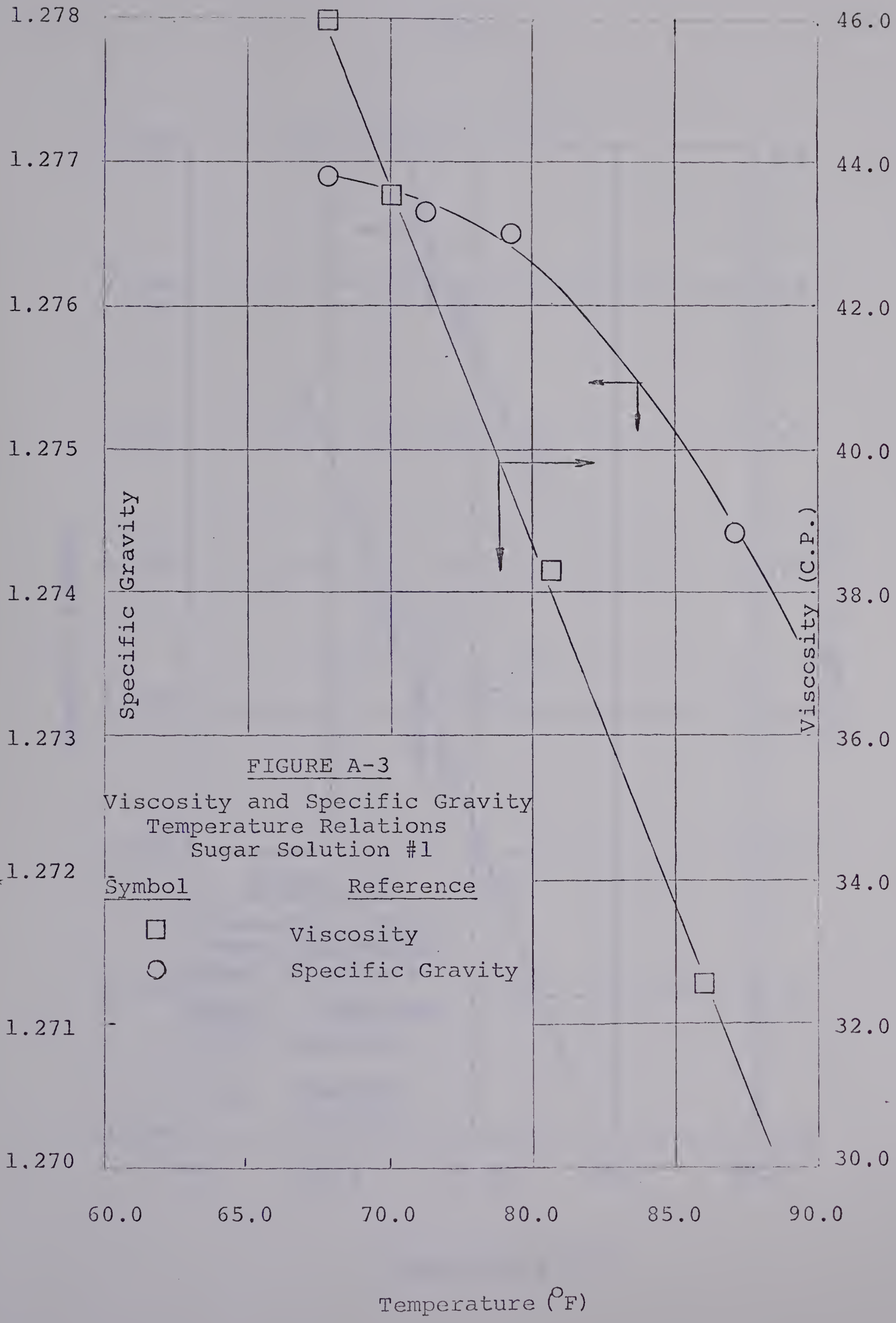

FIGURE A-3

Viscosity and Specific Gravity
Temperature Relations
Sugar Solution #1

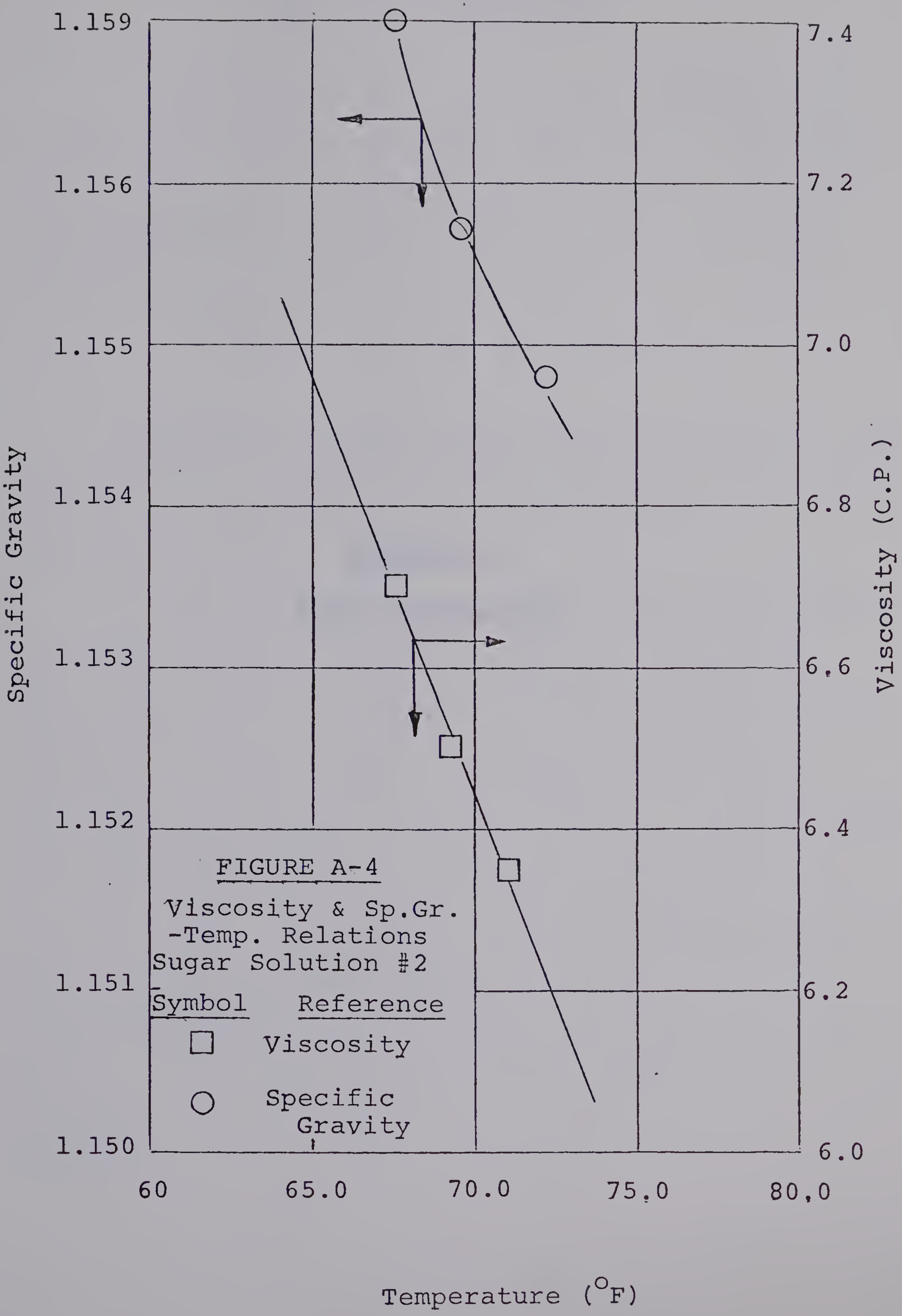

FIGURE A-4

Viscosity & Sp.Gr. -Temp. Relations Sugar Solution #2

# Appendix B

# Flow Calibration

# CALIBRATION DATA

## FLOW METER CALIBRATION

Calibration from 0 - 65.0 Imp. Gal./Min. was accomplished by direct weighing and from 30.0 to 200.0 Imp. Gal/Min. by one employing the Newtonian Von Karman correlation

$$\sqrt{\frac{1}{f}} = 4.0 \log (N_{Re}\sqrt{f}) - .40$$

Calibration from weighing and by the correlation were within 1.0% and 1½% respectively of the full scale repeatability of the flowmeter.

For flow rates ranging from 0-25 Imp. Gal./Min. the converter was set at span number 2. This high sensitivity setting resulted in a more accurate reading for these low flow rates. The results tabulated on Table (B-1) are plotted on Figure (B-1). For the higher flow rates the converter setting was altered to span number 1. Both weighing and employing the Von Karman equation as tabulated on Tables (B-2) and (B-3) are plotted on Figure (B-2). In this case, the weighing served to check the accuracy of the pressure drop readings.

## TABLE B-1

## 0-25 IMP. G.P.M. CALIBRATION (HIGH SENSITITY)

Settings: Amplifier - IV/cm. Room Temp. 72°F

Converter - Span No. 2 Flow Temp. 70°F

| RUN NO. | WEIGHT (LB) | TIME (SEC) | FLOW (IMP.G.P.M.) | RECORDER DIVISIONS |
|---|---|---|---|---|
| 1 | 40.0 | 58.70 | 4.08 | 3.30 |
| 2 | 60.0 | 54.65 | 6.58 | 5.30 |
| 3 | 60.0 | 48.20 | 7.47 | 5.80 |
| 4 | 75.0 | 58.00 | 7.75 | 6.00 |
| 5 | 75.0 | 35.10 | 12.81 | 10.05 |
| 6 | 100.0 | 45.80 | 13.10 | 10.50 |
| 7 | 100.0 | 43.20 | 13.89 | 11.00 |
| 8 | 90.0 | 40.00 | 13.50 | 10.75 |
| 9 | 100.0 | 27.00 | 24.45 | 19.25 |

## TABLE B-2

## 0-65 IMP. G.P.M. CALIBRATION (LOW SENSITIVITY)

Settings: Amplifier - 1 volt/cm. Room Temp. 72°F

Converter - Span No. 1. Flow Temp. 70°F

| RUN NO. | WEIGHT (LB) | TIME (SEC) | FLOW (IMP.G.P.M.) | RECORDER DIVISIONS |
|---|---|---|---|---|
| 1 | 55.00 | 44.00 | 5.50 | 2.00 |
| 2 | 75.00 | 37.30 | 12.08 | 3.25 |
| 3 | 60.00 | 29.60 | 12.15 | 3.25 |
| 4 | 65.00 | 32.60 | 11.98 | 3.20 |
| 5 | 90.00 | 44.30 | 12.20 | 3.30 |
| 6 | 80.00 | 25.00 | 19.20 | 5.00 |
| 7 | 140.00 | 25.10 | 33.50 | 8.70 |
| 8 | 140.00 | 19.00 | 44.25 | 11.35 |
| 9 | 150.00 | 21.10 | 42.60 | 11.20 |
| 10 | 150.00 | 25.80 | 58.10 | 15.00 |
| 11 | 190.00 | 17.20 | 66.30 | 17.20 |

## TABLE B-3

## 0-170 IMP. G.P.M. CALIBRATION

Settings: Amplifier - IV/cm. Room Temp: 72°F

Converter - Span No. 1 Flow Temp: 70°F

| RUN NO. | PRESSURE DROP/20 FEET (IN. OF WATER) | FLOW (IMP. G.P.M.) | RECORDER DIVISIONS |
|---|---|---|---|
| 1 | 110.90 | 165.30 | 44.80 |
| 2 | 91.50 | 146.20 | 40.00 |
| 3 | 80.50 | 136.80 | 37.50 |
| 4 | 67.70 | 124.00 | 34.00 |
| 5 | 61.10 | 117.00 | 30.40 |
| 6 | 45.80 | 99.80 | 26.30 |
| 7 | 32.70 | 82.80 | 22.20 |
| 8 | 23.30 | 68.50 | 18.40 |
| 9 | 17.60 | 58.65 | 15.80 |
| 10 | 13.00 | 49.50 | 13.10 |
| 11 | 9.40 | 41.25 | 11.00 |
| 12 | 5.60 | 30.90 | 8.00 |
| 13 | 3.53 | 23.80 | 6.00 |
| 14 | 6.13 | 32.45 | 8.00 |
| 15 | 10.25 | 43.30 | 11.00 |
| 16 | 17.50 | 58.30 | 14.75 |

## FIGURE B-1
## Low Flow Rate Calibration

Amplifier: IV/cm.

Converter: Span No. 2

Room Temp: 72°F

Flow Temp: 70°F

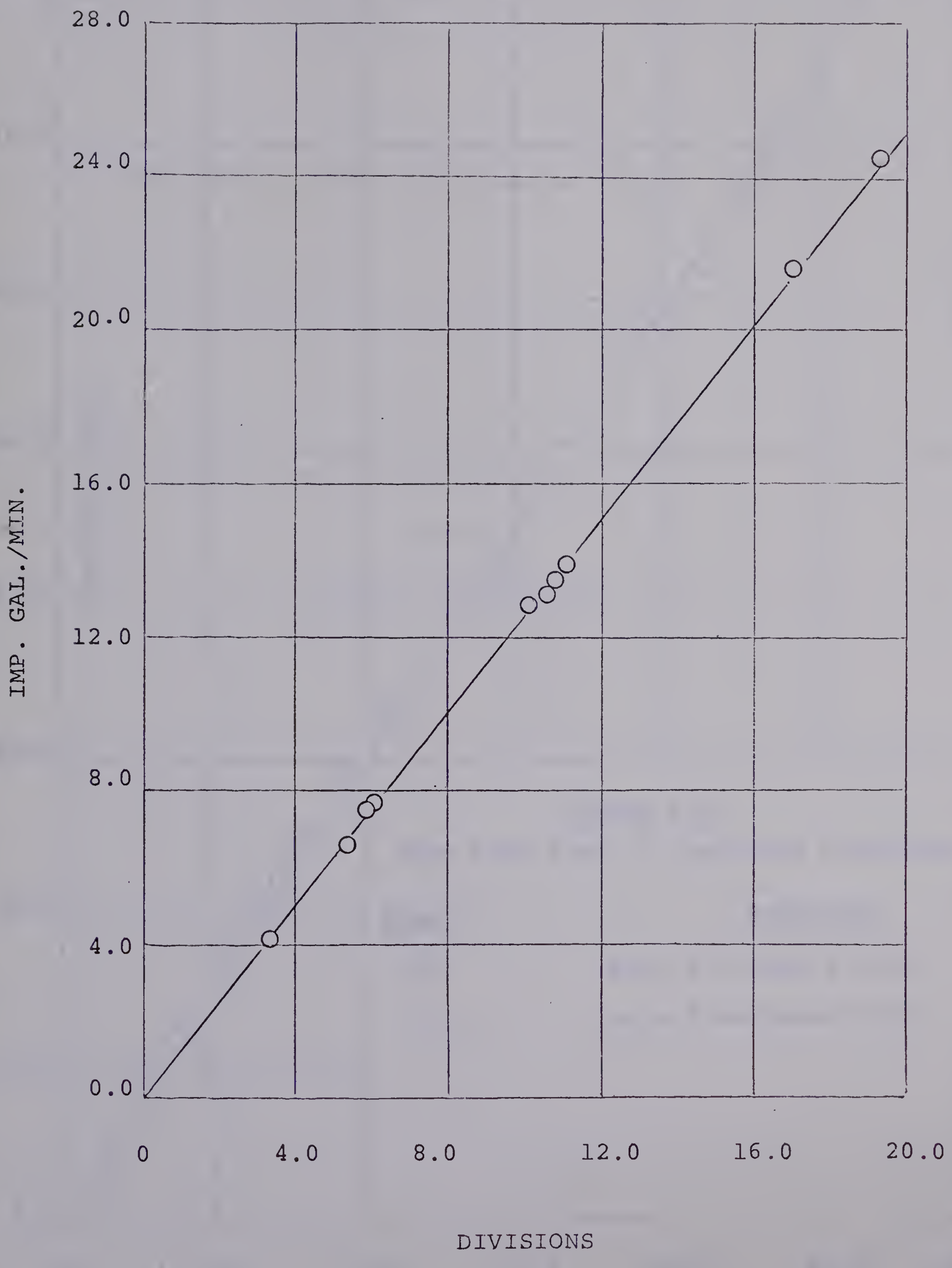

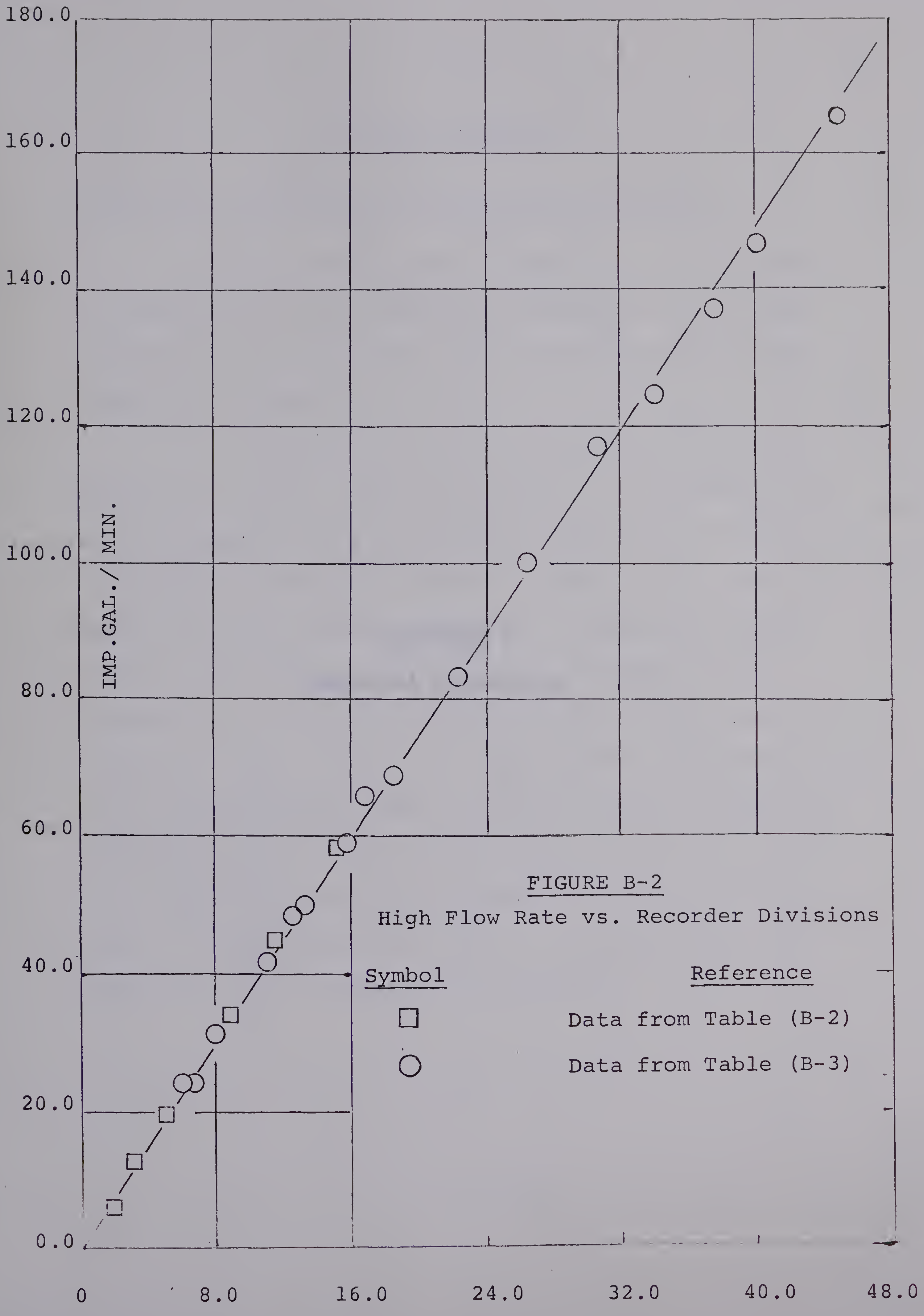

FIGURE B-2

High Flow Rate vs. Recorder Divisions

# Appendix C

# Physical Properties

# PHYSICAL PROPERTIES

## TABLE C-1: PHYSICAL AND RHEOLOGICAL PROPERTIES

The flow curves used for the two concentrations of Separan AP-30 were obtained from Seyer (66) and are reproduced in Figure (C-1). The densities used were the densities of water.

The relaxation time as a function of the shear stress at the wall for the 0.20% and 0.01% Separan AP-30 were obtained from the available literature of Oliver (57) and Seyer (66) and as plotted on Figure (C-2). As noted, for the 0.01% solution, there is a discrepancy between Oliver's and Seyer's data which is accounted for by degradation. Since the 0.01% solution is this study resulted in two discrete friction factor relationships, it is to be expected that each would possess a different relaxation time - shear stress curve; however, no capillary jet thrust apparatus was available and as a result Seyer's relationship was chosen to represent both the degradated and non-degradated solutions.

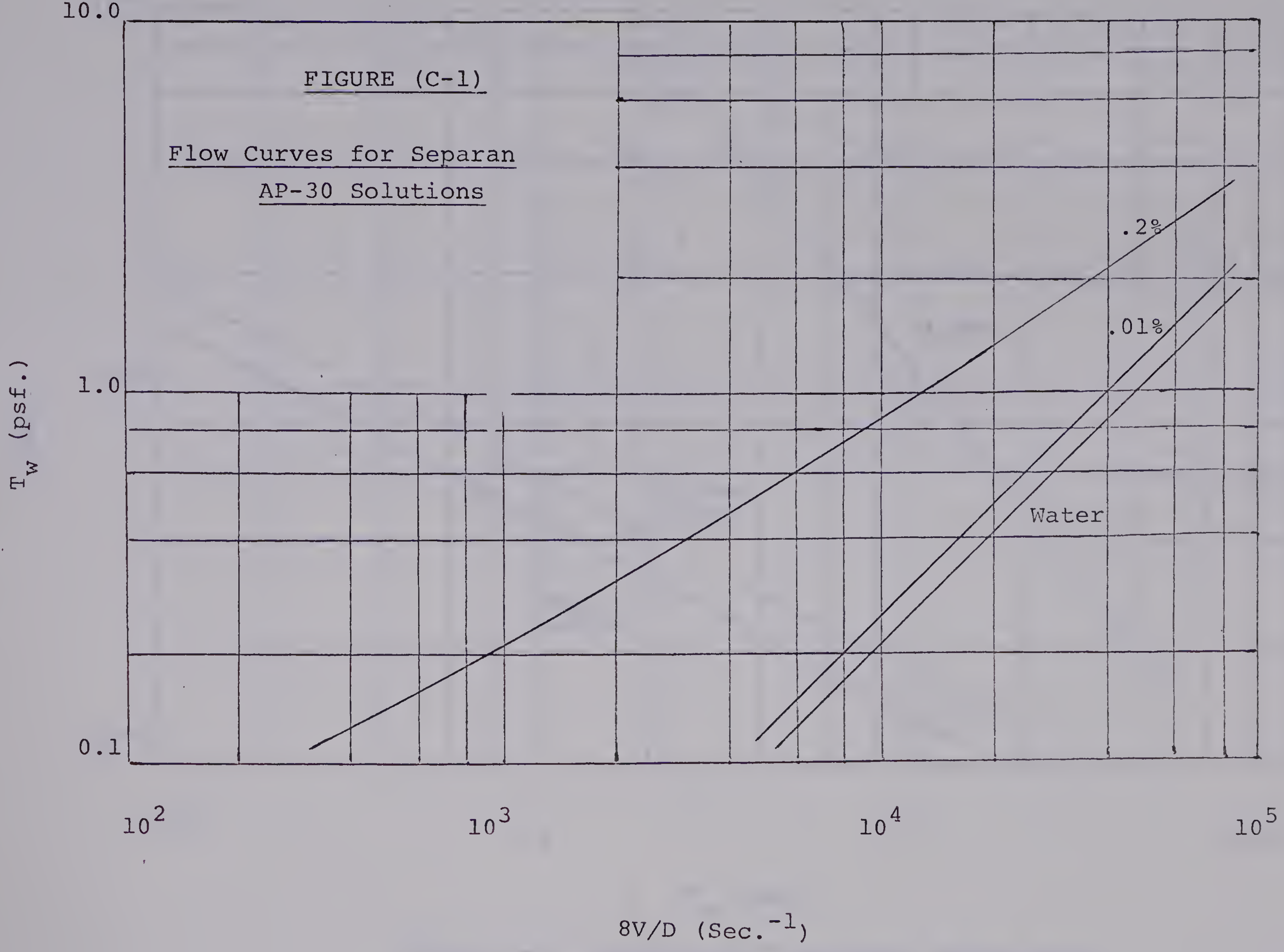

FIGURE (C-1)

Flow Curves for Separan AP-30 Solutions

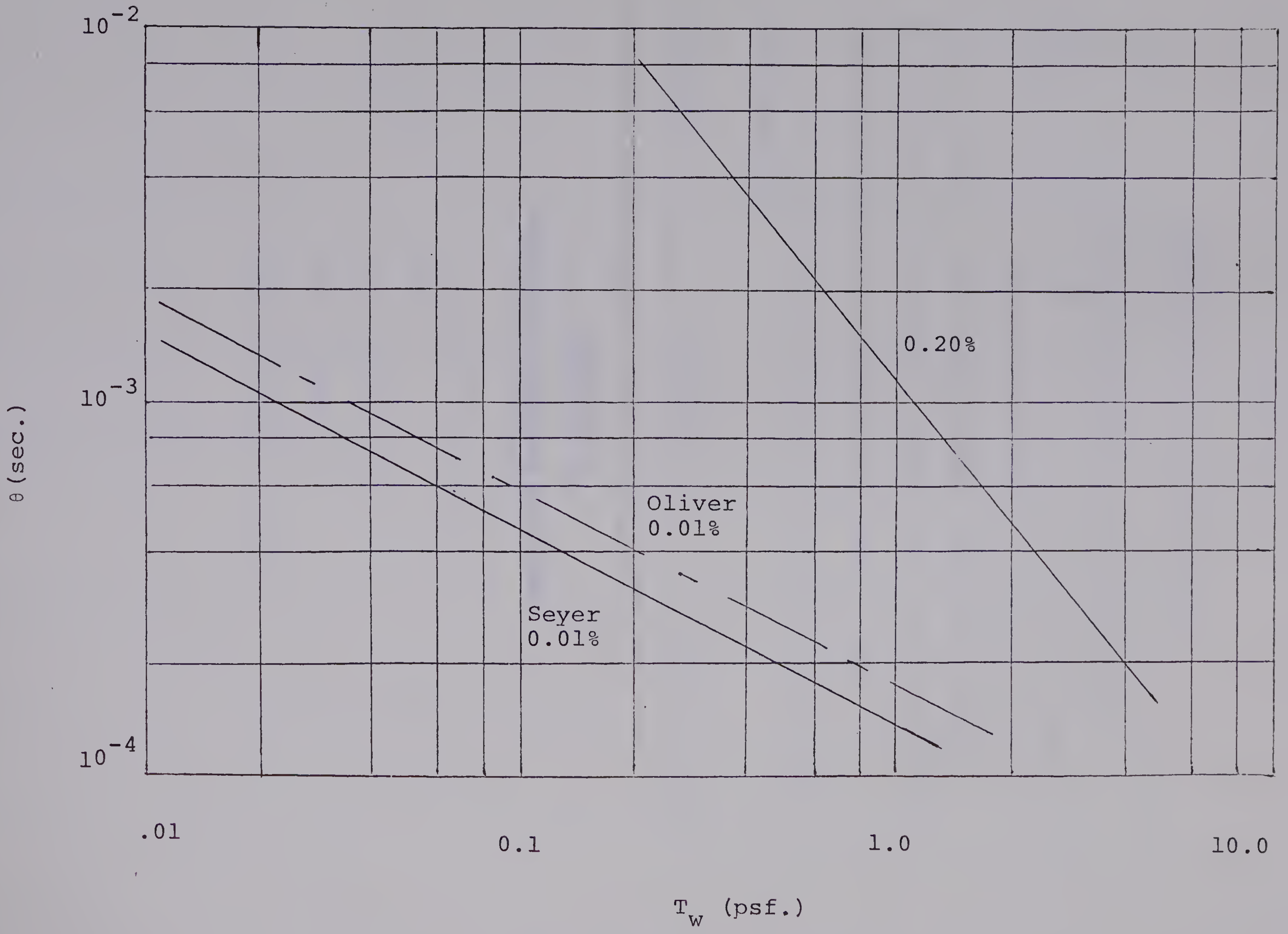

Figure C-2: Relaxation Time-Shear Stress Data

# Appendix D

# Newtonian Pressure Profiles

## Newtonian Pressure Profiles

The tabulated experimental pressure drops given on Tables (D-2) to (D-6) are plotted on Figures (D-1) to (D-8). From these pressure profiles one is able to measure entry lengths and contraction losses and calculate the Reynolds numbers and friction factors. These quantities are tabulated on Table (D-1).

The following outlines the order in which the figures appear.

| Figure No. | Solution | Pipe Dia. (in.) |
|---|---|---|
| 1 | Water | 2 |
| 2 | Sugar Solution #1 | 2 |
| 3 | Sugar Solution #2 | 2 |
| 4 | Sugar Solutions 1 and 2 | 2 |
| 5 | Water | 1/2 |
| 6 | Sugar Solution #1 | 1/2 |
| 7 | Sugar Solution #2 | 1/2 |
| 8 | Sugar Solutions 1 and 2 | 1/2 |

## TABLE (D-1)

| FLUID | PIPE DIA. (IN) | RUN NO. | $N_{Re}$ | $\Delta P_c$ (IN.$H_2O$) | $L_e/D$ | $fx10^3$ |
|---|---|---|---|---|---|---|
| WATER<br>(70.5°F) | 2 | 1 | $1.42x10^5$ | 26.0 | 2.32 | 4.21 |
| | 2 | 2 | $1.74x10^5$ | 40.0 | 2.32 | 4.06 |
| | 2 | 3 | $2.16x10^5$ | 60.0 | 5.83 | 3.96 |
| | 2 | 4 | $2.10x10^5$ | 60.0 | 5.83 | 4.01 |
| | 2 | 5 | $2.5\ x10^5$ | 84.0 | 5.83 | 3.66 |
| | 2 | 6 | $3.10x10^5$ | 129.0 | 6.00 | 3.77 |
| | 1/2 | 1 | $4.73x10^4$ | 25.0 | 5.00 | 5.76 |
| | 1/2 | 2 | $7.75x10^4$ | 78.0 | 5.75 | 5.30 |
| | 1/2 | 3 | $10.08x10^4$ | 130.0 | 5.75 | 5.01 |
| | 1/2 | 4 | $13.15x10^4$ | 220.0 | 9.60 | 4.37 |
| | 1/2 | 5 | $16.60x10^4$ | 366.0 | 9.60 | 4.51 |
| | 1/2 | 6 | $19.85x10^4$ | 487.0 | 9.60 | 4.32 |
| SUGAR SOL'N<br>NO. 1<br>(70.5°F) | 2 | 1 | 416. | ____ | ____ | 39.6 |
| | 2 | 2 | 607. | ____ | ____ | 25.7 |
| | 2 | 3 | 882. | ____ | ____ | 19.95 |
| | 2 | 4 | 1164. | 8.50 | 29.00 | 14.20 |
| | 2 | 5 | 1302. | ____ | ____ | 12.80 |
| | 2 | 6 | 1995. | 3.85 | 34.90 | 8.10 |
| | 2 | 7 | 3550. | 18.00 | 34.80 | 10.30 |
| | 2 | 8 | 4610. | 26.00 | 4.55 | 10.45 |
| | 2 | 9 | 6640. | 38.00 | 8.14 | 9.35 |
| | 2 | 10 | 7560. | 47.00 | 8.72 | 8.80 |
| | 2 | 11 | 9225. | 73.00 | 10.43 | 8.38 |

TABLE (D-1) CONTINUED

| FLUID | PIPE DIA. (IN) | RUN NO. | $N_{Re}$ | $\Delta P_c$ (IN. $H_2O$) | $L_e/D$ | $f \times 10^3$ |
|---|---|---|---|---|---|---|
| | 1/2 | 1 | 326. | ______ | ____ | 49.40 |
| | 1/2 | 2 | 470. | ______ | ____ | 34.80 |
| | 1/2 | 3 | 538. | ______ | ____ | 28.20 |
| | 1/2 | 4 | 859. | 17.00 | 52.00 | 18.86 |
| | 1/2 | 5 | 1530. | ______ | ____ | 9.50 |
| | 1/2 | 6 | 1732. | 92.00 | 95.00 | 10.60 |
| | 1/2 | 7 | 2700. | 90.00 | 6.70 | 10.50 |
| | 1/2 | 8 | 3294. | 122.00 | 6.70 | 10.72 |
| | 1/2 | 9 | 3970. | 190.00 | 6.70 | 10.57 |
| | 1/2 | 10 | 4630. | 213.00 | 6.70 | 10.07 |
| | 1/2 | 11 | 5230. | 300.00 | 7.30 | 10.00 |
| SUGAR SOL'N NO. 2 (66.0°F) | 2 | 1 | 6970. | 17.45 | 3.67 | 7.00 |
| | 2 | 2 | 9275. | ______ | ____ | 7.25 |
| | 2 | 3 | 12640. | 9.08 | 2.91 | 9.65 |
| | 2 | 4 | 18870. | ______ | ____ | 6.48 |
| | 2 | 5 | 21700. | 17.20 | 2.91 | 6.30 |
| | 2 | 6 | 24850. | ______ | ____ | 6.46 |
| | 2 | 7 | 30700. | 31.00 | 8.70 | 5.62 |
| | 2 | 8 | 39430. | 65.00 | 2.33 | 5.14 |
| | 2 | 9 | 44900. | 82.00 | 17.42 | 5.62 |
| | 2 | 10 | 52850. | 107.00 | 8.14 | 4.81 |

TABLE (D-1) CONTINUED

| FLUID | PIPE DIA. (IN) | RUN NO. | $N_{Re}$ | $\Delta P_c$ (IN.$H_2O$) | $L_e/D$ | $f \times 10^3$ |
|---|---|---|---|---|---|---|
| | 1/2 | 1 | 622. | 13.00 | 7.65 | 8.45 |
| | 1/2 | 2 | 9980. | 36.00 | 7.65 | 7.21 |
| | 1/2 | 3 | 14380. | 78.00 | 4.80 | 6.81 |
| | 1/2 | 4 | 21800. | 190.00 | 5.75 | 6.60 |
| | 1/2 | 5 | 28500. | 372.00 | 11.00 | 6.01 |
| | 1/2 | 6 | 33700. | 428.00 | 11.50 | 5.76 |
| | 1/2 | 7 | 37550. | 570.00 | 13.40 | 5.48 |

## TABLE (D-2)

### Pressure Drops (in.Water)

Solution: Water

Fluid Temp. 70.5$^{\circ}$F

| PIPE DIA. (IN) | RUN NO. | FLOW (GAL./MIN.) | PRESSURE TAP LOCATION | | | | | | | | |
|---|---|---|---|---|---|---|---|---|---|---|---|
| | | | 1A-2A | 2A-3A | 3A-1 | 1-2 | 2-3 | 3-4 | 4-5 | 5-6 | 6-7 |
| 2 | 1 | 76.0 | - | - | 25.60 | 2.60 | 2.80 | 9.80 | 12.40 | 13.50 | 16.00 |
| | 2 | 93.5 | - | - | 39.80 | 3.63 | 3.73 | 4.95 | 18.70 | 19.20 | 23.20 |
| | 3 | 116.0 | - | - | 60.90 | 5.60 | 4.40 | 14.00 | 27.00 | 29.70 | 34.80 |
| | 4 | 173.0 | - | - | 83.00 | 6.80 | 7.00 | 16.30 | 34.30 | 45.80 | 33.90 |
| | 5 | 134.5 | - | - | 128.00 | 10.00 | 6.80 | 25.00 | 54.50 | 54.30 | 69.70 |
| | 6 | 166.0 | - | - | 61.30 | 2.60 | 5.70 | 13.70 | 26.70 | 31.30 | 30.30 |

## TABLE (D-2) CONTINUED

## Pressure Drops (in. Water)

Solution: Water

Fluid Temp. 70.5°F

| PIPE DIA. (IN) | RUN NO. | FLOW (GAL./MIN.) | PRESSURE TAP LOCATION | | | | | | | | | |
|---|---|---|---|---|---|---|---|---|---|---|---|---|
| | | | 1A-3A | 3A-4A | 4A-1 | 1-2 | 2-3 | 3-4 | 4-5 | 5-6 | 6-7 | 7-8 |
| 1/2 | 1 | 7.70 | - | - | 24.50 | 1.70 | 3.40 | 6.20 | 21.70 | 22.10 | 19.60 | 18.70 |
| | 2 | 12.60 | - | - | 79.00 | 6.00 | 9.70 | 17.05 | 58.90 | 53.70 | 57.00 | 60.70 |
| | 3 | 16.40 | - | - | 131.80 | 11.30 | 16.90 | 25.40 | 96.00 | 84.70 | 91.70 | 96.80 |
| | 4 | 21.40 | 0.40 | 0.00 | 219.00 | 16.20 | 25.10 | 42.60 | 143.20 | 127.40 | 132.20 | 145.50 |
| | 5 | 27.00 | - | - | 352.00 | 38.40 | 48.30 | 61.70 | 237.10 | 205.00 | 222.70 | 236.50 |
| | 6 | 32.30 | - | - | 497.40 | 33.00 | 49.70 | 92.30 | 324.80 | 294.00 | 299.00 | 317.00 |

## TABLE (D-3)

### Pressure Drops (in. Water)

Sugar Solution No. 1
Pipe Dia. 2 in.

Fluid Temp. 70.5$^{\circ}$F

| RUN NO. | FLOW (GAL./MIN.) | PRESSURE TAP LOCATION | | | | | | | | |
|---|---|---|---|---|---|---|---|---|---|---|
| | | 1A-2A | 2A-3A | 3A-1 | 1-2 | 2-3 | 3-4 | 4-5 | 5-6 | 6-7 |
| 1 | 8.30 | - | - | - | - | - | - | 6.00 | | |
| 2 | 12.10 | - | - | - | - | - | - | 7.70 | | |
| 3 | 17.40 | - | - | - | - | - | - | 12.50 | | |
| 4 | 22.80 | 0.521 | -0.40 | 4.76 | 1.24 | 1.11 | 2.45 | 5.30 | 5.60 | 5.30 |
| 5 | 26.00 | - | - | - | - | - | - | 19.50 | | |
| 6 | 38.20 | 1.47 | 0.184 | 9.15 | 2.30 | 2.35 | 3.40 | 9.00 | 8.82 | 8.72 |
| 7 | 68.00 | 1.65 | -0.83 | 25.30 | 4.70 | 5.21 | 8.75 | 34.80 | 34.80 | 35.10 |
| 8 | 86.20 | 0.81 | 3.56 | 37.60 | 7.15 | 8.45 | 14.92 | 56.60 | 56.70 | 57.60 |
| 9 | 119.50 | 1.73 | 2.48 | 70.70 | 14.10 | 15.80 | 29.90 | 96.80 | 96.80 | 100.00 |
| 10 | 134.50 | 1.96 | 2.22 | 88.20 | 17.30 | 18.20 | 37.00 | 115.00 | 115.80 | 119.80 |
| 11 | 160.00 | 2.06 | 1.84 | 126.80 | 22.10 | 25.80 | 50.30 | 155.00 | 154.90 | 161.70 |

## TABLE (D-4)

### Pressure Drops (in. Water)

Sugar Solution No. 1
Pipe Dia. 1/2 in.

Fluid Temp. 70.5$^{\circ}$F

<table>
<tr><th rowspan="2">RUN NO.</th><th rowspan="2">FLOW<br>(GAL./MIN.)</th><th colspan="10">PRESSURE TAP LOCATIONS</th></tr>
<tr><th>1A-3A</th><th>3A-4A</th><th>4A-1</th><th>1-2</th><th>2-3</th><th>3-4</th><th>4-5</th><th>5-6</th><th>6-7</th><th>7-8</th></tr>
<tr><td>1</td><td>1.804</td><td>-</td><td>-</td><td>-</td><td>-</td><td>-</td><td>-</td><td colspan="4">57.00</td></tr>
<tr><td>2</td><td>2.604</td><td>-</td><td>-</td><td>-</td><td>-</td><td>-</td><td>-</td><td colspan="4">84.80</td></tr>
<tr><td>3</td><td>3.03</td><td>-</td><td>-</td><td>-</td><td>-</td><td>-</td><td>-</td><td colspan="4">96.20</td></tr>
<tr><td>4</td><td>5.00</td><td>1.45</td><td>0.00</td><td>24.40</td><td>5.70</td><td>7.00</td><td>15.70</td><td>41.00</td><td>42.80</td><td>42.00</td><td>44.10</td></tr>
<tr><td>5</td><td>8.60</td><td>-</td><td>-</td><td>-</td><td>-</td><td>-</td><td>-</td><td colspan="4">253.10</td></tr>
<tr><td>6</td><td>11.30</td><td>0.535</td><td>1.30</td><td>95.10</td><td>10.60</td><td>23.90</td><td>39.30</td><td>107.00</td><td>100.00</td><td>96.90</td><td>101.70</td></tr>
<tr><td>7</td><td>15.90</td><td>1.70</td><td>1.70</td><td>172.00</td><td>19.70</td><td>39.10</td><td>64.60</td><td>231.60</td><td>238.80</td><td>237.20</td><td>249.00</td></tr>
<tr><td>8</td><td>19.00</td><td>1.40</td><td>1.60</td><td>250.30</td><td>26.10</td><td>54.40</td><td>97.80</td><td>343.00</td><td>344.80</td><td>343.00</td><td>359.20</td></tr>
<tr><td>9</td><td>22.60</td><td>2.20</td><td>1.60</td><td>378.00</td><td>32.85</td><td>46.20</td><td>141.70</td><td>480.80</td><td>480.50</td><td>480.80</td><td>502.90</td></tr>
<tr><td>10</td><td>25.80</td><td>3.80</td><td>1.60</td><td>483.00</td><td>39.70</td><td>65.90</td><td>174.20</td><td>598.00</td><td>594.50</td><td>598.00</td><td>625.00</td></tr>
<tr><td>11</td><td>28.30</td><td>2.90</td><td>0.00</td><td>591.00</td><td>46.70</td><td>115.00</td><td>207.80</td><td>713.10</td><td>709.80</td><td>716.80</td><td>746.50</td></tr>
</table>

## TABLE (D-5)

### Pressure Drops (in. Water)

Sugar Solution No. 2
Pipe Dia. 2 in.

Fluid Temp. 66.0°F

| RUN NO. | FLOW (GAL./MIN.) | PRESSURE TAP LOCATION | | | | | | | | |
|---|---|---|---|---|---|---|---|---|---|---|
| | | 1A-2A | 2A-3A | 3A-1 | 1-2 | 2-3 | 3-4 | 4-5 | 5-6 | 6-7 |
| 1 | 22.50 | 0.184 | 0.460 | 3.28 | 0.92 | 0.89 | 1.06 | 2.28 | 2.30 | 2.48 |
| 2 | 30.00 | - | - | - | - | - | - | 13.00 | | |
| 3 | 40.90 | 1.75 | 0.43 | 12.45 | 1.66 | 2.31 | 2.88 | 9.16 | 9.80 | 11.00 |
| 4 | 61.00 | - | - | - | - | - | - | 48.00 | | |
| 5 | 70.15 | 1.76 | 0.09 | 16.20 | 2.79 | 3.78 | 5.35 | 20.30 | 19.60 | 21.90 |
| 6 | 80.30 | - | - | - | - | - | - | 83.00 | | |
| 7 | 99.00 | 1.30 | 0.00 | 40.80 | 5.20 | 6.70 | 12.90 | 35.70 | 37.60 | 36.00 |
| 8 | 127.00 | 1.60 | 0.00 | 87.40 | 3.90 | 10.30 | 20.20 | 52.60 | 56.00 | 56.50 |
| 9 | 143.50 | 1.50 | -0.50 | 103.00 | 10.50 | 13.50 | 26.00 | 65.40 | 68.60 | 71.00 |
| 10 | 167.00 | 1.20 | 0.00 | 139.50 | 12.80 | 15.40 | 37.80 | 82.30 | 87.50 | 96.70 |

## TABLE (D-6)

### Pressure Drops (in. Water)

Sugar Solution No. 2
Pipe Dia. 1/2 in.

Fluid Temp. 66.8$^{O}$F

| RUN NO. | FLOW (GAL./MIN.) | PRESSURE TAP LOCATION | | | | | | | | | |
|---|---|---|---|---|---|---|---|---|---|---|---|
| | | 1A-3A | 3A-4A | 4A-1 | 1-2 | 2-3 | 3-4 | 4-5 | 5-6 | 6-7 | 7-8 |
| 1 | 6.00 | 1.01 | 0.43 | 21.10 | 2.60 | 3.10 | 6.80 | 24.30 | 24.30 | 24.30 | 25.20 |
| 2 | 9.70 | 0.74 | 0.45 | 52.80 | 4.90 | 8.60 | 15.70 | 54.60 | 53.80 | 54.90 | 58.10 |
| 3 | 14.00 | 0.80 | 0.34 | 119.20 | 8.90 | 17.10 | 32.20 | 109.50 | 105.50 | 110.10 | 116.10 |
| 4 | 21.20 | 1.12 | 0.21 | 272.50 | 17.90 | 41.50 | 64.80 | 242.10 | 239.70 | 236.50 | 250.50 |
| 5 | 27.50 | 1.10 | 0.00 | 450.00 | 26.10 | 69.20 | 97.80 | 380.50 | 343.00 | 369.70 | 390.00 |
| 6 | 32.00 | 1.80 | 0.30 | 595.00 | 30.70 | 93.00 | 122.50 | 488.20 | 434.00 | 473.00 | 496.50 |
| 7 | 35.00 | - | - | 702.00 | 39.60 | 105.80 | 140.30 | 565.00 | 505.00 | 544.00 | 574.00 |

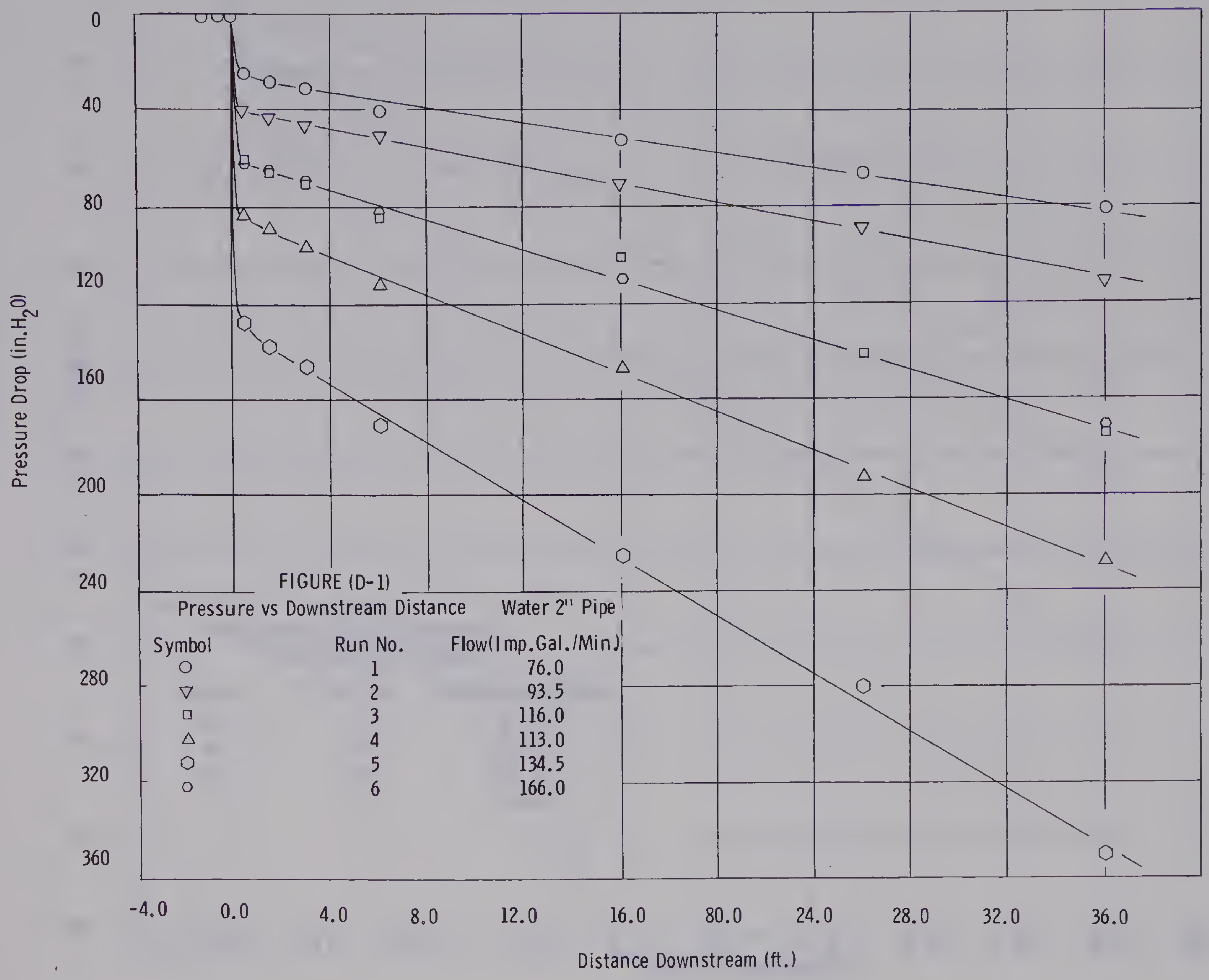

FIGURE (D-1)
Pressure vs Downstream Distance Water 2" Pipe

| Symbol | Run No. | Flow(Imp.Gal./Min.) |
|---|---|---|
| ○ | 1 | 76.0 |
| ▽ | 2 | 93.5 |
| □ | 3 | 116.0 |
| △ | 4 | 113.0 |
| ⬡ | 5 | 134.5 |
| ⬡ | 6 | 166.0 |

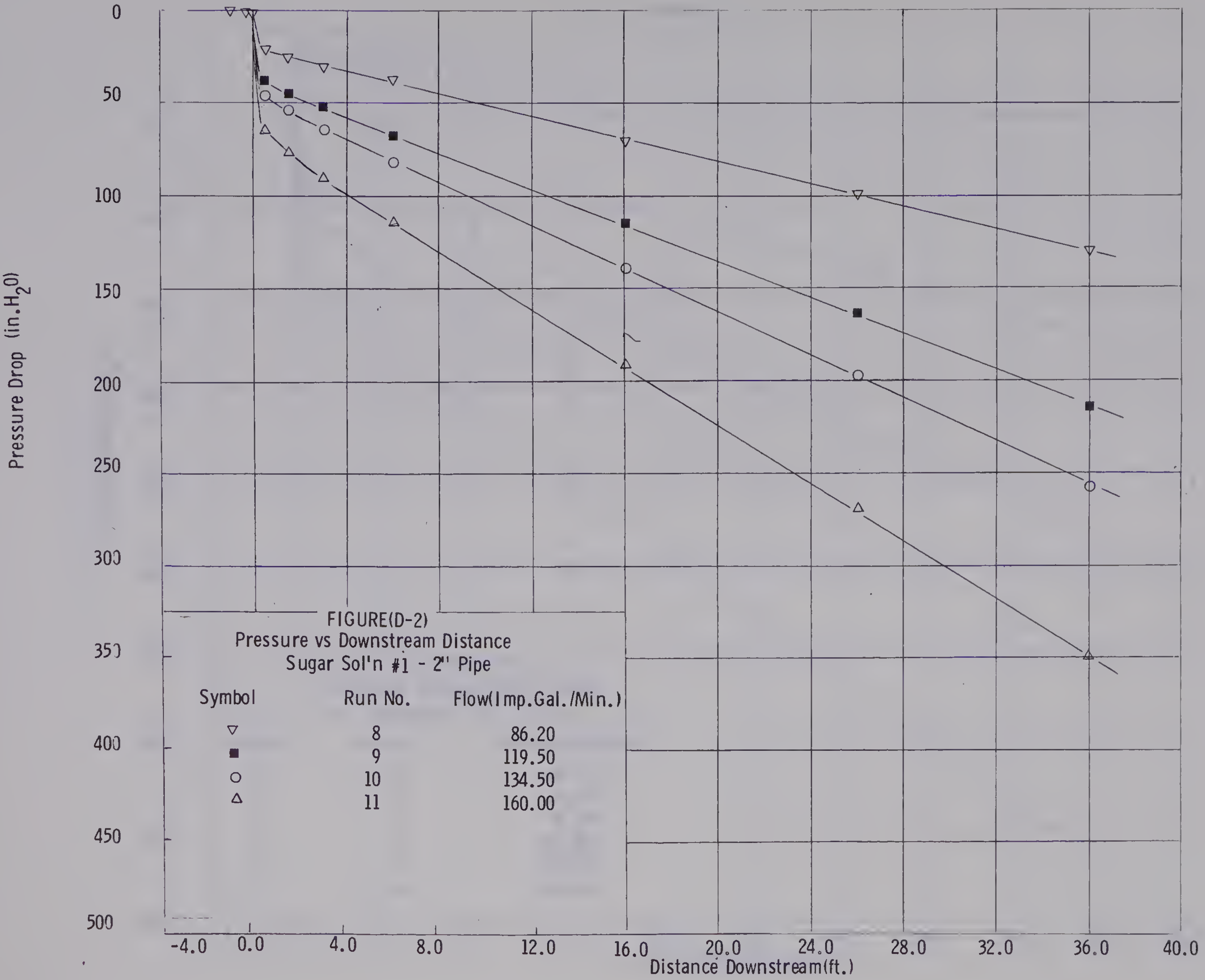

FIGURE(D-2)
Pressure vs Downstream Distance
Sugar Sol'n #1 - 2" Pipe

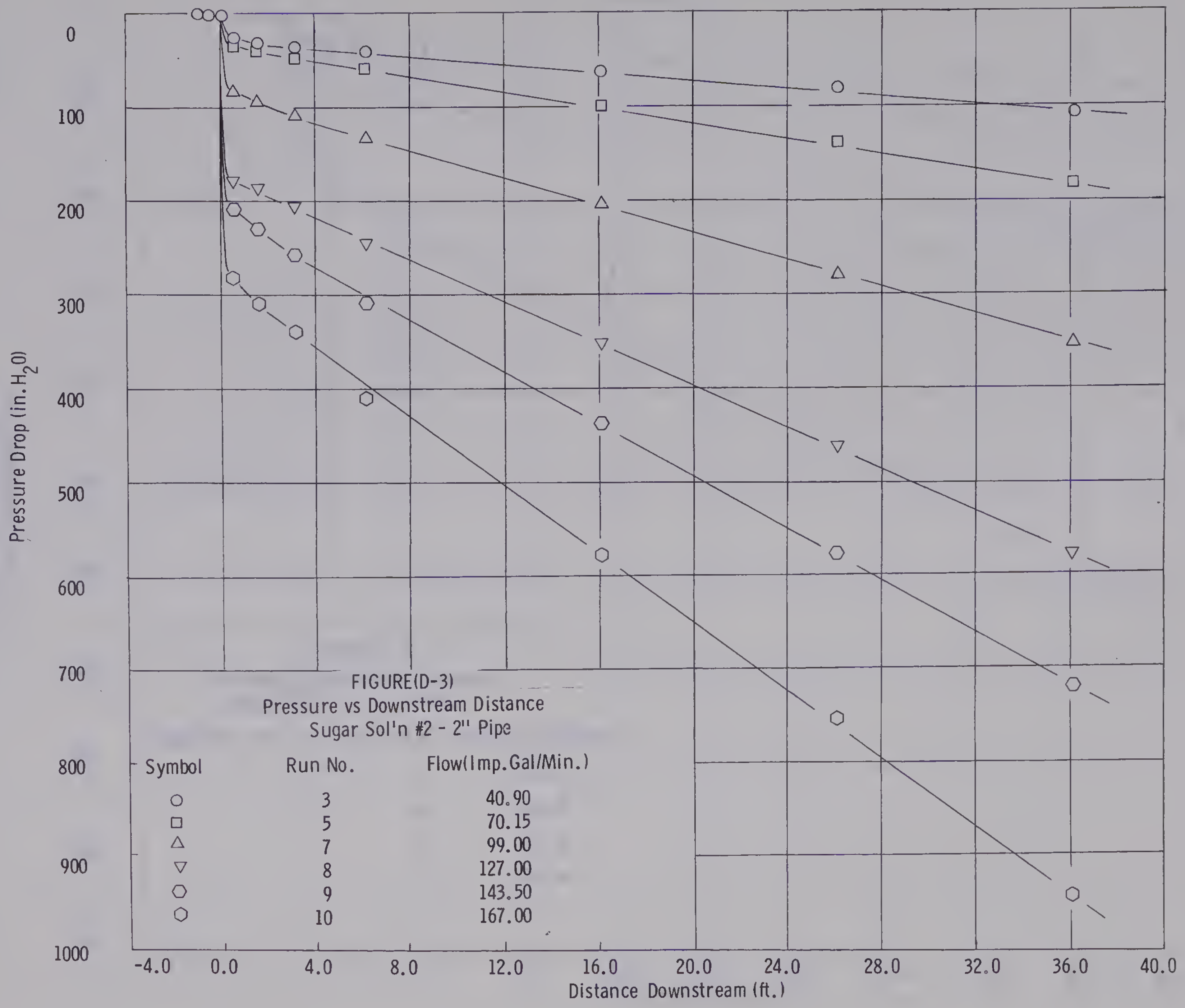

FIGURE(D-3)
Pressure vs Downstream Distance
Sugar Sol'n #2 - 2" Pipe

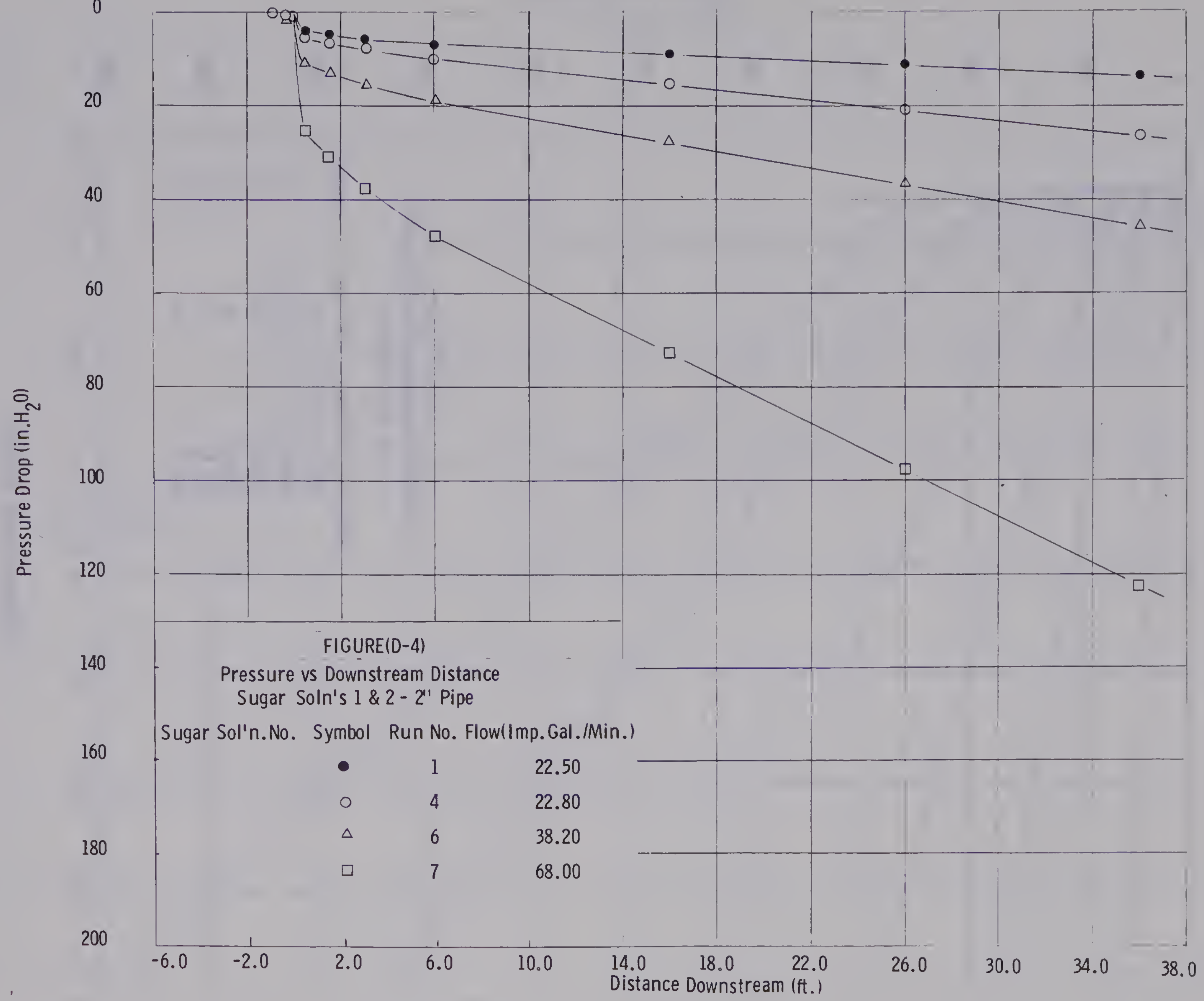

FIGURE(D-4)
Pressure vs Downstream Distance
Sugar Soln's 1 & 2 - 2" Pipe

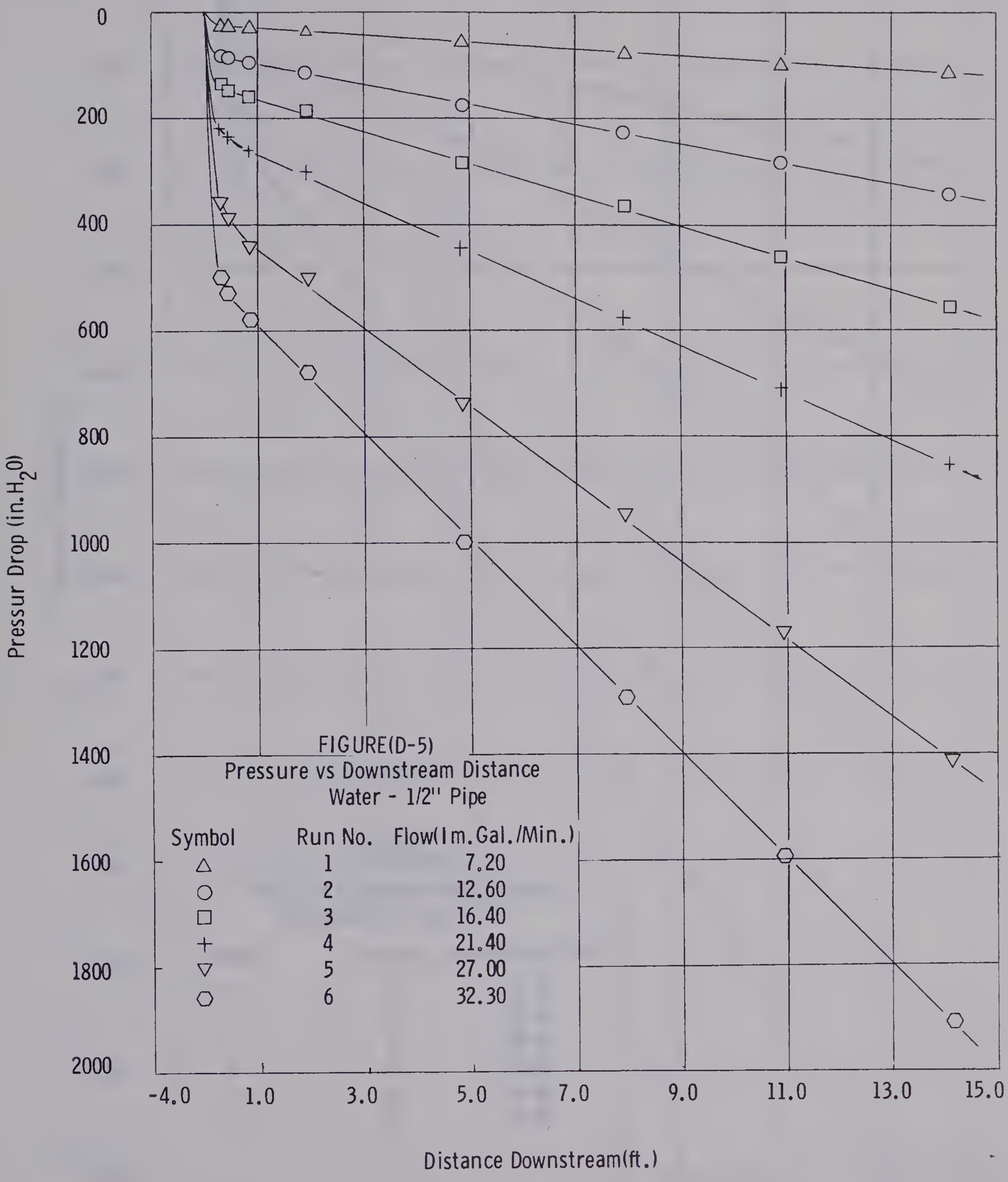

FIGURE(D-5)
Pressure vs Downstream Distance
Water - 1/2" Pipe

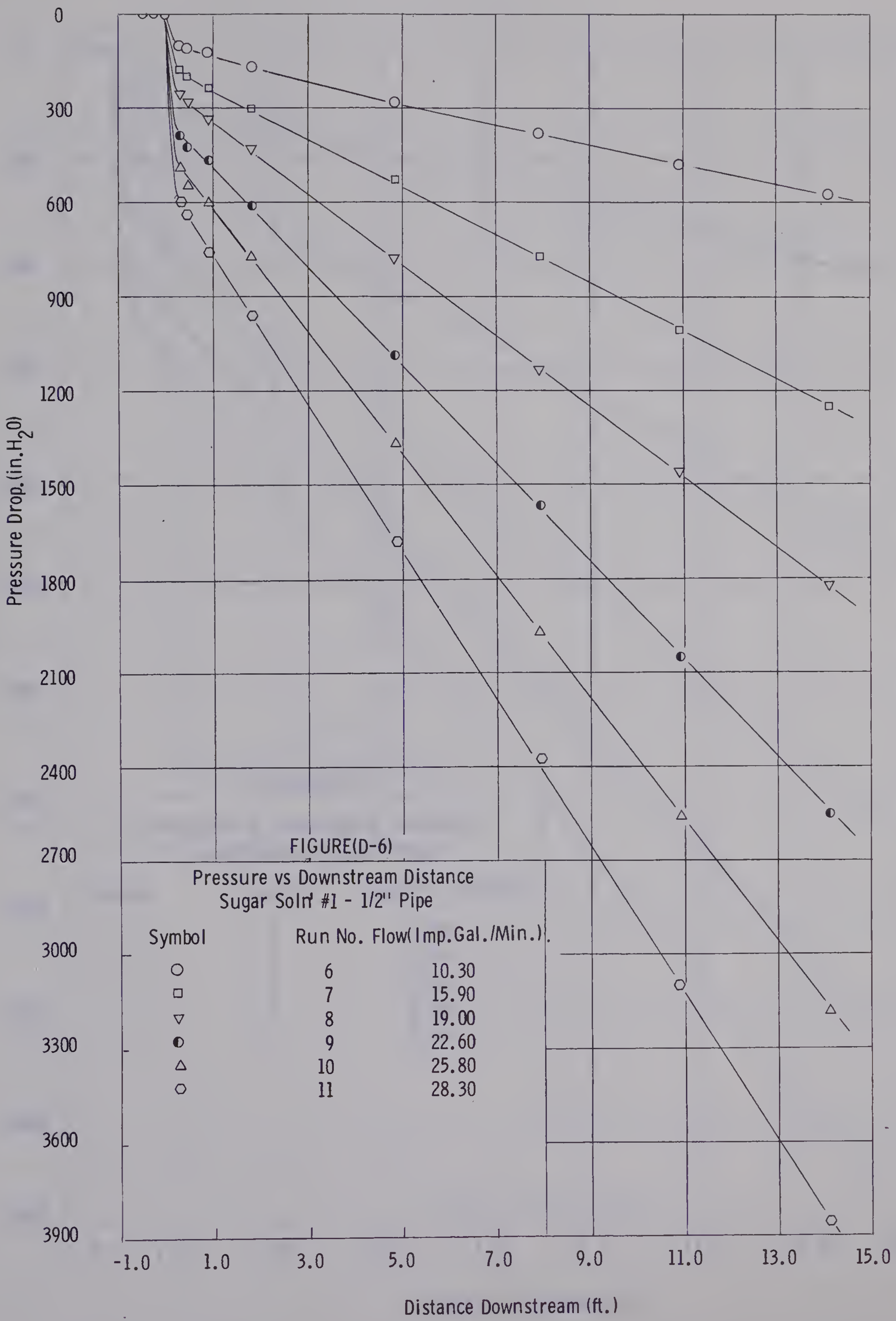

FIGURE(D-6)

Pressure vs Downstream Distance
Sugar Soln #1 - 1/2" Pipe

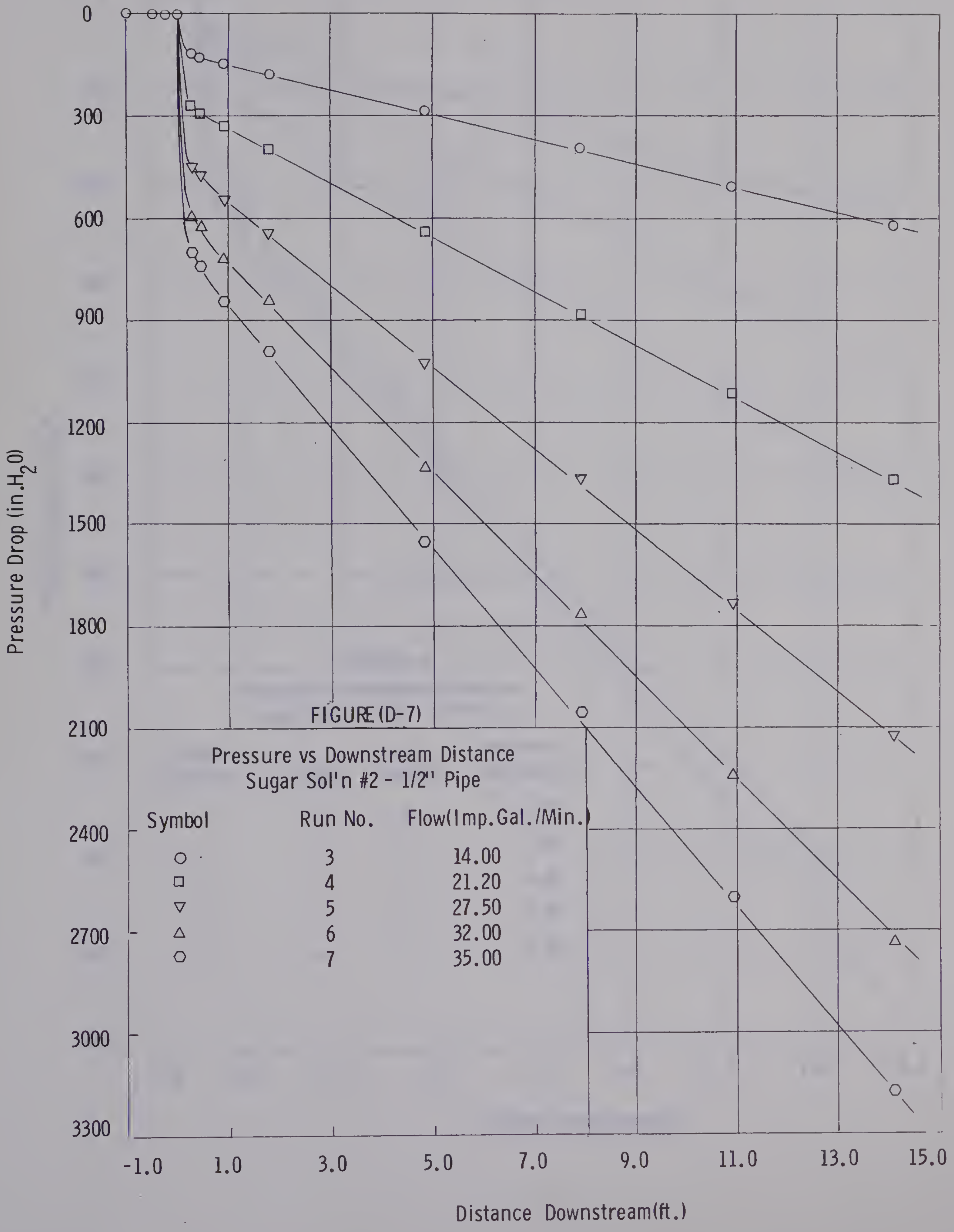

FIGURE (D-7)

Pressure vs Downstream Distance
Sugar Sol'n #2 - 1/2" Pipe

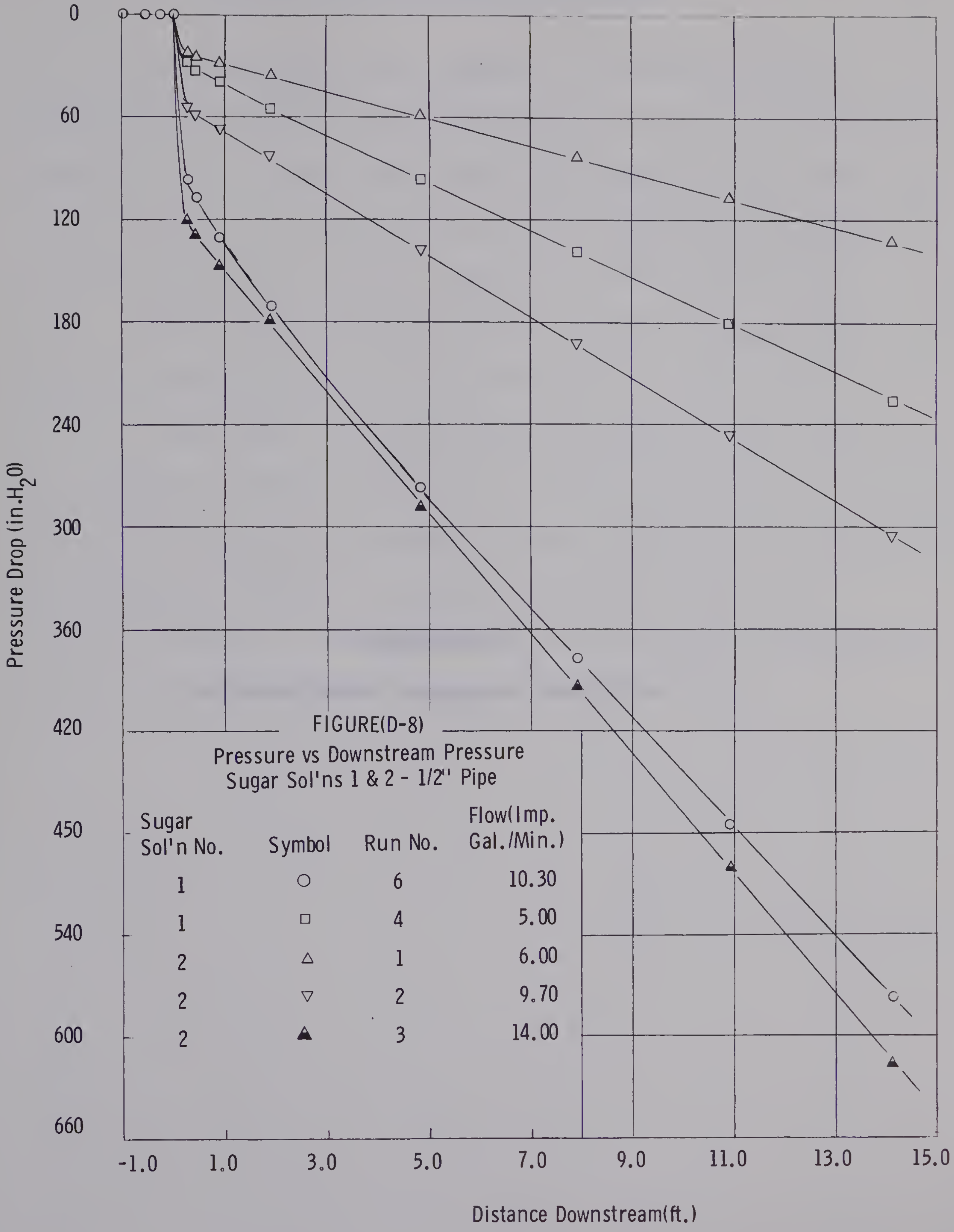

FIGURE(D-8)
Pressure vs Downstream Pressure
Sugar Sol'ns 1 & 2 - 1/2" Pipe

# Appendix E

# Viscoelastic Pressure Profiles

# VISCOELASTIC PRESSURE PROFILES

Due to significant amounts of degradation and the unusual types of pressure profiles for the solutions studied new solutions were used extensively. This provided a check for reproducibility and clearly indicated the above effects on entry length and contraction loss.

Table (E-1) lists the order of the figures and describes when fresh solutions were used. Table (E-6) to (E-9) tabulates the experimental pressure drops that are plotted in Figures (E-1) to (E-18). From these figures one is able to measure entry lengths and contraction losses as well as calculating Reynolds numbers and friction factors. These measured and calculated variables are tabulated on Tables (E-2) to (E-5) inclusive.

TABLE (E-1)

| FIGURE NO. | ET-597 % CONC. | PIPE DIA. (IN) | COMMENTS |
|---|---|---|---|
| E-1 to E-3 | 0.20 | 2 | - Fresh solution<br>- Low to high flow rates<br>- Figure E-3 reproduce data with another fresh solution (Runs 10 to 20). |
| E-4 to E-7 | 0.20 | 1/2 | - Used solution from above<br>- Low to high flow rates |
| E-8 to E-10 | 0.01 | 2 | - Fresh solution<br>- Low to high flow rates for runs (1-14).<br>- Runs (15-22) reproduce the above data, with another fresh solution. Located in Chapter 4, Figure (4.10) |
| E-11 to E-13 | 0.01 | 1/2 | - Fresh solution<br>- Low to high flow rates for runs 1 to 11 inclusive. |
| E-14 to E-16 | 0.01 | 1/2 | - Fresh solution<br>- High to low flow rates for runs 12 to 24 inclusive. |
| E-17 to E-18 | 0.01 | 1/2 | - Fresh non-degradated solution<br>- Low flow rates only for runs 25 to 29 inclusive. |

## TABLE (E-2)

% Conc.: 0.20 Fluid Temp.: 68.0°F

Pipe Dia.: 2 in. Room Temp.: 70.0°F

| RUN NO. | $\frac{V\theta}{D} \times 10^2$ | $N_{Re}'$ | $f \times 10^3$ | $\Delta P_c$ (IN.$H_2O$) | $L_e/D$ |
|---|---|---|---|---|---|
| 1 | 35.93 | 1236 | 18.033 | 2.32 | 8.70 |
| 2 | 39.09 | 2659 | 8.874 | 5.55 | 17.50 |
| 3 | 50.89 | 5326 | 4.014 | 16.05 | 93.00 |
| 4 | 54.30 | 9564 | 2.316 | 36.50 | 40.60 |
| 5 | 51.56 | 14364 | 1.710 | 54.00 | 75.70 |
| 6 | 42.12 | 20117 | 1.513 | 82.50 | 35.00 |
| 7 | 49.80 | 25225 | 1.085 | 116.00 | 122.00 |
| 8 | 47.59 | 19211 | 1.422 | 85.00 | 110.00 |
| 9 | 53.21 | 29643 | 0.900 | 154.00 | 134.00 |
| 10 | 46.99 | 19490 | 1.422 | 89.50 | 93.00 |
| 11 | 38.47 | 24786 | 1.365 | 119.50 | 139.00 |
| 12 | 29.47 | 18306 | 2.183 | 78.00 | 35.00 |
| 13 | 30.58 | 31797 | 1.337 | 149.00 | 35.00 |
| 14 | 33.04 | 25658 | 1.503 | 110.00 | 47.00 |
| 15 | 30.78 | 19826 | 1.983 | 76.50 | 35.00 |
| 16 | 36.46 | 2267 | 1.072 | 5.30 | 47.00 |
| 17 | 38.91 | 1265 | 1.661 | 2.30 | 8.70 |
| 18 | 51.17 | 17302 | 1.466 | 73.50 | 64.00 |
| 19 | 39.14 | 23297 | 1.423 | 106.00 | 116.00 |
| 20 | 38.37 | 31068 | 1.133 | 152.50 | 116.00 |

## TABLE (E-3)

% Conc.: 0.20

Pipe Dia.: 1/2 in.

Fluid Temp.: 69.0°F

Room Temp.: 70.0°F

| RUN NO. | $\frac{V\theta}{D} \times 10^2$ | $N_{Re}'$ | $f \times 10^3$ | $\Delta P_c$ ($IN.H_2O$) | $L_e/D$ |
|---|---|---|---|---|---|
| 1 | 89.06 | 3948 | 4.706 | 34.00 | 40.30 |
| 2 | 71.79 | 7872 | 3.091 | 80.00 | 86.50 |
| 3 | 70.13 | 14411 | 1.873 | 168.00 | 93.00 |
| 4 | 62.92 | 21641 | 1.441 | 293.00 | 92.00 |
| 5 | - | - | - | - | - |
| 6 | 53.56 | 32053 | 1.170 | 508.00 | 110.00 |
| 7 | 51.16 | 39108 | 1.020 | 673.00 | 124.00 |
| 8 | 43.01 | 45799 | 1.029 | 813.00 | 110.00 |
| 9 | - | - | - | - | - |
| 10 | 38.56 | 41266 | 1.238 | 24.75 | 86.30 |
| 11 | 34.59 | 50910 | 1.115 | 37.00 | 62.50 |
| 12 | 30.65 | 57913 | 1.123 | 38.75 | 67.20 |
| 13 | 29.60 | 71683 | 0.962 | 46.50 | 24.00 |
| 14 | 25.50 | 82836 | 0.968 | 66.75 | 28.80 |
| 15 | 24.31 | 88178 | 0.952 | 74.40 | 25.00 |
| 16 | 21.30 | 92145 | 1.027 | 73.25 | 13.50 |
| 17 | 24.30 | 81525 | 1.019 | 61.75 | 30.60 |
| 18 | 26.47 | 73679 | 1.435 | 47.50 | 44.00 |

[illegible]

[illegible] [illegible]

[illegible] [illegible]

| [illegible] | [illegible] | [illegible] | [illegible] | [illegible] | [illegible] |
|---|---|---|---|---|---|
| [illegible] | [illegible] | [illegible] | [illegible] | [illegible] | [illegible] |
| [illegible] | [illegible] | [illegible] | [illegible] | [illegible] | [illegible] |
| [illegible] | [illegible] | [illegible] | [illegible] | [illegible] | [illegible] |
| [illegible] | [illegible] | [illegible] | [illegible] | [illegible] | [illegible] |
|  | – | – | – | – | [illegible] |
| [illegible] | [illegible] | [illegible] | [illegible] | [illegible] | [illegible] |
| [illegible] | [illegible] | [illegible] | [illegible] | [illegible] | [illegible] |
| [illegible] | [illegible] | [illegible] | [illegible] | [illegible] | [illegible] |
| – | – | – | – | – | [illegible] |
| [illegible] | [illegible] | [illegible] | [illegible] | [illegible] | [illegible] |
| [illegible] | [illegible] | [illegible] | [illegible] | [illegible] | [illegible] |
| [illegible] | [illegible] | [illegible] | [illegible] | [illegible] | [illegible] |
| [illegible] | [illegible] | [illegible] | [illegible] | [illegible] | [illegible] |
| [illegible] | [illegible] | [illegible] | [illegible] | [illegible] | [illegible] |
| [illegible] | [illegible] | [illegible] | [illegible] | [illegible] | [illegible] |
| [illegible] | [illegible] | [illegible] | [illegible] | [illegible] | [illegible] |
| [illegible] | [illegible] | [illegible] | [illegible] | [illegible] | [illegible] |
| [illegible] | [illegible] | [illegible] | [illegible] | [illegible] | [illegible] |

## TABLE (E-4)

% Conc.: 0.01 Fluid Temp.: 65.5°F

Pipe Dia.: 2 in. Room Temp.: 73.0°F

| RUN NO. | $\frac{V\theta}{D} \times 10^2$ | $N'_{Re}$ | $f \times 10^3$ | $\Delta P_c$ (IN. $H_2O$) | $L_e/D$ |
|---|---|---|---|---|---|
| 1 | 1.30 | 33841 | 5.145 | 2.30 | 35.00 |
| 2 | 1.38 | 45755 | 4.433 | 3.60 | 40.60 |
| 3 | 1.44 | 70790 | 3.902 | 7.70 | 23.20 |
| 4 | 1.40 | 58013 | 4.183 | 5.40 | 46.50 |
| 5 | 1.47 | 103941 | 3.547 | 15.50 | 35.00 |
| 6 | 1.52 | 104632 | 3.334 | 15.20 | 24.20 |
| 7 | 1.56 | 123797 | 3.113 | 24.00 | 46.50 |
| 8 | 1.62 | 138128 | 2.875 | 31.00 | 26.10 |
| 9 | 1.54 | 172660 | 3.078 | 46.50 | 175.00 |
| 10 | 1.50 | 207192 | 3.158 | 62.00 | 185.00 |
| 11 | 1.54 | 239134 | 2.945 | 88.00 | 93.00 |
| 12 | 1.57 | 290587 | 2.760 | 128.00 | 174.00 |
| 13 | 1.81 | 203394 | 2.206 | 62.00 | 163.00 |
| 14 | 1.40 | 288343 | 3.424 | 130.00 | 174.00 |
| 15 | 1.31 | 30215 | 5.140 | 1.20 | 2.90 |
| 16 | 1.75 | 174387 | 2.400 | 43.00 | 151.00 |
| 17 | 1.81 | 208919 | 2.210 | 69.00 | 174.00 |
| 18 | 1.85 | 221523 | 2.104 | 78.00 | 163.00 |
| 19 | 1.83 | 241724 | 2.124 | 87.00 | 180.00 |
| 20 | 1.86 | 270213 | 2.019 | 112.00 | 182.00 |
| 21 | 1.84 | 296112 | 2.057 | 136.00 | 188.00 |
| 22 | 1.81 | 290587 | 2.112 | 132.00 | 186.00 |

## TABLE (E-5)

% Conc.: 0.01 | Fluid Temp.: 67.5°F

Pipe Dia.: 1/2 in. | Room Temp.: 74.0°F

| RUN NO. | $\frac{8V}{D} \times 10^2$ | $N'_{Re}$ | $f \times 10^3$ | $\Delta P_c$ (IN. $H_2O$) | $L_e/D$ |
|---|---|---|---|---|---|
| 1* | 4.91 | 28517 | 3.523 | 12.00 | 48.00 |
| 2* | 5.94 | 55893 | 2.274 | 43.00 | 58.00 |
| 3* | 6.00 | 77566 | 2.142 | 82.00 | 58.00 |
| 4* | 6.15 | 107794 | 1.960 | 175.00 | 48.00 |
| 5* | 5.74 | 145437 | 2.153 | 325.00 | 25.00 |
| 6* | 5.67 | 169391 | 2.160 | 430.00 | 24.00 |
| 7 | 5.43 | 193916 | 2.304 | 57.00 | 9.60 |
| 8 | 5.18 | 221292 | 2.481 | 76.00 | 9.60 |
| 9 | 5.02 | 250950 | 2.582 | 95.00 | 5.00 |
| 10 | 4.79 | 274905 | 2.793 | 119.00 | 5.00 |
| 11** | 4.48 | 288023 | 3.151 | 131.00 | 19.00 |
| 12 | 4.98 | 292015 | 2.569 | 1370.00 | 153.00 |
| 13** | 4.74 | 275475 | 2.839 | 1220.00 | 210.00 |
| 14** | 4.42 | 246388 | 3.279 | 1055.00 | 173.00 |
| 15** | 4.39 | 232129 | 3.352 | 927.00 | 180.00 |
| 16** | 4.33 | 196768 | 3.521 | 615.00 | 170.00 |
| 17** | 4.16 | 174524 | 3.848 | 470.00 | 38.00 |
| 18** | 4.51 | 157985 | 3.345 | 328.00 | 27.00 |
| 19** | 4.46 | 138023 | 3.472 | 275.00 | 9.60 |
| 20** | 4.29 | 102091 | 3.867 | 153.00 | 9.50 |
| 21** | 4.18 | 71863 | 4.260 | 75.00 | 14.30 |
| 22** | 3.86 | 34220 | 5.406 | 17.50 | 5.50 |
| 23** | 3.92 | 28517 | 5.360 | 8.50 | 5.50 |
| 24** | 3.76 | 51330 | 5.411 | 43.00 | 7.70 |
| 25* | 6.18 | 37072 | 2.214 | 20.00 | 19.30 |
| 26* | 5.62 | 27376 | 2.747 | 9.80 | 14.50 |
| 27* | 5.83 | 13688 | 2.796 | 1.55 | 86.00 |
| 28* | 5.61 | 7699 | 3.227 | 0.75 | 96.00 |
| 29* | 4.94 | 19962 | 3.646 | 5.00 | 5.50 |

---

* These runs were used to determine the friction factors for the non-degradated solution on Figure (4.5).

** These runs were used to determine the friction factors for the degradated solution on Figure (4.5).

## TABLE (E-6)

## PRESSURE DROP (in. WATER)

% Conc.: 0.20

Pipe Dia. 2 in.

Fluid Temp.: 68.8°F

Room Temp.: 70.8°F

| RUN NO. | FLOW (GAL./MIN.) | PRESSURE TAP LOCATION | | | | | | | | |
|---|---|---|---|---|---|---|---|---|---|---|
| | | 1A-2A | 2A-3A | 3A-1 | 1-2 | 2-3 | 3-4 | 4-5 | 5-6 | 6-7 |
| 1 | 18.80 | - | - | 2.58 | 0.58 | 0.57 | 1.04 | 3.31 | 3.29 | 3.32 |
| 2 | 30.50 | - | - | 5.21 | 0.84 | 0.84 | 1.38 | 4.29 | 4.48 | 4.68 |
| 3 | 49.50 | - | - | 14.50 | 1.18 | 1.31 | 2.19 | 5.90 | 5.75 | 5.61 |
| 4 | 74.50 | - | - | 31.05 | 1.44 | 1.56 | 3.19 | 8.15 | 8.05 | 7.35 |
| 5 | 99.00 | 0.214 | 0.036 | 51.10 | 1.47 | 1.77 | 4.32 | 10.83 | 10.41 | 9.58 |
| 6 | 125.00 | 0.199 | 0.199 | 81.00 | 0.47 | 2.40 | 6.68 | 13.70 | 15.08 | 13.52 |
| 7 | 147.50 | 0.323 | -0.430 | 107.60 | -0.86 | 1.50 | 7.55 | 16.90 | 21.40 | 8.37 |
| 8 | 121.50 | 0.392 | 0.392 | 81.70 | -1.47 | 2.11 | 6.32 | 14.10 | 16.70 | 7.00 |
| 9 | 165.00 | 0.735 | -1.622 | 138.80 | -1.93 | 2.38 | 10.70 | 19.20 | 26.60 | 7.30 |
| 10 | 122.50 | - | - | 84.50 | 0.61 | 0.29 | 6.09 | 15.46 | 23.80 | 1.08 |
| 11 | 144.50 | - | - | 114.80 | -0.09 | 1.48 | 6.46 | 17.90 | 19.90 | 12.30 |

## TABLE (E-6) CONTINUED

## PRESSURE DROP (in.WATER)

| RUN NO. | FLOW (GAL./MIN.) | PRESSURE TAP LOCATION | | | | | | | | |
|---|---|---|---|---|---|---|---|---|---|---|
| | | 1A-2A | 2A-3A | 3A-1 | 1-2 | 2-3 | 3-4 | 4-5 | 5-6 | 6-7 |
| 12 | 116.70 | - | - | 76.70 | 0.48 | 2.37 | 7.20 | 14.70 | 15.00 | 15.00 |
| 13 | 171.20 | - | - | 153.70 | -3.10 | 1.96 | 10.30 | 21.70 | 24.90 | 22.40 |
| 14 | 147.50 | - | - | 112.30 | -2.14 | 2.12 | 8.90 | 19.20 | 19.10 | 18.70 |
| 15 | 122.80 | - | - | 79.20 | -1.66 | 2.62 | 7.30 | 16.60 | 19.90 | 17.10 |
| 16 | 27.30 | - | - | 4.69 | 0.65 | 0.75 | 1.58 | 3.98 | 3.87 | 3.96 |
| 17 | 18.30 | - | - | 2.31 | 0.86 | | 1.00 | 2.99 | 3.24 | 3.18 |
| 18 | 113.00 | - | - | 69.50 | 0.06 | 2.46 | 6.50 | 12.90 | 17.70 | 4.70 |
| 19 | 138.00 | - | - | 99.00 | -1.57 | 3.06 | 9.00 | 16.30 | 21.30 | 12.80 |
| 20 | 169.00 | - | - | 145.00 | -1.39 | 2.70 | 10.40 | 20.50 | 29.20 | 10.80 |

## TABLE (E-7)

## PRESSURE DROPS (in. WATER)

% Conc.: 0.20 Fluid Temp.: 69.0$^{o}$F

Pipe Dia.: 1/2 in. Room Temp.: 70.0$^{o}$F

| RUN NO. | FLOW (GAL.MIN.) | PRESSURE TAP LOCATION | | | | | | | | | | |
|---|---|---|---|---|---|---|---|---|---|---|---|---|
| | | 1A-2A | 2A-3A | 3A-4A | 4A-1 | 1-2 | 2-3 | 3-4 | 4-5 | 5-6 | 6-7 | 7-8 |
| 1 | 6.00 | 0.291 | 0.505 | 0.061 | 28.20 | 1.81 | 3.03 | 7.30 | 10.93 | 11.75 | 11.30 | 12.10 |
| 2 | 9.80 | 0.061 | 0.061 | - .153 | 71.77 | 2.67 | 5.12 | 9.08 | 23.00 | 19.30 | 19.40 | 21.20 |
| 3 | 15.10 | - | 0.230 | -0.306 | 153.90 | 4.03 | 8.80 | 12.88 | 34.30 | 29.00 | 28.50 | 32.60 |
| 4 | 20.20 | 0.123 | 0.123 | -0.750 | 260.90 | 5.65 | 12.42 | 16.80 | 49.80 | 38.50 | 39.10 | 45.10 |
| 5 | 26.80 | 0.565 | 0.245 | - .583 | 445.00 | 7.05 | 18.30 | 25.30 | 74.20 | 51.80 | 56.50 | 65.70 |
| 6 | 26.80 | - | - | - | 468.00 | 7.10 | 18.70 | 25.70 | 77.20 | 53.20 | 58.90 | 66.40 |
| 7 | 31.00 | -0.50 | -0.70 | -1.20 | 615.10 | 8.30 | 24.40 | 29.70 | 97.50 | 61.70 | 72.00 | 80.30 |
| 8 | 34.60 | - | - | - | 755.00 | 9.30 | 31.90 | 30.00 | 116.10 | 72.50 | 87.80 | 100.50 |
| 9 | - | - | - | - | - | - | - | - | - | - | - | - |
| 10 | 31.90 | - | - | - | 636.00 | 9.30 | 26.50 | 30.50 | 100.60 | 63.30 | 74.80 | 83.70 |
| 11 | 37.50 | - | - | - | 995.00 | 9.45 | 29.80 | 29.90 | 128.80 | 80.90 | 101.90 | 120.80 |

## TABLE (E-7) CONTINUED

### PRESSURE DROPS (in. WATER)

| RUN NO. | FLOW (GAL/MIN.) | PRESSURE TAP LOCATION | | | | | | | | | | |
|---|---|---|---|---|---|---|---|---|---|---|---|---|
| | | 1A-2A | 2A-3A | 3A-4A | 4A-1 | 1-2 | 2-3 | 3-4 | 4-5 | 5-6 | 6-7 | 7-8 |
| 12 | 40.50 | - | - | - | 1080.00 | 7.10 | 38.00 | 31.70 | 158.80 | 96.00 | 125.50 | 149.80 |
| 13 | 47.20 | - | - | - | 1302.00 | 8.30 | 45.00 | 36.40 | 176.20 | 107.50 | 146.80 | 176.70 |
| 14 | 52.00 | - | - | - | 1847.00 | 6.20 | 57.30 | 36.50 | 211.00 | 124.00 | 182.10 | 215.50 |
| 15 | 54.50 | - | - | - | 2042.00 | -2.10 | 68.00 | 41.50 | 223.00 | 133.50 | 199.50 | 231.00 |
| 16 | 56.00 | - | - | - | 2020.00 | 5.20 | 66.50 | 47.50 | 244.30 | 147.00 | 218.00 | 252.00 |
| 17 | 51.50 | - | - | - | 1683.00 | 9.20 | 34.00 | 30.00 | 114.50 | 67.00 | 95.00 | 114.00 |
| 18 | 48.00 | - | - | - | 1297.00 | 7.50 | 28.80 | 26.70 | 91.50 | 58.50 | 80.00 | 96.50 |

## TABLE (E-8)

## PRESSURE DROPS (in. WATER)

% Conc.: 0.01 Fluid Temp.: 65.5$^{O}$F

Pipe Dia.: 2 in. Room Remp.: 73.0$^{O}$F

| RUN NO. | FLOW (GAL./MIN.) | PRESSURE TAP LOCATION | | | | | | | | |
|---|---|---|---|---|---|---|---|---|---|---|
| | | 1A-2A | 2A-3A | 3A-1 | 1-2 | 2-3 | 3-4 | 4-5 | 5-6 | 6-7 |
| 1 | 19.60 | 0.093 | 0.093 | 1.59 | 0.29 | 0.32 | 0.62 | 0.98 | 1.33 | 1.12 |
| 2 | 26.50 | 0.093 | 0.031 | 2.84 | 0.35 | 0.49 | 0.80 | 1.63 | 2.14 | 1.77 |
| 3 | 41.00 | 0.124 | 0.000 | 6.95 | 0.64 | 0.85 | 1.74 | 3.29 | 3.20 | 3.80 |
| 4 | 33.60 | 0.093 | 0.031 | 4.35 | 0.55 | 0.65 | 1.26 | 2.51 | 2.62 | 2.78 |
| 5 | 60.20 | 0.154 | -0.123 | 14.95 | 1.04 | 1.04 | 2.68 | 5.55 | 8.61 | 7.35 |
| 6 | 60.60 | 0.154 | 0.031 | 14.80 | 1.06 | 1.01 | 2.48 | 5.70 | 5.70 | 7.00 |
| 7 | 71.70 | 0.061 | -0.123 | 22.50 | 1.41 | 1.18 | 3.46 | 7.27 | 7.37 | 9.15 |
| 8 | 80.00 | 0.107 | -0.245 | 29.30 | 1.62 | 1.32 | 4.28 | 8.20 | 8.55 | 10.52 |
| 9 | 100.00 | 0.153 | 0.261 | 46.80 | 1.16 | 1.89 | 6.15 | 10.97 | 13.10 | 17.18 |
| 10 | 120.00 | 0.093 | -0.276 | 61.30 | 2.76 | 2.10 | 8.31 | 15.23 | 16.90 | 23.30 |
| 11 | 138.50 | 0.062 | -0.400 | 82.80 | 4.07 | 2.53 | 11.88 | 21.00 | 23.50 | 32.30 |

# TABLE (E-8) CONTINUED

## PRESSURE DROPS (in. WATER)

| RUN NO. | FLOW (GAL./MIN.) | PRESSURE TAP LOCATION | | | | | | | | |
|---|---|---|---|---|---|---|---|---|---|---|
| | | 1A-2A | 2A-3A | 3A-1 | 1-2 | 2-3 | 3-4 | 4-5 | 5-6 | 6-7 |
| 12 | 168.30 | - | -0.461 | 129.20 | 5.95 | 2.68 | 16.50 | 22.65 | 39.70 | 44.70 |
| 13 | 117.80 | 0.030 | -0.122 | 60.60 | 1.24 | 2.01 | 7.45 | 11.00 | 16.40 | 23.50 |
| 14 | 167.00 | - | - | 124.80 | 6.60 | 6.80 | 16.70 | 27.00 | 32.10 | 54.60 |
| 15 | 17.50 | - | - | 1.13 | 0.34 | | 1.07 | | 0.80 | 0.90 |
| 16 | 101.00 | - | - | 42.50 | 1.44 | 1.39 | 4.87 | 10.20 | 11.30 | 14.00 |
| 17 | 121.00 | - | - | 63.40 | 4.50 | 4.30 | 7.40 | 13.10 | 14.60 | 18.50 |
| 18 | 128.30 | - | - | 70.70 | 4.40 | 4.40 | 8.30 | 14.00 | 16.40 | 19.80 |
| 19 | 140.00 | - | - | 84.50 | 4.60 | 4.50 | 9.80 | 15.60 | 18.40 | 23.80 |
| 20 | 156.50 | - | - | 105.00 | 4.40 | 4.20 | 11.90 | 18.00 | 21.40 | 28.10 |
| 21 | 171.50 | - | - | 128.50 | 4.50 | 4.50 | 14.20 | 21.50 | 25.10 | 34.60 |
| 22 | 168.30 | - | - | 126.00 | 5.30 | 3.80 | 14.80 | 26.30 | 24.00 | 34.20 |

### TABLE (E-9)

### PRESSURE DROPS (in.WATER)

% Conc.: 0.01 Fluid Temp.: 67.5°F

Pipe Dia.: 1/2 in. Room Temp.: 74°F

| RUN NO. | FLOW (GAL./MIN.) | PRESSURE TAP LOCATION | | | | | | | | | | |
|---|---|---|---|---|---|---|---|---|---|---|---|---|
| | | 1A-2A | 2A-3A | 3A-4A | 4A-1 | 1-2 | 2-3 | 3-4 | 4-5 | 5-6 | 6-7 | 7-8 |
| 1 | 5.00 | 0.091 | 0.091 | 0.091 | 11.92 | 0.53 | 1.14 | 1.87 | 5.86 | 5.66 | 5.86 | 6.29 |
| 2 | 9.80 | 0.091 | 0.076 | 0.091 | 42.40 | 1.42 | 2.92 | 4.15 | 15.32 | 13.40 | 15.23 | 15.60 |
| 3 | 13.60 | 0.122 | 0.091 | 0.106 | 82.00 | 2.72 | 4.88 | 6.84 | 28.70 | 23.70 | 28.10 | 28.30 |
| 4 | 18.90 | 0.122 | 0.030 | 0.060 | 168.80 | 6.08 | 8.48 | 14.10 | 52.50 | 42.00 | 50.50 | 50.00 |
| 5 | 25.50 | 0.122 | 0.061 | 0.061 | 327.00 | 12.15 | 16.00 | 22.00 | 101.90 | 78.20 | 97.30 | 100.50 |
| 6 | 29.70 | - | - | - | 425.50 | 16.80 | 20.40 | 29.30 | 137.40 | 104.10 | 130.00 | 136.10 |
| 7 | 34.00 | 0.50 | 1.00 | 1.50 | 561.70 | 24.30 | 40.40 | 34.90 | 193.50 | 139.70 | 181.50 | 190.20 |
| 8 | 38.80 | 0.20 | 0.30 | 0.50 | 738.00 | 27.00 | 49.30 | 46.80 | 263.00 | 188.20 | 247.20 | 266.70 |
| 9 | 44.00 | 0.16 | 0.31 | 0.61 | 940.61 | 30.50 | 65.80 | 61.70 | 351.50 | 256.60 | 331.20 | 357.00 |
| 10 | 48.20 | - | - | - | 1183.00 | 36.70 | 85.60 | 79.80 | 149.00 | 344.50 | 411.40 | 463.50 |
| 11 | 50.50 | 0.20 | 0.32 | 0.40 | 1312.40 | 43.20 | 104.10 | 103.70 | 552.20 | 427.80 | 513.30 | 574.00 |

## TABLE (E-9) CONTINUED

## PRESSURE DROPS (in. WATER)

| RUN NO. | FLOW (GAL./MIN.) | PRESSURE TAP LOCATION | | | | | | | | | | |
|---|---|---|---|---|---|---|---|---|---|---|---|---|
| | | 1A-2A | 2A-3A | 3A-4A | 4A-1 | 1-2 | 2-3 | 3-4 | 4-5 | 5-6 | 6-7 | 7-8 |
| 12 | 51.20 | - | - | - | 1454.00 | 17.40 | 85.80 | 55.00 | 465.00 | 329.00 | 426.00 | 481.00 |
| 13 | 48.30 | - | - | - | 1246.00 | 24.70 | 94.00 | 81.50 | 454.00 | 332.00 | 416.50 | 473.50 |
| 14 | 43.20 | - | - | - | 1080.00 | 24.80 | 92.00 | 76.40 | 419.50 | 312.40 | 390.30 | 437.10 |
| 15 | 40.70 | - | - | - | 997.00 | 23.60 | 79.80 | 71.90 | 382.50 | 290.00 | 347.50 | 396.50 |
| 16 | 34.50 | - | - | - | 651.00 | 18.20 | 59.40 | 56.20 | 286.80 | 321.30 | 264.10 | 299.30 |
| 17 | 30.60 | - | - | - | 516.20 | 10.20 | 56.90 | 50.50 | 246.60 | 193.10 | 227.40 | 257.30 |
| 18 | 27.70 | - | - | - | 381.50 | 12.10 | 36.00 | 35.60 | 172.00 | 135.30 | 161.50 | 183.50 |
| 19 | 24.20 | - | - | - | 280.50 | 9.50 | 28.70 | 28.50 | 135.80 | 108.50 | 127.60 | 145.20 |
| 20 | 17.90 | - | - | - | 152.70 | 7.60 | 17.20 | 18.00 | 84.30 | 69.90 | 79.00 | 88.50 |
| 21 | 12.60 | - | - | - | 74.30 | 3.80 | 9.20 | 10.60 | 45.80 | 39.00 | 43.60 | 48.30 |
| 22 | 6.00 | - | - | - | 18.50 | 0.742 | 2.43 | 3.46 | 12.90 | 12.00 | 12.85 | 13.96 |
| 23 | 5.00 | - | - | - | 10.53 | 0.070 | 1.62 | 2.51 | 8.85 | 8.34 | 8.87 | 9.57 |
| 24 | 9.00 | - | - | - | 43.30 | 1.71 | 6.80 | 7.40 | 29.90 | 26.20 | 28.60 | 31.30 |
| 25 | 6.50 | - | - | - | 19.80 | 0.462 | 1.49 | 1.88 | 6.54 | 5.63 | 6.08 | 6.68 |
| 26 | 4.80 | - | - | - | 10.00 | 1.11 | | 1.27 | 4.32 | 3.83 | 4.18 | 4.52 |
| 27 | 2.30 | - | - | - | 1.36 | 0.254 | | 0.60 | 0.97 | 1.00 | 1.05 | 1.15 |
| 28 | 1.35 | - | - | - | 0.316 | 0.917 | | | 0.354 | | 0.800 | |
| 29 | 3.50 | - | - | - | 5.19 | 0.676 | | 1.14 | 2.83 | 2.74 | 3.00 | 3.19 |

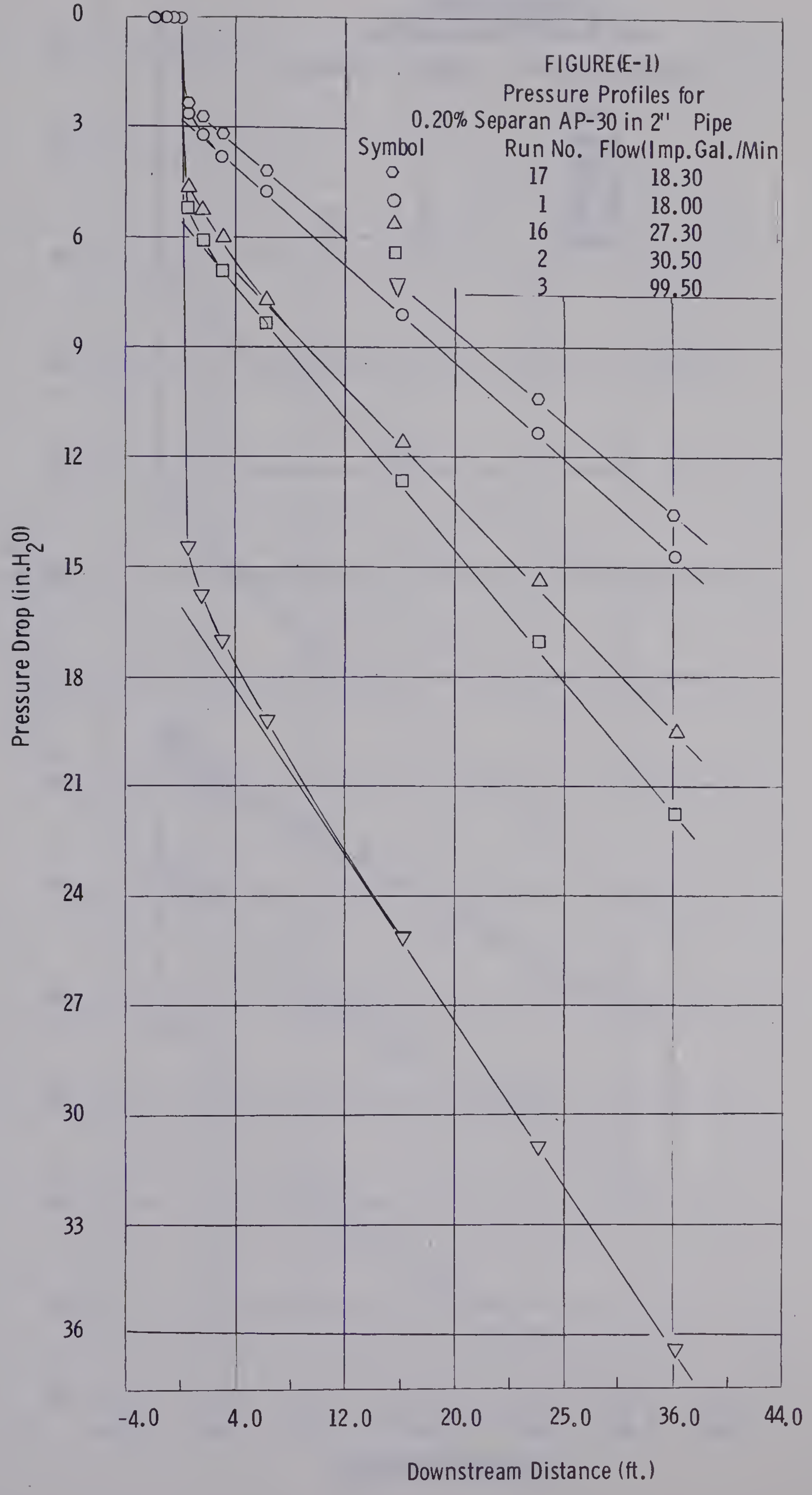

FIGURE(E-1)
Pressure Profiles for
0.20% Separan AP-30 in 2" Pipe

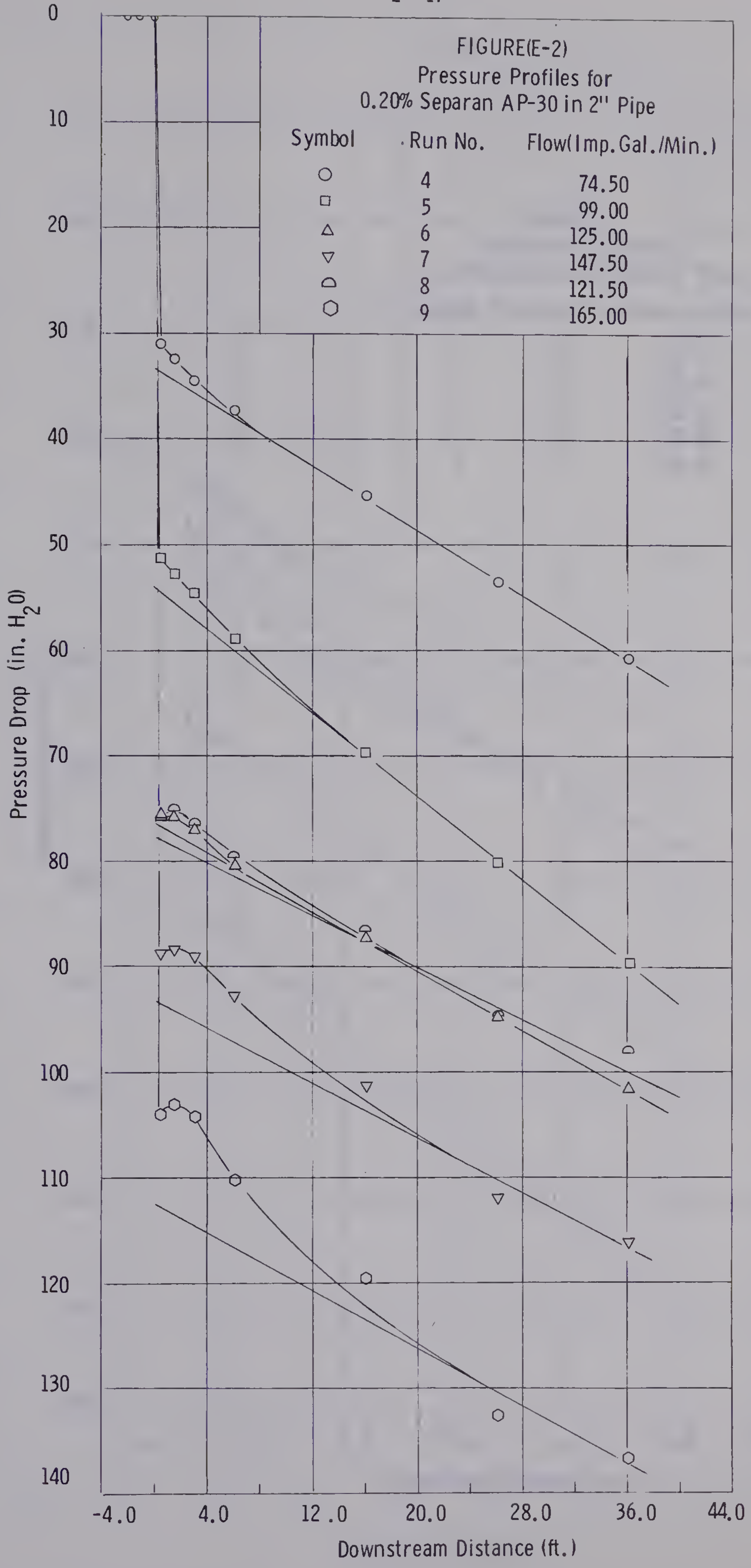

FIGURE(E-2)
Pressure Profiles for
0.20% Separan AP-30 in 2" Pipe

| Symbol | Run No. | Flow(Imp.Gal./Min.) |
|---|---|---|
| ○ | 4 | 74.50 |
| □ | 5 | 99.00 |
| △ | 6 | 125.00 |
| ▽ | 7 | 147.50 |
| ◠ | 8 | 121.50 |
| ⬡ | 9 | 165.00 |

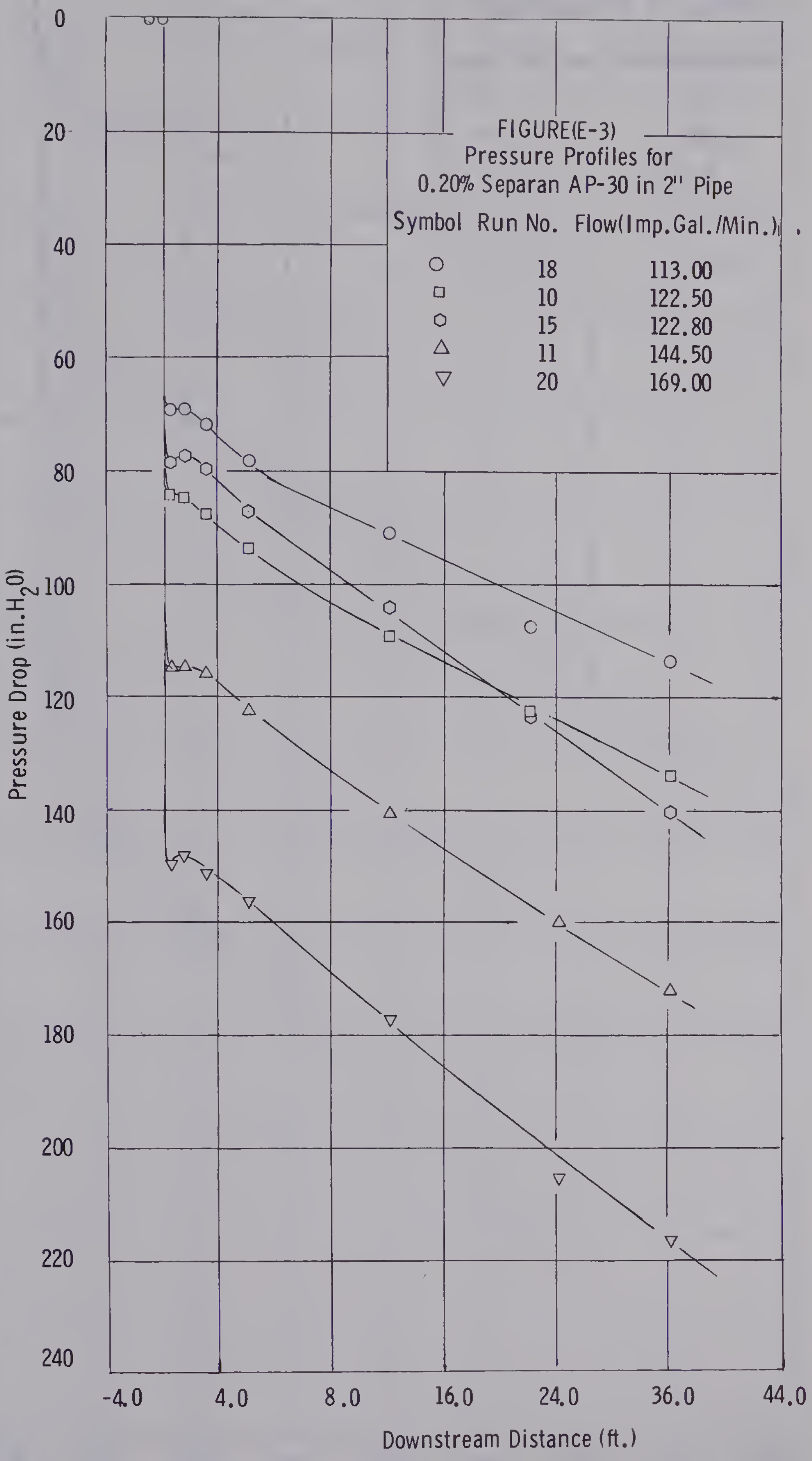

FIGURE(E-3)
Pressure Profiles for
0.20% Separan AP-30 in 2" Pipe

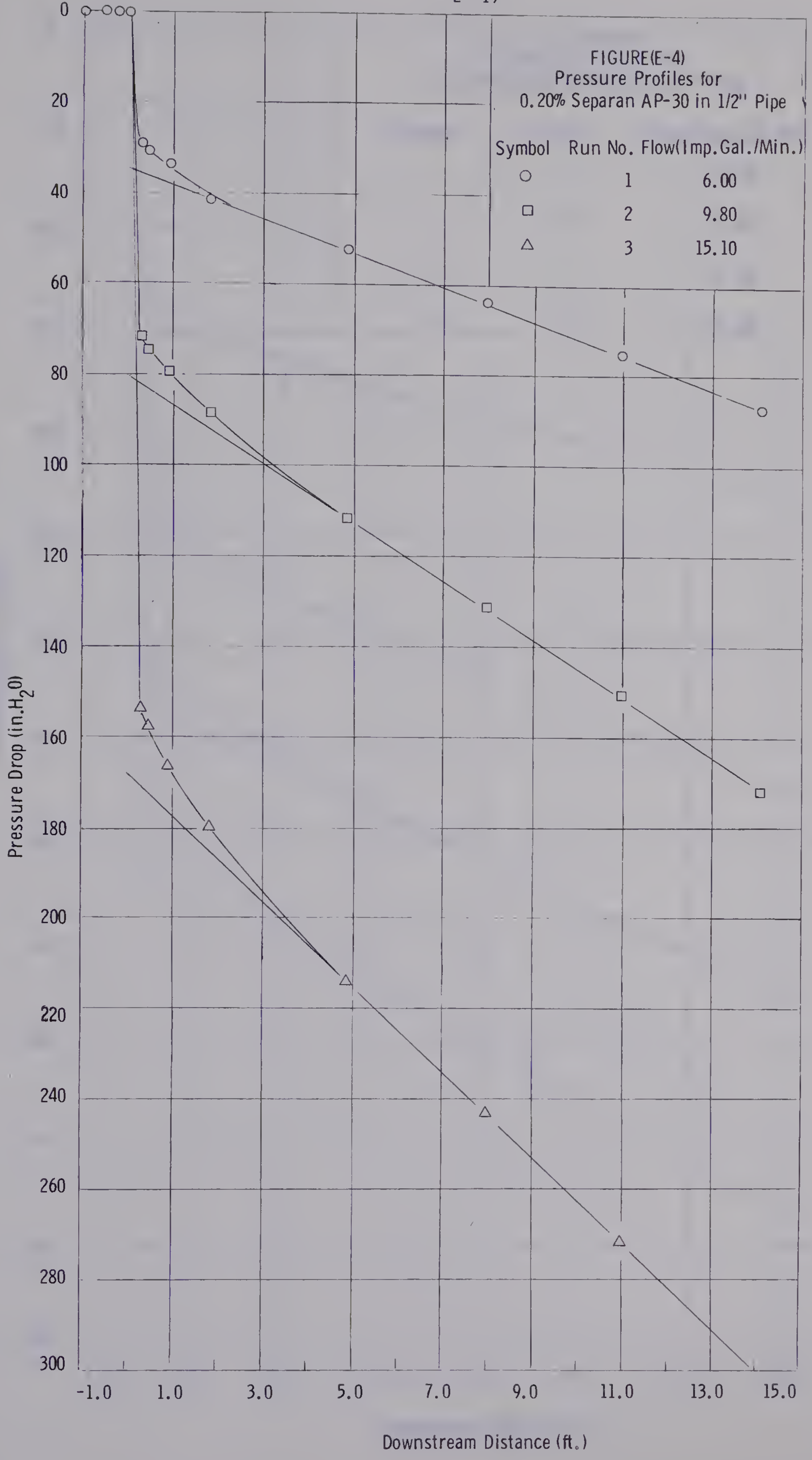

FIGURE(E-4)
Pressure Profiles for
0.20% Separan AP-30 in 1/2" Pipe

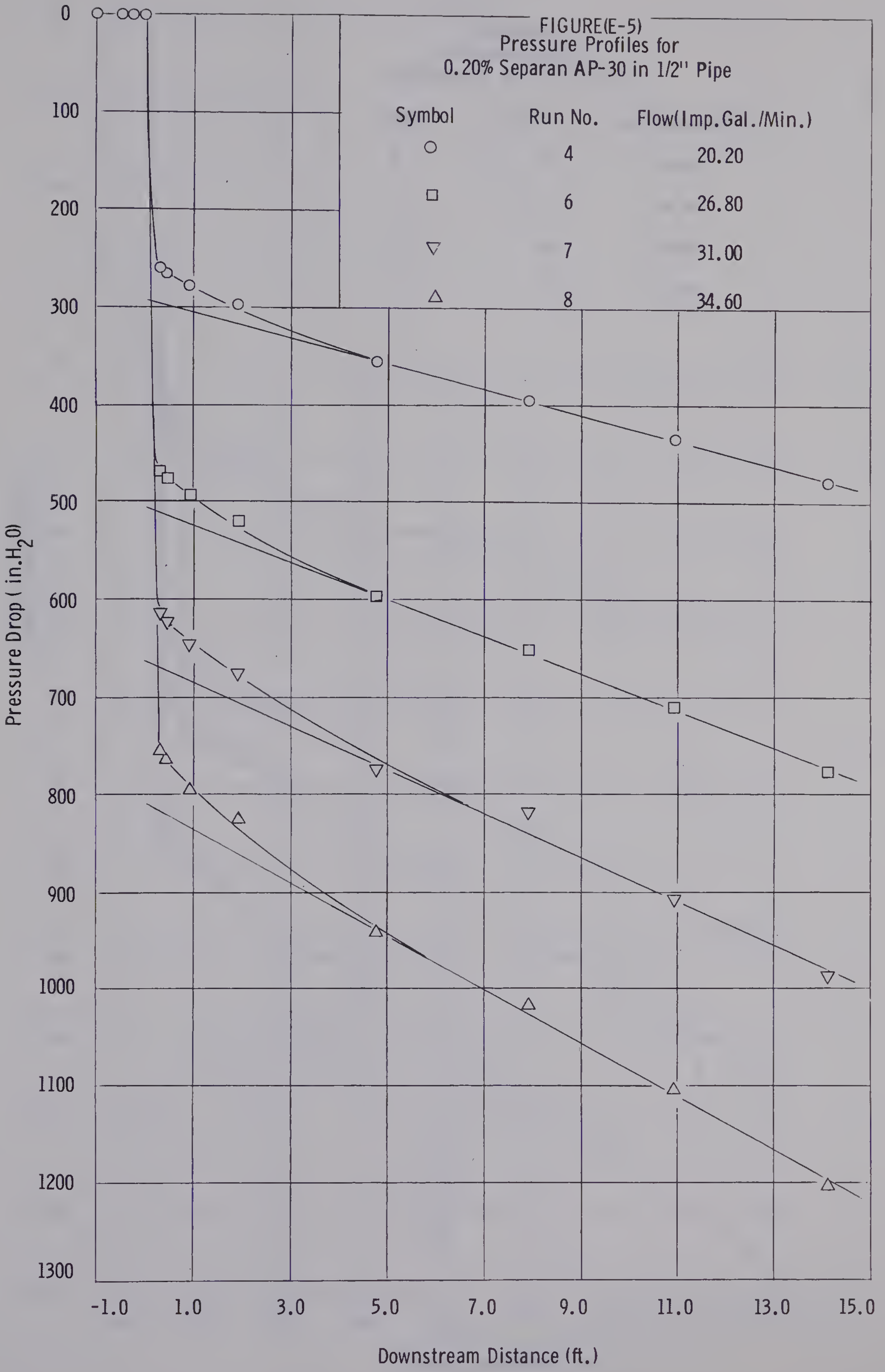

FIGURE(E-5) Pressure Profiles for 0.20% Separan AP-30 in 1/2" Pipe

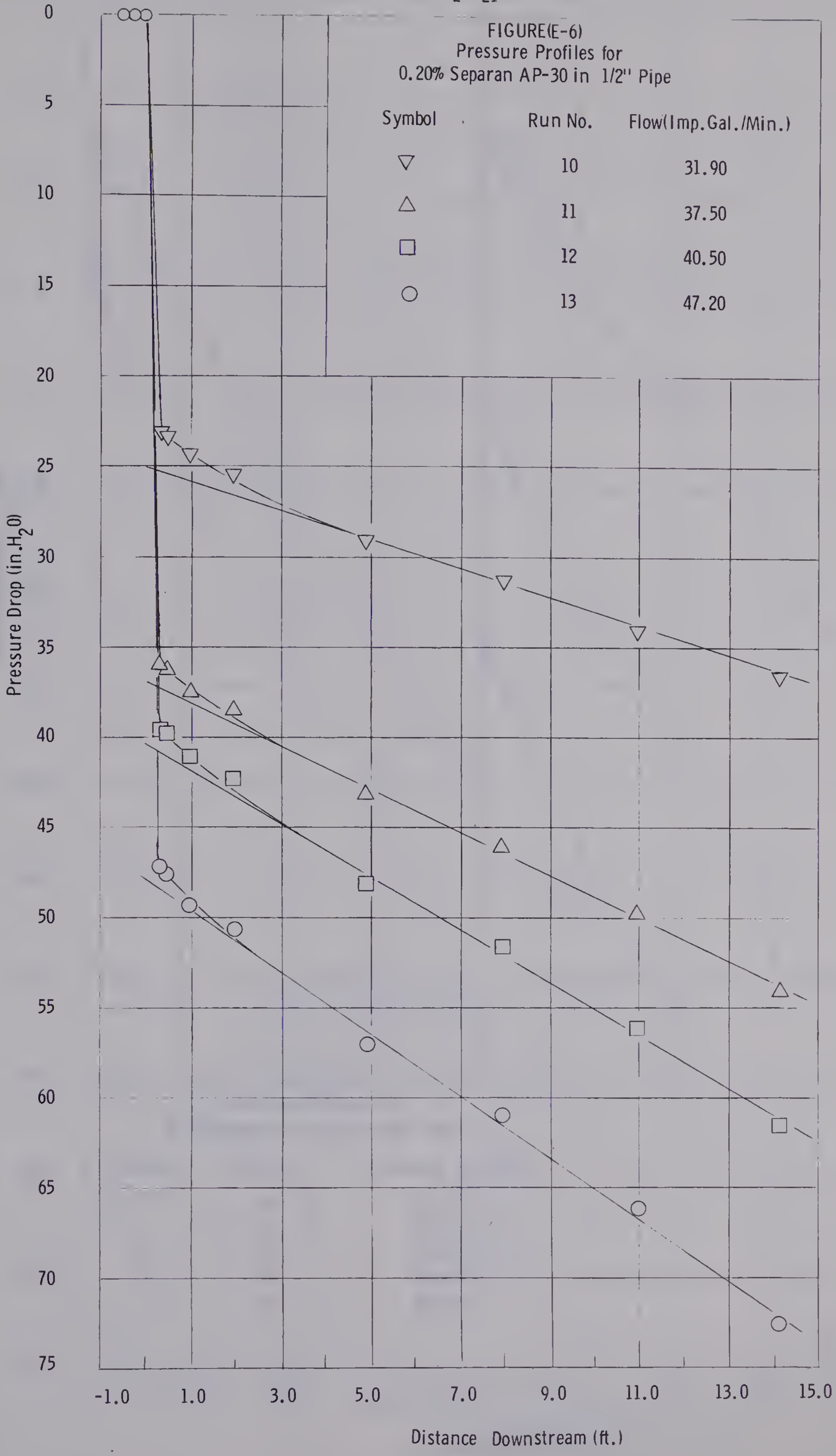

FIGURE(E-6)
Pressure Profiles for
0.20% Separan AP-30 in 1/2" Pipe

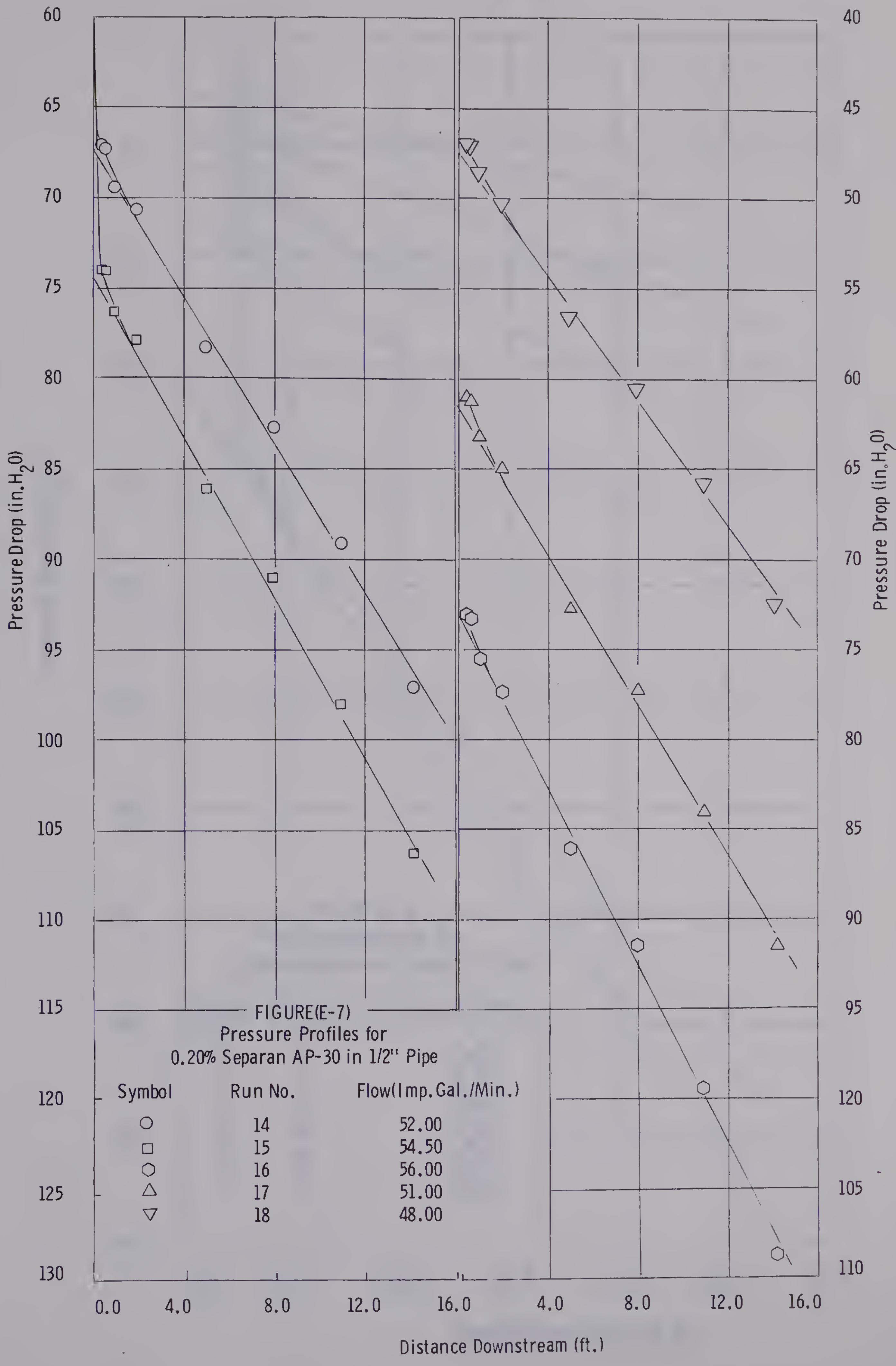

FIGURE(E-7)
Pressure Profiles for
0.20% Separan AP-30 in 1/2" Pipe

| Symbol | Run No. | Flow(Imp.Gal./Min.) |
|---|---|---|
| ○ | 14 | 52.00 |
| □ | 15 | 54.50 |
| ⬡ | 16 | 56.00 |
| △ | 17 | 51.00 |
| ▽ | 18 | 48.00 |

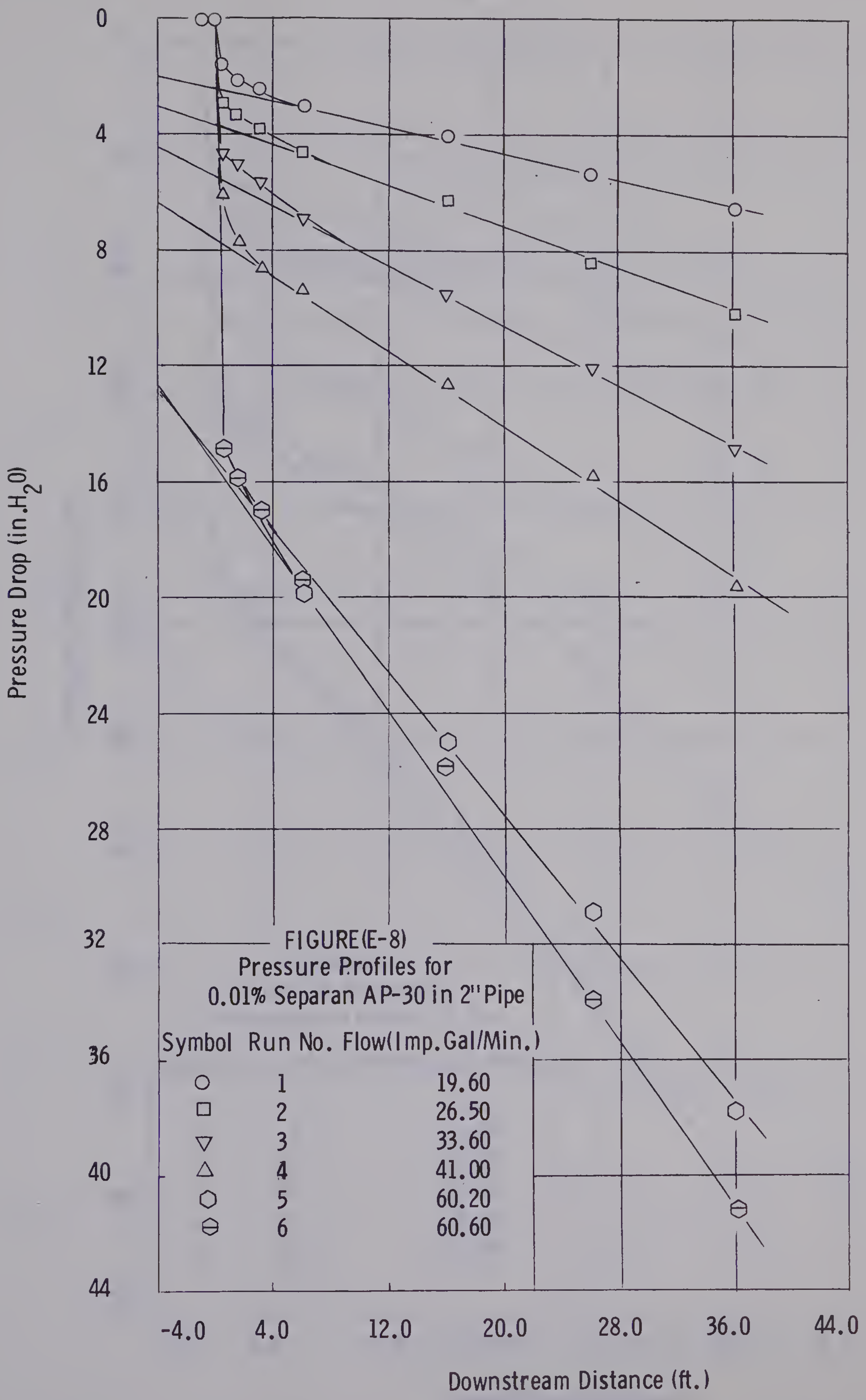

FIGURE(E-8)
Pressure Profiles for
0.01% Separan AP-30 in 2" Pipe

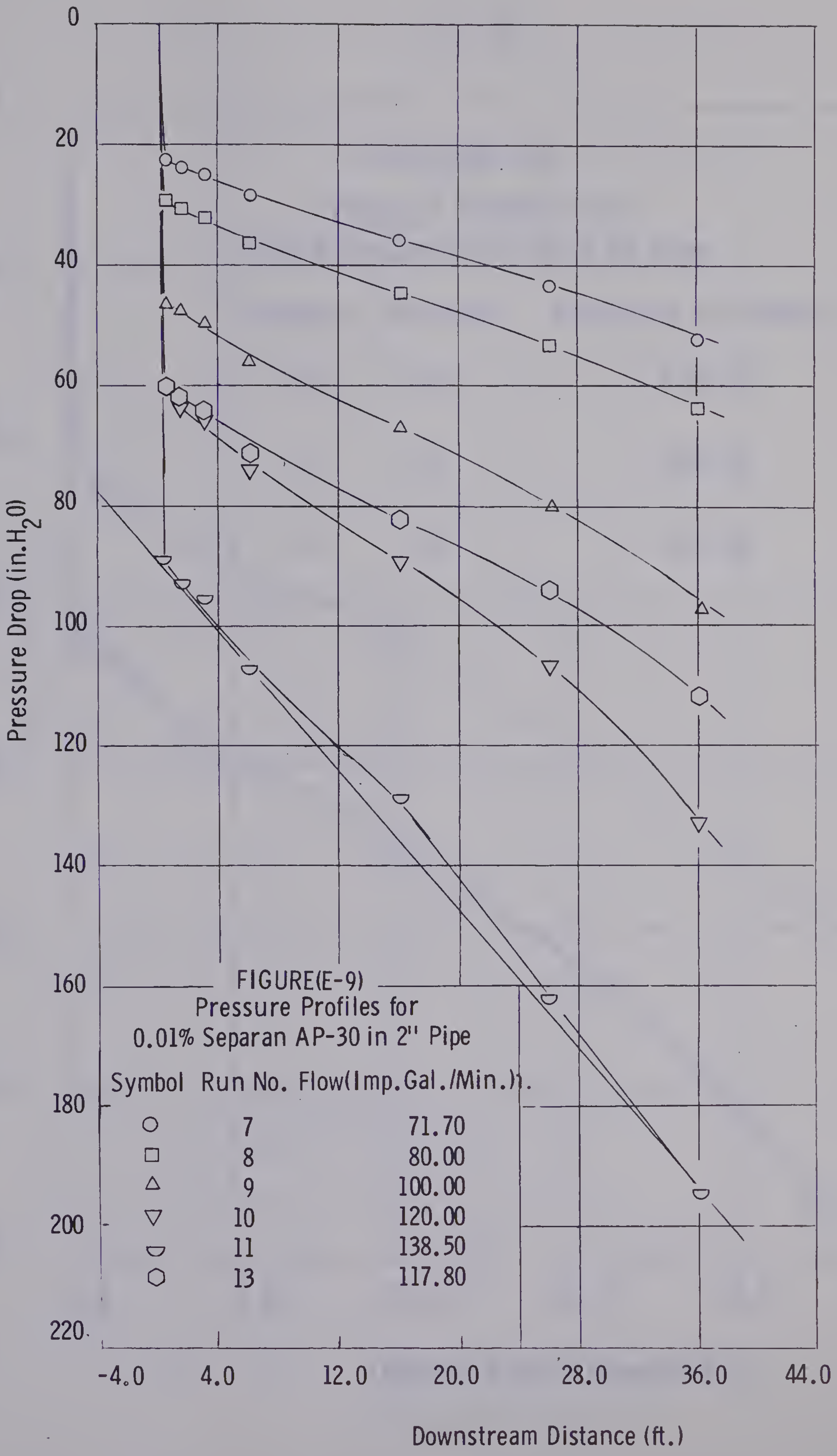

FIGURE(E-9)
Pressure Profiles for
0.01% Separan AP-30 in 2" Pipe

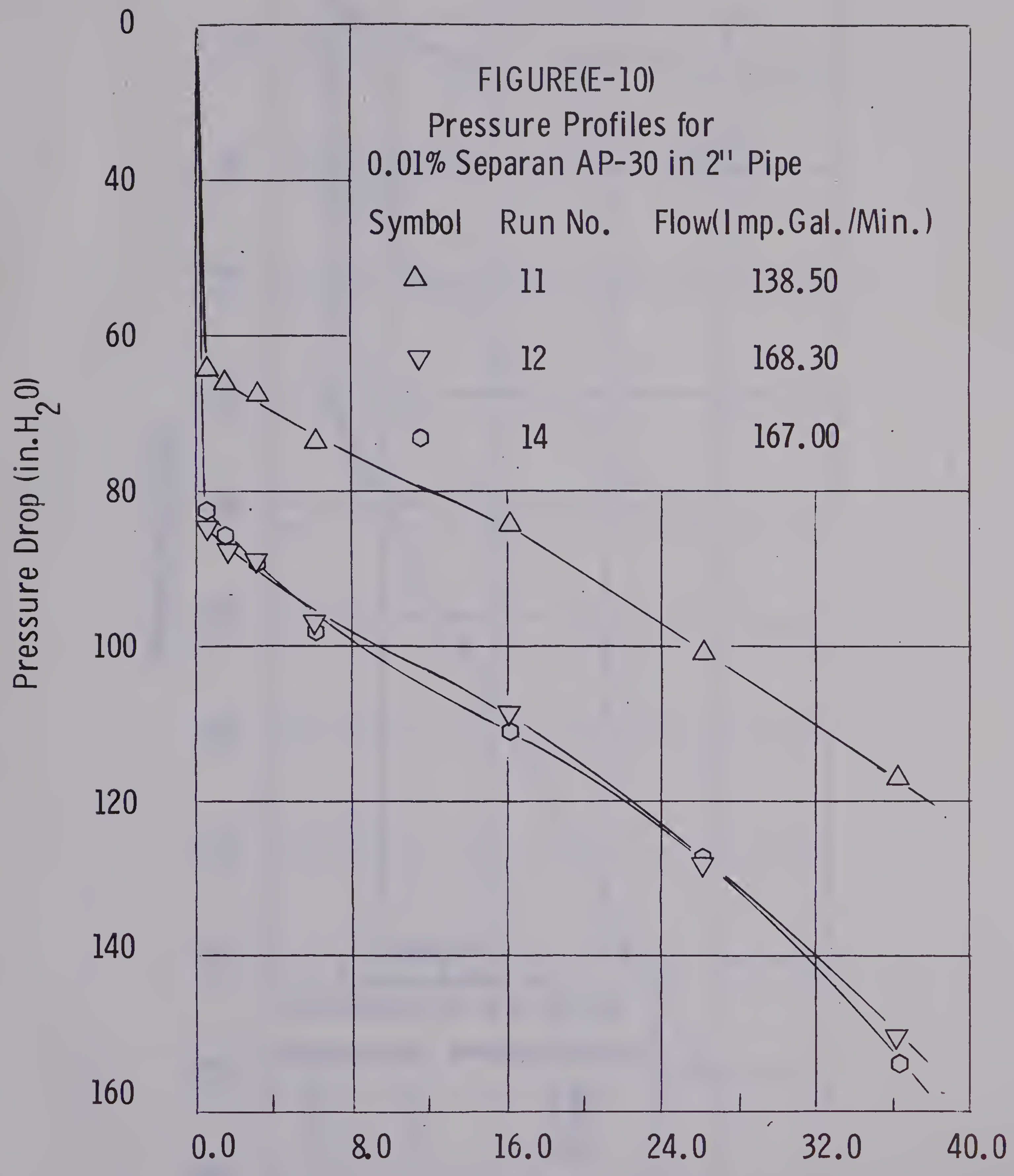
FIGURE(E-10)
Pressure Profiles for
0.01% Separan AP-30 in 2" Pipe
Symbol
Run No.
Flow(Imp.Gal./Min.)
△
11
138.50
▽
12
168.30
⬡
14
167.00
Pressure Drop (in.H2O)
0
40
60
80
100
120
140
160
0.0
8.0
16.0
24.0
32.0
40.0
Downstream Distance (ft.)

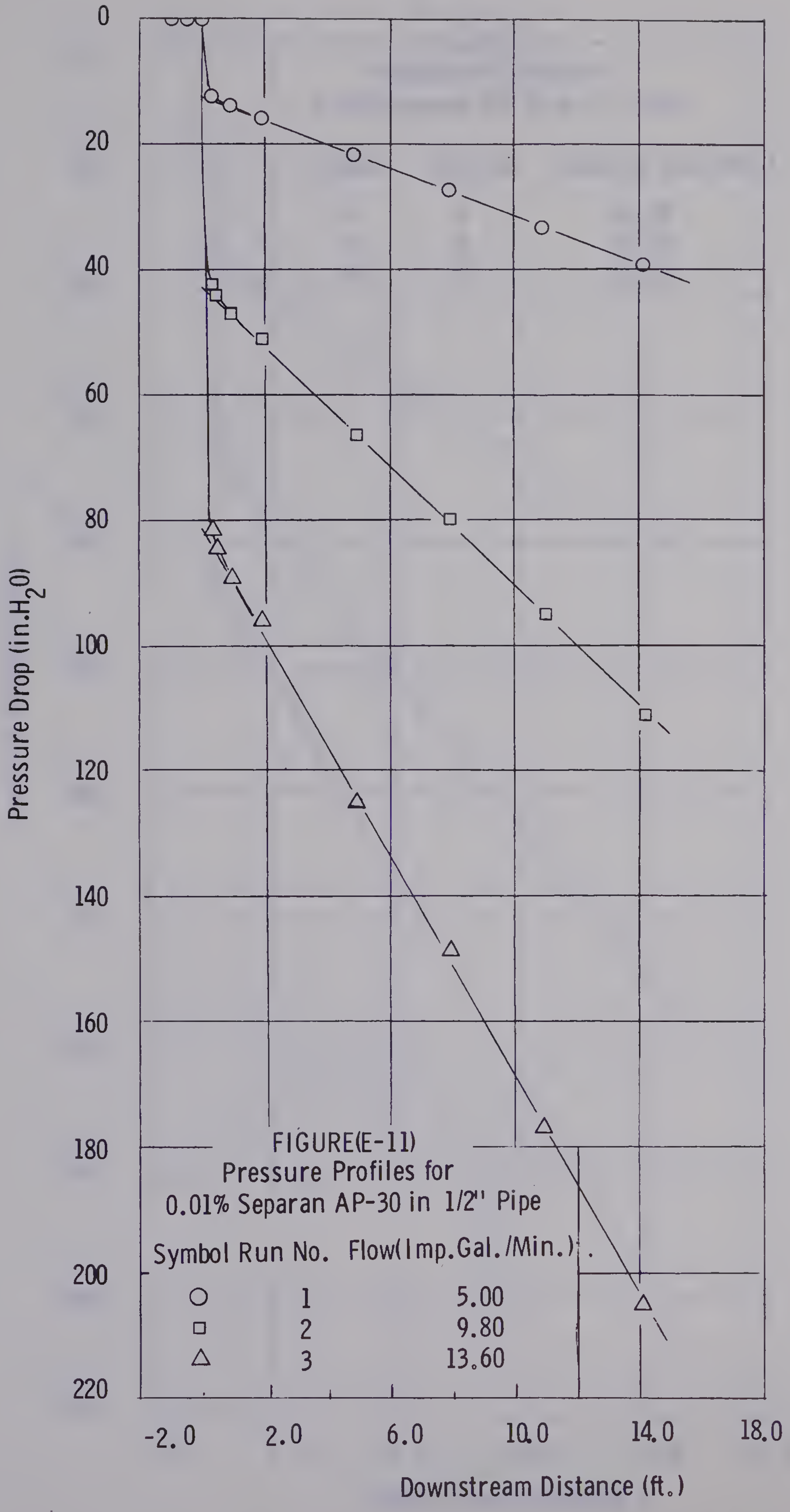

FIGURE(E-11) Pressure Profiles for 0.01% Separan AP-30 in 1/2" Pipe

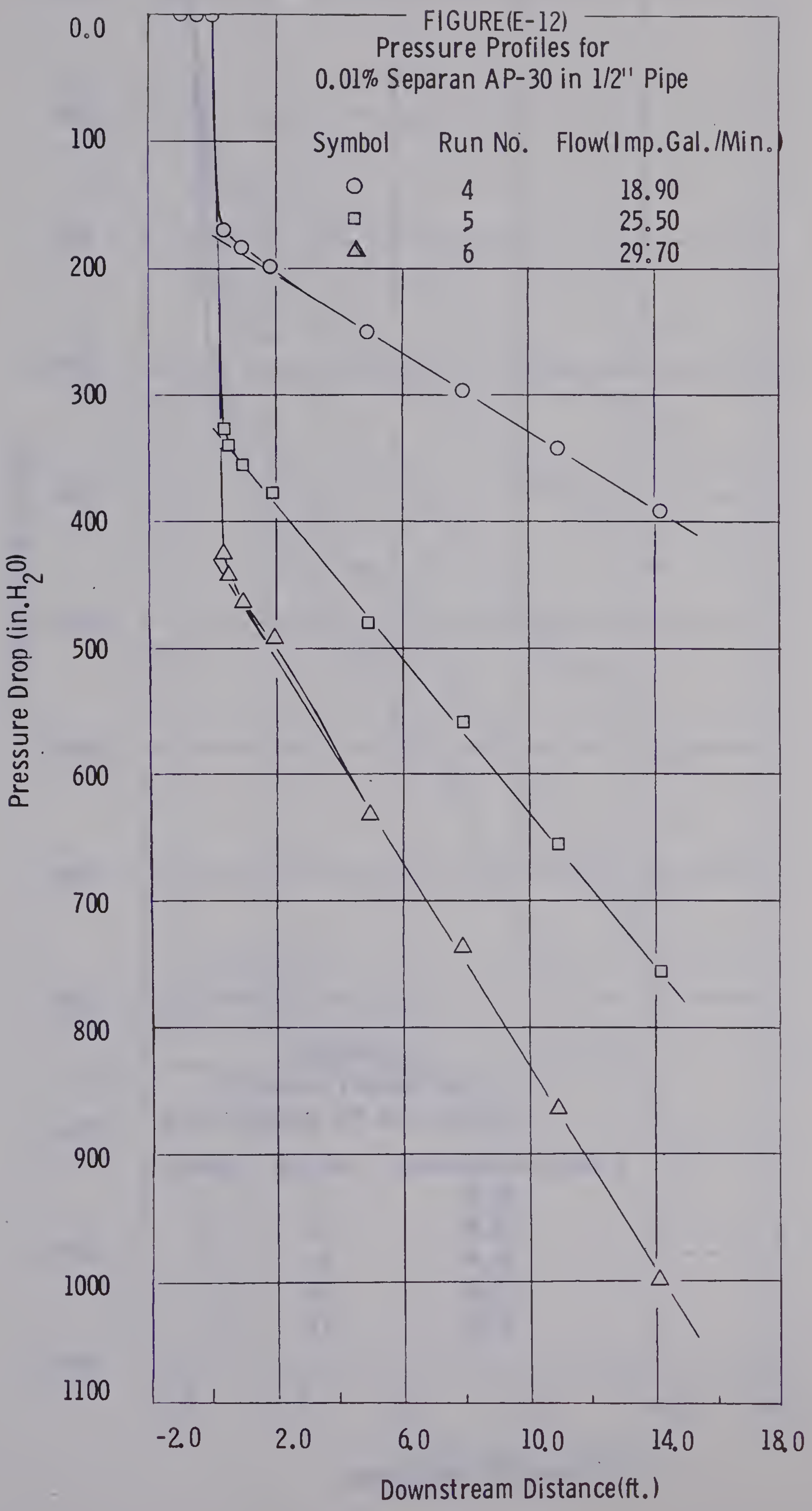

FIGURE(E-12)
Pressure Profiles for
0.01% Separan AP-30 in 1/2" Pipe

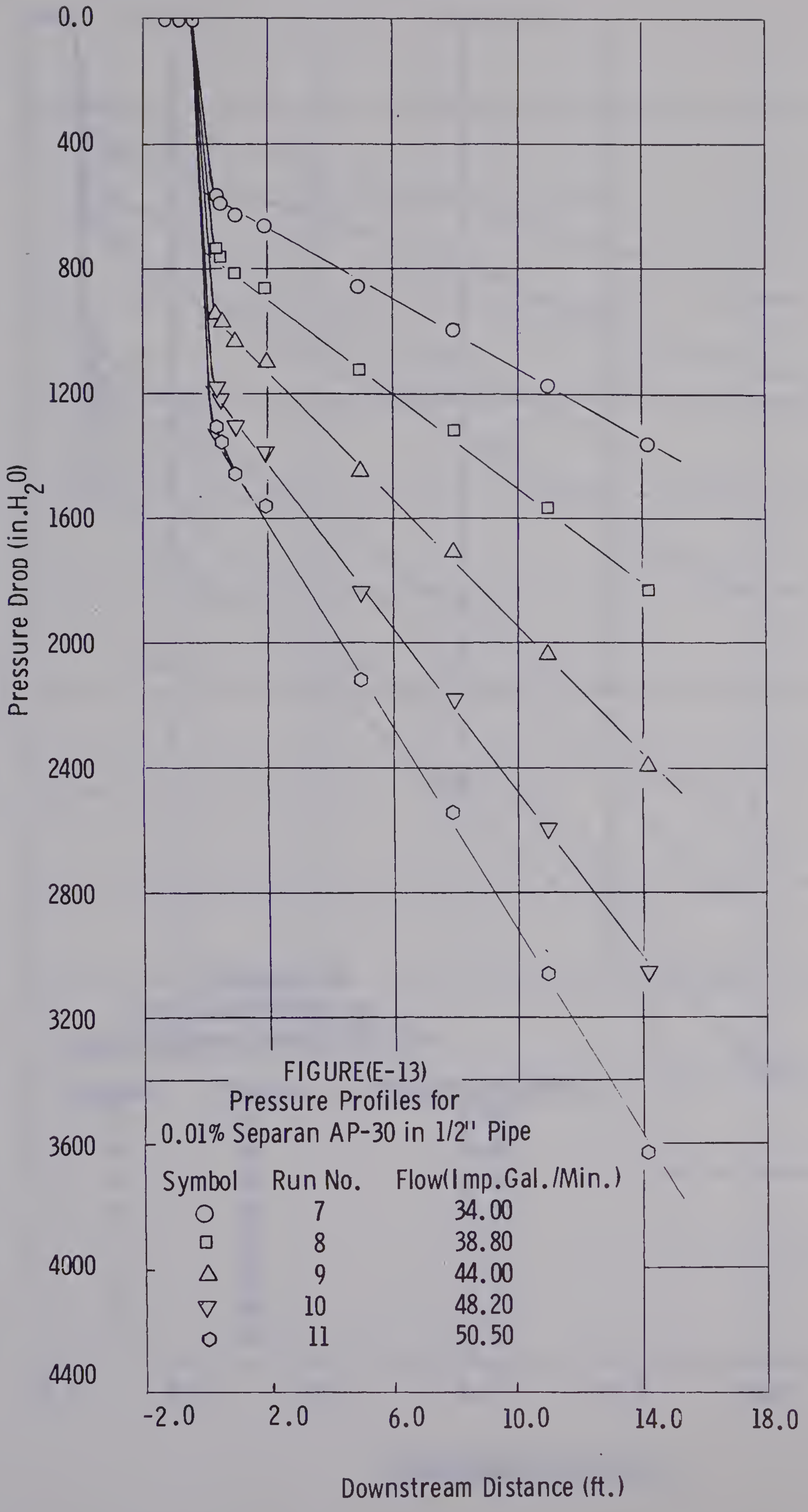

FIGURE(E-13)
Pressure Profiles for
0.01% Separan AP-30 in 1/2" Pipe

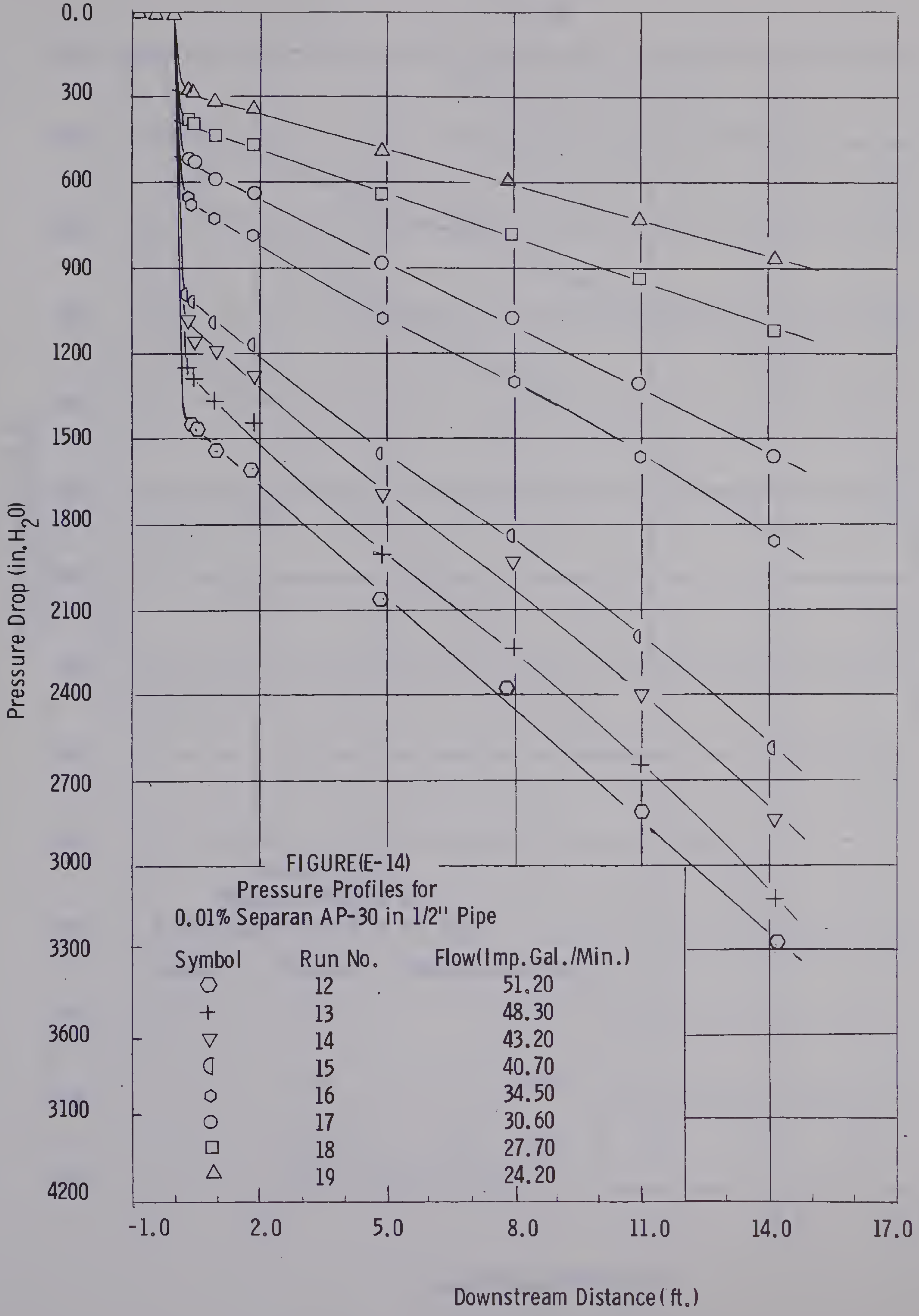

FIGURE(E-14)
Pressure Profiles for
0.01% Separan AP-30 in 1/2" Pipe

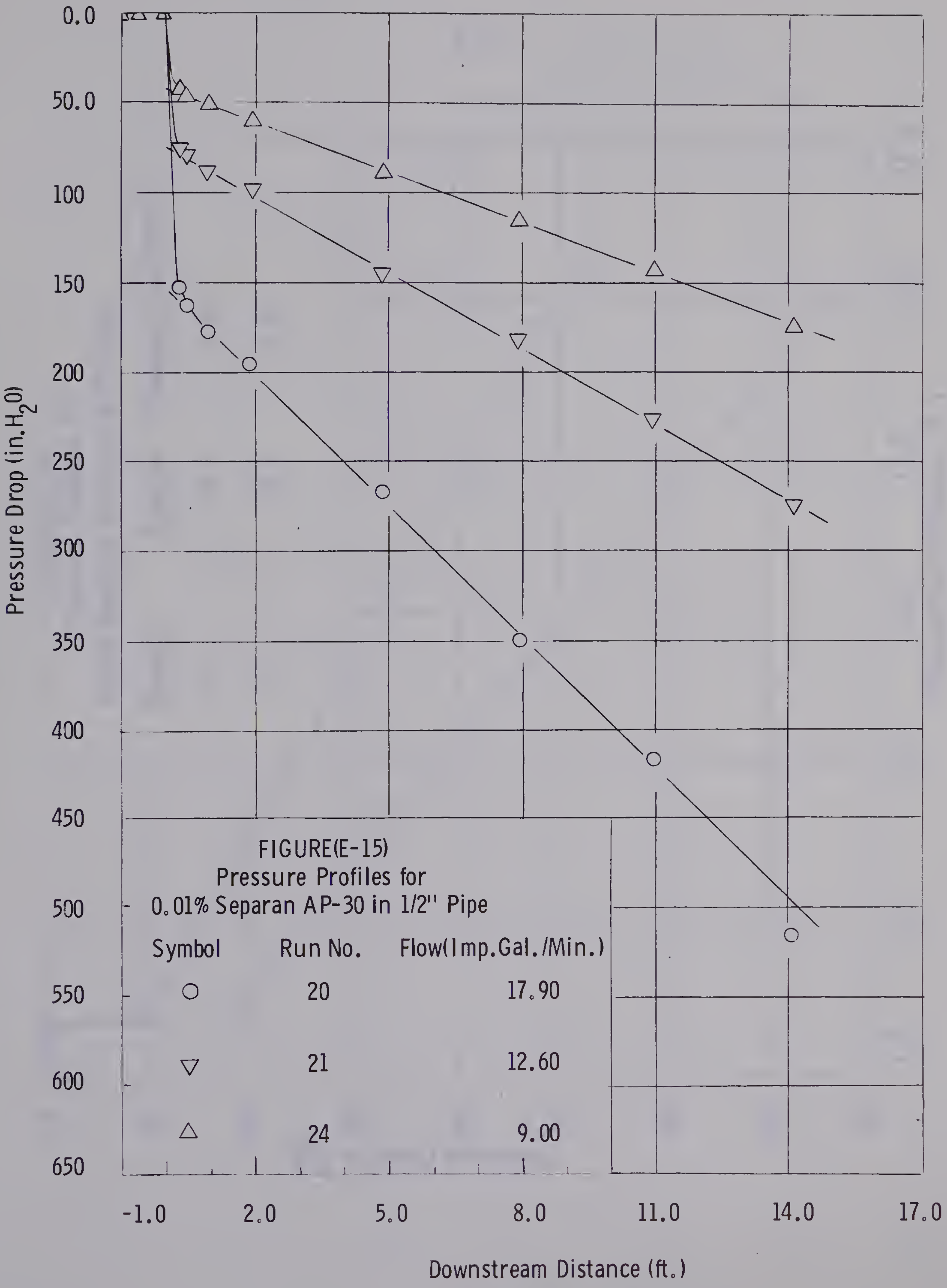

FIGURE(E-15)
Pressure Profiles for
0.01% Separan AP-30 in 1/2" Pipe

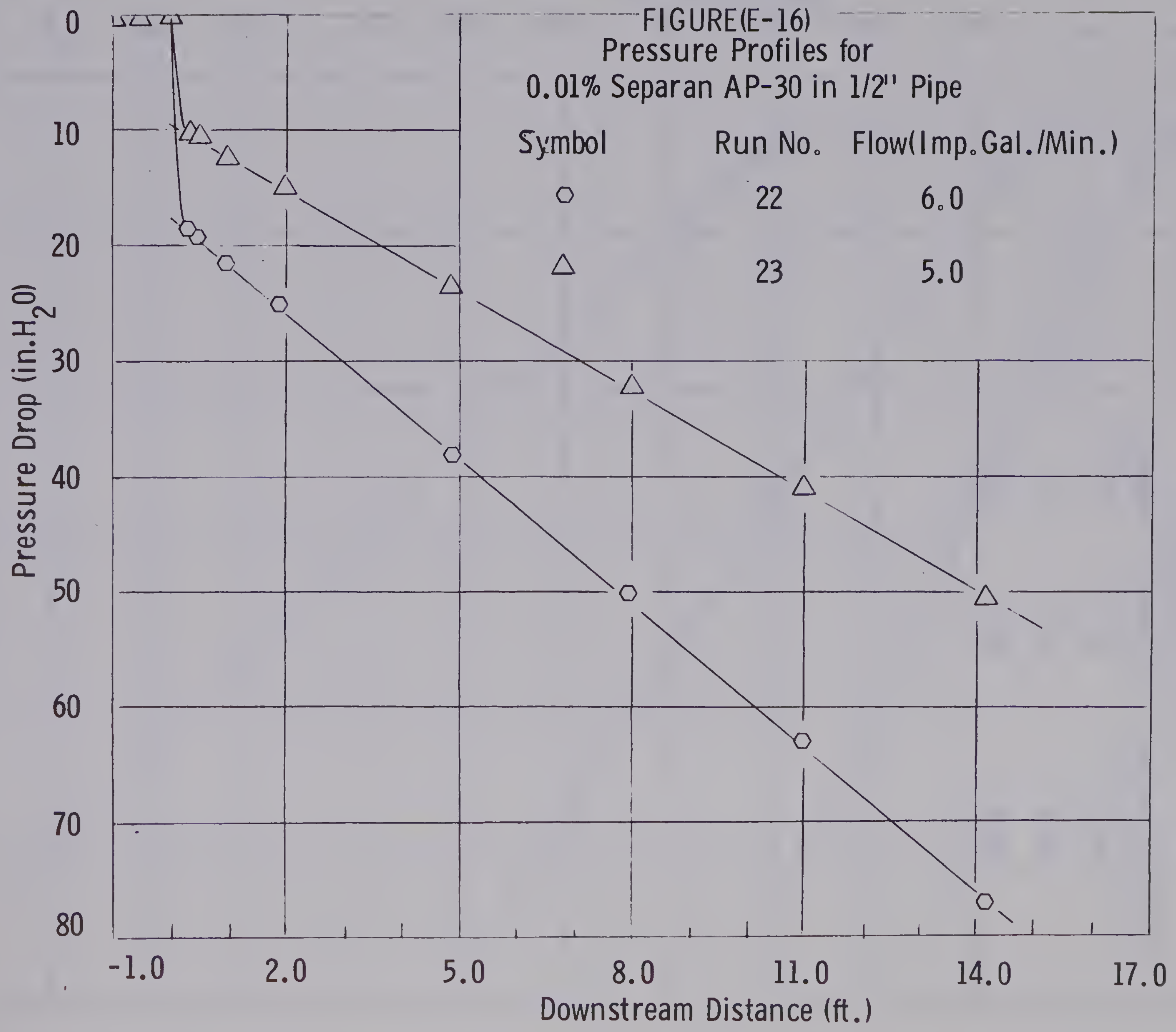

FIGURE(E-16)
Pressure Profiles for
0.01% Separan AP-30 in 1/2'' Pipe

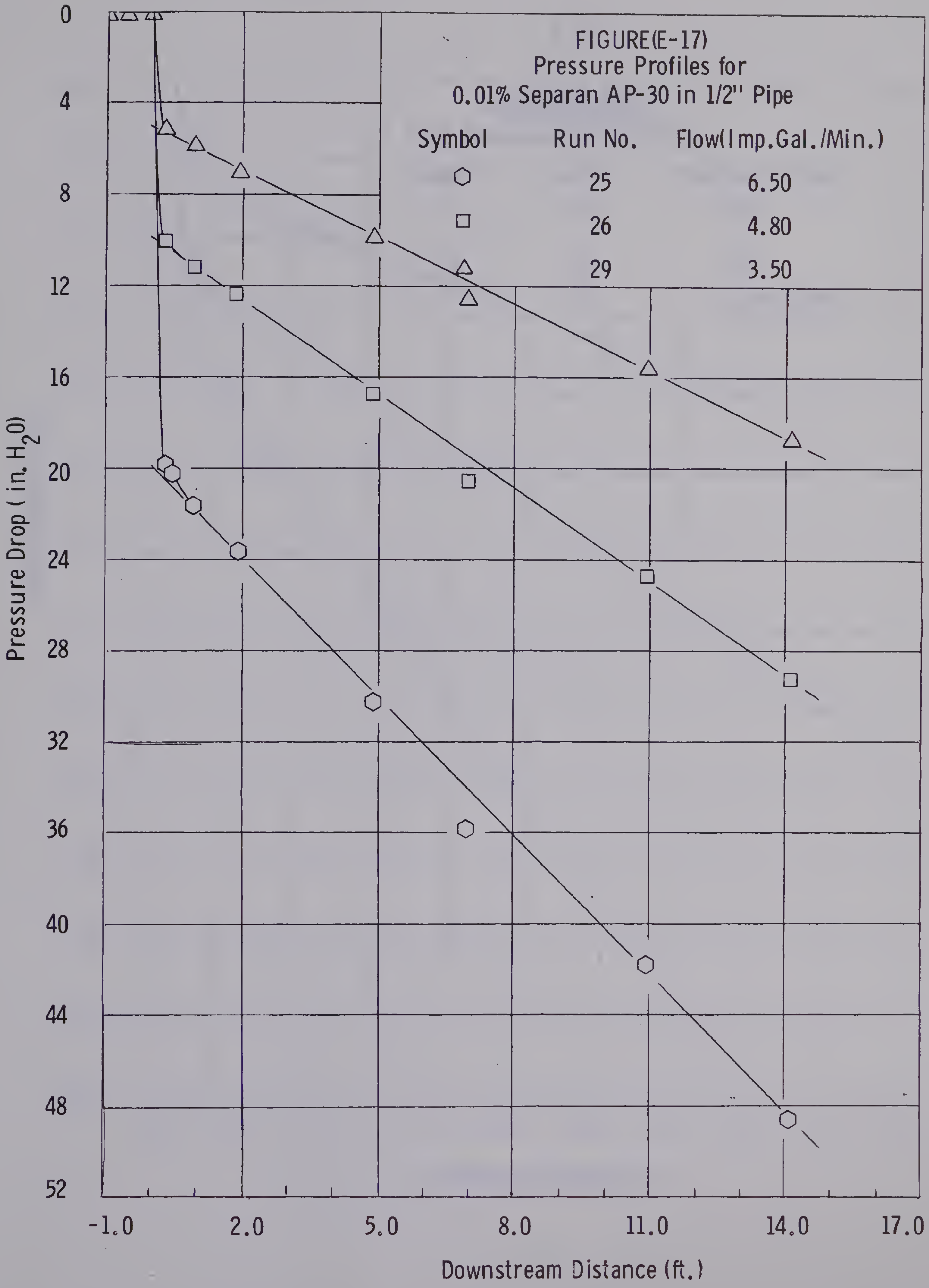

FIGURE(E-17)
Pressure Profiles for
0.01% Separan AP-30 in 1/2" Pipe

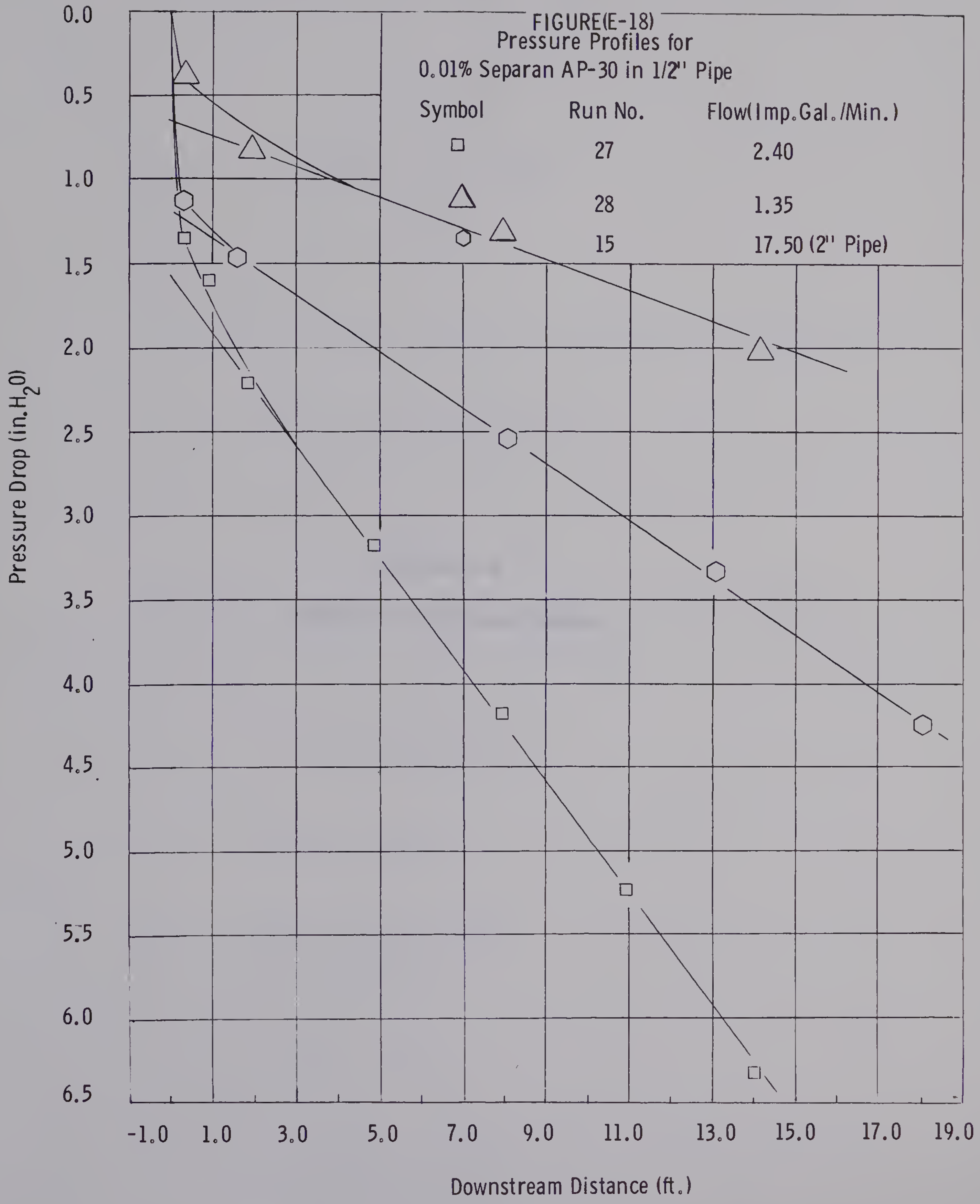
FIGURE(E-18)
Pressure Profiles for
0.01% Separan AP-30 in 1/2" Pipe
Symbol
Run No.
Flow(Imp.Gal./Min.)
□ 27 2.40
△ 28 1.35
⬡ 15 17.50 (2" Pipe)
Pressure Drop (in.H2O)
0.0
0.5
1.0
1.5
2.0
2.5
3.0
3.5
4.0
4.5
5.0
5.5
6.0
6.5
-1.0
1.0
3.0
5.0
7.0
9.0
11.0
13.0
15.0
17.0
19.0
Downstream Distance (ft.)

# Appendix F

# Sample Calculations

The sample calculations given below are based on Run 1 of the 0.20% Separan AP30 data in the 2" pipe.

Table G-1:

For Run 1:

$$Q = 18.00 \text{ Imp. Gal./Min.}$$

$$\Delta P = 3.34 \text{ in. water.}$$

$$L = 10 \text{ ft.}$$

For the 2" pipe the bulk velocity is given by:

$$V = \frac{(18.00)(4.0)(.1336)(1.2)}{(60.0)(\pi)(.1721)^2}$$

$$= 2.069 \text{ ft./sec.}$$

The shear stress at the wall is obtained by converting the pressure drop to psf by

$$\Delta P = \frac{(3.34)(14.7)(144.0)}{(33.91)(12.00)}$$

$$= 17.375 \text{ (psf.)}$$

and

$$T_w = \frac{(17.375)(0.1721)}{(4.0)(10.0)}$$

$$= 0.0748 \text{ (psf.)}$$

Now the friction factor can be determined as

$$f = \frac{(0.0748)(2.0)(32.2)}{(62.4)(2.069)^2}$$

$$= 0.01803$$

With the value of the shear stress at the wall and use of Figure (C-1) in Appendix C the flow behavior index, consistency index and the laminar shear rate can be determined.

$$n' = 0.557$$

$$K' = 0.004216$$

$$\frac{8V}{D} = 96.0$$

The generalized Reynolds number can now be calculated as

$$N_{Re}' = \frac{(.1721)^{.557}(2.069)^{2.0-.557}(62.4)\ 8^{1.0-.557}}{(0.004216)(32.2)}$$

$$= 1236.51$$

From Figure (C-2) in Appendix C the relaxation time of 0.02990 sec. is obtained. This is now used to determine the normal stress difference

$$(P_{11}-P_{22})_w = (0.0299)(2.0)(0.0748)(175.0)$$

$$= 0.7796 \text{ (psf.)}$$

The Deborah number and inertia-viscous number can now be determined as

$$N_{DEB} = \frac{V\theta}{D}$$

$$= \frac{(2.069)(0.0299)}{(0.1721)}$$

$$= (0.359)$$

and

$$N_{IV} = \frac{(P_{11}-P_{22})_w g_c}{\rho V^2}$$

$$= \frac{(.7796)(32.2)}{(62.4)(2.069)^2}$$

$$= 0.094$$

To determine the dimensionless contraction loss and entry length one must obtain these values from Figure (E-1) Appendix E.

$$(\Delta P_c)_{VE} = 2.32 \text{ (in. water)}$$

$$L_e = 1.50 \text{ ft.}$$

Thus, the dimensionless contraction loss becomes

$$\frac{(\Delta P_c)_{VE}}{\rho V^2/g_c} = \frac{(2.32)(14.7)(144.0)(32.2)}{(12.0)(33.91)(62.4)(2.069)^2}$$

$$= 1.458$$

and

$$\frac{L_e}{D} = \frac{1.50}{0.1721}$$

$$= 8.70$$

# Appendix G

# Nomenclature

| | |
|---|---|
| a | constant |
| $A, A'$ | arbitrary functions |
| $A_1, A_1'$ | arbitrary functions |
| b | distance between parallel flat plates |
| $C_{(\xi,f)}$ | constant defined by (16) |
| D | pipe diameter |
| $d_{ij}$ | deformation rate tensor defined as $\frac{1}{2}(\partial_i V_j + \partial_j V_i)$ |
| f | Fanning friction factor |
| $F_{entry}$ | frictional loss in the entry |
| $F_{dev}$ | frictional loss in developed flow |
| $F_{upstream}$ | frictional loss in the upstream reservoir |
| $F_E$ | frictional loss due to elasticity |
| $\Delta E$ | elastic stored energy per unit mass |
| $g_c$ | constant $\left(32.174 \frac{ft.lbm}{sec.^2 lbf}\right)$ |
| K | constant defined by equation (1.2.1) |
| $K'$ | consistency index defined by equation (2.2.1) |
| $K_2$ | Hagenbach correction factor defined by equation (1.2.6) |
| $\frac{K_1}{N_{Re}}$ | Couette correction factor |
| $\Delta KE$ | kinetic energy change |
| L | distance downstream from the contraction |
| Le | entry length |
| $\left(\frac{L_e}{D}\right)_{VE}$ | viscoelastic dimensionless entry length |

| | |
|---|---|
| $(\frac{L_e}{D})_{pV}$ | purely viscous dimensionless entry length |
| $n'$ | flow behavior index |
| $N_{Deb}$ | dimensionless Deborah number defined as $(\frac{V\Theta}{D})$ |
| $N_{ws}$ | dimensionless Weissenberg number defined as $\frac{(P_{11}-P_{22})_w}{T_w}$ |
| $N_{Re}$ | dimensionless Reynolds number |
| $N'_{Re}$ | dimensionless generalized Reynolds number |
| $p$ | hydrostatic pressure |
| $P_{ij}$ | deviatoric stress component defined by equation (2.2.3) |
| $\Delta P$ | pressure loss in developed flow |
| $\Delta P_{DEV}$ | pressure loss in developed flow |
| $\Delta P_{LOSS}$ | defined by Figure (4.9) |
| $\Delta P_{TOT}$ | total pressure drop measured from the contraction |
| $\Delta P_c$ | contraction loss |
| $R$ | pipe radius |
| $s$ | normal stress power law index defined as $(P_{11}-P_{22})_w = \text{const.} (\frac{8V}{D})^s$ |
| $S_{ji}$ | strain tensor (39) |
| $T_w$ | shear stress at the wall |
| $T_{ij}$ | component of stress tensor |
| $u$ | instantaneous axial velocity |
| $u^+$ | dimensionless velocity defined as $(u/u^*)$ |
| $u^*$ | frictional velocity defined as $\sqrt{T_w/\rho}$ |

| | |
|---|---|
| $V$ | average velocity |
| $y$ | distance from pipe wall |
| $y^+$ | dimensionless distance defined as $(yu^*/\nu)$ |

## Greek Symbols

| | |
|---|---|
| $\beta$ | dimensionless diameter ratio |
| $\Delta_{LOSS}$ | defined by Figure (4.9) |
| $\delta_{ij}$ | Kronecker delta |
| $\frac{\delta}{\delta t}$ | contravariant convective derivative (52) |
| $\rho$ | density |
| $\Theta$ | relaxation time defined by equation (2.4.7) |
| $\phi$ | Hagenbach correction factor |
| $\nu$ | kinematic viscosity |
| $\sigma(n',s)$ | constant defined by equation (1.2.2) |
| $\mu$ | viscosity |

# Appendix H

# Bibliography

1. Acrivos, A., M.J. Shah and E.E. Peterson, Chem. Eng. Sc., 20, 101 (1965).

2. Adams, E.B., and D.C. Bogue, Paper presented at the Symposium on Mechanics of Viscoelastic Fluids, Part 1, Dec. (1965).

3. Astarita, G., Ind. Eng. Chem. Fund., 4, 354 (1965).

4. Astarita, G., A.I.Ch.E. J., 5, 237 (1966).

5. Astarita, G., I.&E.C. Fund., 6, 257 (1966).

6. Astarita, G., and G. Greco, I.&.E.C. Fund., 7, 27 (1968).

7. Astarita, G., G. Greco and L. Peluso, to be published.

8. Astarita, G., and L. Nicodemo, A.I.Ch.E. J., 12, 478 (1966).

9. Bagley, E.B., Trans. Soc. Rheol., 5, 355 (1961).

10. Bakewell Jr., H.P., and J.T. Lumley, Phy. of Fluids, 10, 1880 (1967).

11. Barbin, A.R., and J.B. Jones, J. Basic Eng., 85, 29 (1963).

12. Bernstein, B., E. Kearsley and T. Zapas, Trans. Soc. Rheol., 9, 27 (1965).

13. Bogue, D.C., I.&E.C. Fund., 7, 874 (1959).

14. Bogue, D.C., I.&E.C. Fund., 5, 253 (1966).

15. Bogue, D.C., and J.O. Doughty, I.&E.C. Fund., 5, 243 (1966).

16. Bogue, D.C., and A.B. Metzner, I.&E.C. Fund., 2, 143 (1963).

17. Brodkey, R.S., A.I.Ch.E. J., 9, 448 (1963).

18. Campbell, W.D., and J.C. Slattery, J. Basic Eng., March (1963).

19. Castro, W.E., Ph.D. Dissertation, The University of West Virginia (1966).

20. Christiansen, E.B., and H.E. Lemmon, A.I.Ch.E. J., 11, 995 (1965).

21. Collins, M., and W.R. Schowalter, A.I.Ch.E. J., 9, 804 (1963).

22. Dalla Lana, I.G., and E.B. Christiansen, Can. J. Chem. Eng., 45, 275 (1967).

23. Dealy, J.M., Paper presented at the Chem. Eng. Colloquium, August 4, (1964).

24. Dealy, J.M., A.I.Ch.E. J., 11, 745 (1965).

25. Denn, M.M., Chem. Eng. Sc., 22, 395 (1967).

26. Dodge, D.W., and A.B. Metzner, A.I.Ch.E. J., 5, 189 (1959).

27. Doughty, J.O., and D.C. Bogue, I.&E.C. Fund., 6, 388 (1967).

28. Drexler, L.H., M.Sc. Dissertation, The University of Delaware, June (1967).

29. Ernst, W.D., A.I.A.A., 5, 906 (1967).

30. Feig,J., Masters Dissertation, The University of Delaware, (1966).

31. Goren, Y., and J.F. Norbury, J. Basic Eng., 89, 814 (1967).

32. Granville, P.S., Paper presented to Bureau of Ordnance (Naval Ordnance Systems Command), published in Hydrodynamics Laboratory Technical Note 61, Nov. (1966).

33. Gupta, R.C., A.I.Ch.E. J., 11, 1149 (1965).

34. Gupta, M.K., A.B. Metzner and J.P. Hartnett, Int. J. Heat Mass Transfer, 10, 1211 (1967).

35. Hinze, J.O., "Turbulence", McGraw-Hill (1958).

36. Hershey, H.C., and J.T. Zakin, I.&E.C. Fund., 6, 381 (1967).

37. Huppler, J.D., Trans. Soc. Rheol., 9, 273 (1965).

38. Kirsten, H., "Experimentelle Untersuchungen der Entwicklung der Geschwindigkeitsverteilung der Turbulenten Rohrströmung, Thesis, Leipzig (1927).

39. Lodge, A.S., "Elastic Liquids", Academic Press (1964).

40. Marucci, G., and G. Astarita, A.I.Ch.E. J., 13, 931 (1967).

41. Meter, D.M., A.I.Ch.E. J., 10, 881 (1964).

42. Meter, D.M., and R.B. Bird, A.I.Ch.E. J., 10, 878 (1964).

43. Metzner, A.B., A.I.Ch.E. J., 13, 316 (1967).

44. Metzner, A.B., and G. Astarita, A.I.Ch.E. J., 13, 550 (1967).

45. Metzner, A.B. and M.G. Park, J. Fluid Mech., 20,291 (1964).

46. Metzner, A.B., and J.C. Reed, A.I.Ch.E. J., 1, 434 (1955).

47. Metzner, A.B., and J.L. White, A.I.Ch.E. J., 11, 989 (1965).

48. Metzner, A.B., W.T. Houghton and R.A. Sailor, Trans. Soc. Rheol., 5, 133 (1961).

49. Metzner, A.B., E.A. Uebler and C.F. Chan Man Fong, to be published.

50. Metzner, A.B., J.L. White and M.M. Denn, A.I.Ch.E. J., 12, 863 (1966).

51. Metzner, A.B., J.L. White and M.M. Denn, Chem. Eng. Progr., 62, 81 (1966).

52. Meyer, W.A., A.I.Ch.E. J., 12, 522 (1966).

53. Middleman, S., and J. Gavis, Phy. of Fluids, 4, 355 (1961), 4, 963 (1961).

54. McMillen, E.L., Chem. Eng. Progr., 42, 537 (1948).

55. Nicodemo, L., D. Acierno and G. Astarita, to be published.

56. La Nieve, H.L., and D.C. Bogue, J. Appl. Poly. Sc., 12, 353 (1968).

57. Oliver, D.R., Can. J. Chem. Eng., 44, 100 (1966).

58. Oliver, D.R., and W.M. Macsporran, Can. J. Chem. Eng., Cdn. J.Chem. Eng., 46, 233 (1968).

59. Olson, R.M., and E.M., Sparrow, A.I.Ch.E. J., 9, 766 (1963).

60. Philippoff, W., and F.H. Gaskins, Trans. Soc. Rheol., 2, 263 (1958).

61. Popovich, A.T., and R.L. Hummel, A.I.Ch.E. J., 13, 854 (1967).

62. Ross, D., Trans. A.S.M.E., 78 915 (1956).

63. Rotta, Von J., Ingenieur Archiv., 24, 258 (1956).

64. Ryan, N.W., and M.M. Johnson, A.I.Ch.E. J., 5, 433 (1965).

65. Savins, J.G., Paper pesented to the Society of Petroleum Eng. Symposium on Mechanics of Rheologically Complex Fluids, Dec. (1966).

66. Seyer, F.A., Ph.D. Dissertation, The University of Delaware, June (1967).

67. Seyer, F.A., and A.B. Metzner, Can. J. Chem. Eng., 45, 121 (1967).

68. Seyer, F.A., and A.B. Metzner, to be published.

69. Seyer, F.A., and A.B. Metzner, to be published.

70. Shaver, R.G., and E.W. Merrill, A.I.Ch.E. J., 5, 181 (1959).

71. Shertzer, C.R., I.&E.C. Fund., 4, 225 (1965).

72. Shertzer, C.R., and A.B. Metzner, Trans. Soc. Rheol., 10, 431 (1966).

73. Spriggs, T.W., and R.B. Bird, I.&E.C. Fund., 4, 182, (1965).

74. Spriggs, T.W., J.D. Huppler and R.B. Bird, Trans. Soc. Rheol. 10, 191 (1966).

75. Tomita, Y., Bull. of J.S.M.E., 4, 77 (1961).

76. Tomita, Y., and K. Tsuchiya, Bull. of J.S.M.E., 6, 709 (1963).

77. Uebler, E.A. Ph.D. Dissertation, The University of Delaware (1966).

78. Wang, Y.T., and P.A. Longwell, A.I.Ch.E. J., 10, 323 (1964).

79. Wells Jr., C.S., and J.G. Spangler, Phy. of Fluids, 10, 1890 (1967).

80. White, J.L., and A.B. Metzner, to be published.

81. White, J.L., and A.B. Metzner, A.I.Ch.E. J., 11, 324 (1965).

82. White, J.L., and A.B. Metzner, J. Appl. Poly. Sc., 7, 1867 (1963).

83. White, J.L., and A.B. Metzner, Trans. Soc. Rheol., 8, 295 (1963).

84. White, J.L., and N. Tokita, J. Appl. Poly. Sc., 11, 321 (1967).

85. White, J.L., and N. Tokita, J. of Phy. Soc. Japan, 22, 719 (1967).

86. Williams, M.C., A.I.Ch.E. J., 11, 467 (1965).

B29906